Astronomy & Astrophysics manuscript no. harps-kp
April 24, 2018

Exploring the realm of scaled Solar System analogs with HARPS ⋆

D. Barbato[1,2], A. Sozzetti[2], S. Desidera[3], M. Damasso[2], A.S. Bonomo[2], P. Giacobbe[2], L.S. Colombo[4], C. Lazzoni[4,3], R. Claudi[3], R. Gratton[3], G. LoCurto[5], F. Marzari[4], and C. Mordasini[6]

[1] Dipartimento di Fisica, Università degli Studi di Torino, via Pietro Giuria 1, I-10125 Torino, Italy
[2] INAF – Osservatorio Astrofisico di Torino, Via Osservatorio 20, I-10025 Pino Torinese, Italy
[3] INAF – Osservatorio Astronomico di Padova, Vicolo dell'Osservatorio 5, I-35122, Padova, Italy
[4] Dipartimento di Fisica e Astronomia "G. Galilei", Università di Padova, Vicolo dell'Osservatorio 3, I-35122 Padova, Italy
[5] European Southern Observatory, Alonso de Cordova 3107, Vitacura, Santiago, Chile
[6] Physikalisches Institut, University of Bern, Sidlerstrasse 5, 3012 Bern, Switzerland

Received <date> / Accepted <date>

ABSTRACT

Context. The assessment of the frequency of planetary systems reproducing the Solar System's architecture is still an open problem in exoplanetary science. Detailed study of multiplicity and architecture is generally hampered by limitations in quality, temporal extension and observing strategy, causing difficulties in detecting low-mass inner planets in the presence of outer giant planetary bodies.
Aims. We present the results of high-cadence and high-precision HARPS observations on 20 solar-type stars known to host a single long-period giant planet in order to search for additional inner companions and estimate the occurence rate f_p of scaled Solar System analogs, i.e. systems featuring lower-mass inner planets in the presence of long-period giant planets.
Methods. We carry out combined fits of our HARPS data with literature radial velocities using differential evolution MCMC to refine the literature orbital solutions and search for additional inner planets. We then derive the survey detection limits to provide preliminary estimates of f_p.
Results. We generally find better constrained orbital parameters for the known planets than those found in the literature; significant updates can be especially appreciated on half of the selected planetary systems. While no additional inner planet is detected, we find evidence for previously unreported long-period massive companions in systems HD 50499 and HD 73267. We finally estimate the frequency of inner low mass (10-30 $M_\oplus$) planets in the presence of outer giant planets as $f_p < 9.84\%$ for P<150 days.
Conclusions. Our preliminary estimate of f_p is significantly lower than the values found in the literature for similarly defined mass and period ranges; the lack of inner candidate planets found in our sample can also be seen as evidence corroborating the inward migration formation model for super-Earths and mini-Neptunes. Our results also underline the need for high-cadence and high-precision follow-up observations as the key to precisely determine the occurence of Solar System analogs.

Key words. techniques: radial velocities - methods: data analysis - planetary systems - stars: individual: HD 50499, HD 73267

1. Introduction

The science of exoplanetology has so far produced outstanding results: as of the time of writing (January 2018) the NASA Exoplanet Archive contains data for 3587 confirmed exoplanets, 1509 of which are part of a total of 594 multiple planetary systems. The recent increment in known multiple planets systems, arising in particular from the Kepler mission, has helped produce the first comparative studies on their mass distribution and global architecture (see Winn & Fabrycky 2015; Hobson & Gomez 2017), especially focused on the multiplicity and architecture's role in supporting or disproving the current and competing formation models for both giant and terrestrial planets as expanded upon in Raymond et al. (2008), Cossou et al. (2014), Schlaufman (2014) and Morbidelli & Raymond (2016).

A key parameter in discriminating between different formation models is the fraction of planetary systems featuring both gas giants and lower-mass planets and their relative orbits; for example the numerical simulations reported in Izidoro et al. (2015) suggest that *in situ* and *inward migration* formation models of hot super-Earths, defined as planets 1 to 20 times more massive than the Earth and with orbital periods lower than 100 days, would cause very different systems architecture, the latter creating an anti-correlation between giant planets and close-in super-Earth populations.

However, the investigation of a particular characteristic of multiplanetary systems, namely the frequency of systems featuring a clear mass and dimension hierarchy similar to the one dominating our Solar System, suffers from low-quality literature data and would clearly benefit from larger statistics. Out of the 594 multiple planetary systems confirmed so far only two are generally considered to be clear Solar System analogs, namely the GJ 676A (Sahlmann et al. 2016) and Kepler-90 (Cabrera et al. 2014) systems, and these contain at least one super-Earth, a type of planet noticeably lacking in our own system.

To further support this initial point, lacking a proper review on the subject, we have conducted a preliminary search in the NASA Exoplanet Archive (as retrieved on September 12 2017) in order to provide the needed context on the diverse known system architectures, focusing on those systems in which all planetary components have been studied via radial velocity observa-

⋆ Based on observations collected at the European Organisation for Astronomical Research in the Southern Hemisphere under ESO programmes 093.C-0919(A) and 094.C-0901(A).

tions. Drawing the line between giant planets and smaller ones at 30 $M_{\oplus}$, during this search we found that out of the 102 multiple planetary systems studied by RV surveys in which more than half of the planetary components have a catalogued measure of mass, 57 host only giant planets, 24 host only lower-mass planets and only 11 (namely the systems around stars GJ 676 A, GJ 832, HD 10180, HD 11964, HD 164922, HD 181433, HD 190360, HD 204313, HD 219134, HD 219828, HD 47186) are what could be considered Solar System analogs, featuring inner low-mass planets and outer giant planets orbiting outside the circumstellar habitable zone outer limit, computed here using the model discussed in Kopparapu et al. (2013). Finally we note the existence of 10 mixed-architecture multiple systems, featuring giant planets on close-in orbits or inside the habitable zone. We can therefore provide a preliminary estimate of known Solar System analogs amounting to about 10% of known multiple systems studied by RV surveys.

The value of this fraction is obviously highly dependent on the exact definition of what constitutes a Solar System analog. For example, it is significantly higher if one considers just the giant planets orbital periods instead of their position relative to the system's habitable zone as key to architectural characterization; considering as analogs those systems composed of inner lower-mass planets and outer giants whose orbits are longer than one year this fraction amounts to 15.57% of known multiple systems, and to 19.67% if the lower limit on giant planets orbital period is instead set at 100 days.

Although low, this fraction is an encouraging sign that a sizeable number of planetary systems may reproduce our own planetary architecture, featuring at least one gas giant on a long-period orbit and lower-mass planets on inner orbits; another positive clue can be identified in the findings of Ciardi et al. (2013), suggesting that in up to 60% of Kepler candidate planet pairs the innermost one has a smaller radius than the outer body, and that this fraction rises up to 68% if the pair contains one Neptune-sized planet. Winn & Fabrycky (2015) also reports that approximately half of Sun-like star host at least one small planet (from 1 to 4 $R_{\oplus}$) with an orbital period less than one year.

During the aforementioned preliminary search through the RV-observed known systems we found 229 single-planet systems, 195 of which contain a single long-period (P≥1 yr) giant and 34 containing a single Neptune-like or super-terrestrial planet. In this context, it is clear that this large fraction of single known long-period giant planet systems may represent an unparalleled opportunity for the search of yet undetected inner, smaller planets and therefore of scaled-down Solar System analogs; however, known systems with giant planets are not usually subject to follow-up observations to search for additional, lower mass planetary companions at short orbital period. Furthermore, the available data published on most of these systems do not provide by itself enough solid ground on which to base such a search, being characterized by a sampling frequency and in some case integration time or instrument setup not suited for detecting low-mass and short period planets. To successfully detect such inner planets and their very low amplitude signals compared to those of the more massive and distant companions, an intense monitoring of the host star is needed in order to fully cover their orbital phase; the need for higher precision and more densely sampled observations on already studied planetary systems is therefore clear and urgent in the search for scaled-down Solar System analogs.

The purpose of this paper is therefore to present the results of the observations conducted by the HARPS spectrograph on a small sample of these single-giant systems, in order to provide an estimate on the occurence rate of smaller inner planets in the presence of a single outer giant planet and to fuel further observations; it is also of note that the analysis of a parallel HARPS-N survey on a similarly selected northern hemisphere sample is currently underway and will be the subject of a forthcoming paper.

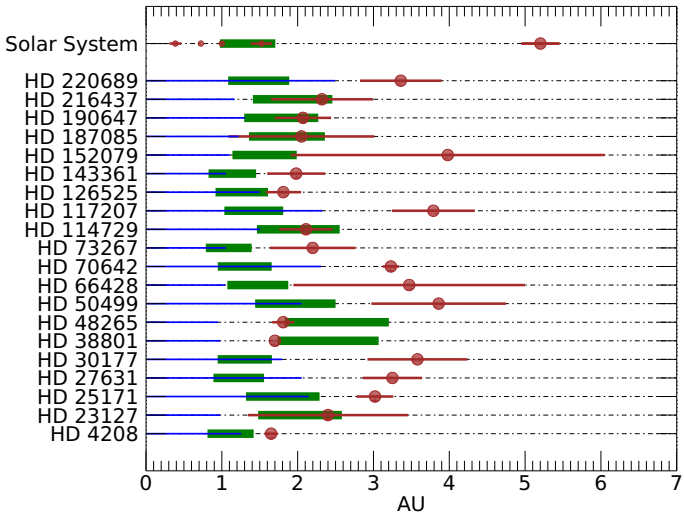

Fig. 1. Overview of the sample systems and a comparison with the inner Solar System's architecture. The sample's known giant planets are shown as brown circles, a thin brown line from periastron to apoastron showing their orbit's span. Each system's habitable zone, computed using the model detailed in Kopparapu et al. (2013), is shown as a thick green band, while the thin blue line indicates each system's region of dynamical stability for additional inner planets as computed through Hill's criterion detailed in Sect. 4.

In Sect. 2 we describe the selection criteria for the analyzed sample, before moving on to describe the HARPS observations structure and setup in Sect. 3; in Sect. 4 we show the results of the new data fits conducted to refine the orbital parameters of the known planets. Finally, in Sect. 5 we calculate the detection limits for each system and the sample as a whole, in order to provide an estimate to the planetary frequency of low-mass inner planets in the presence of outer giant planets to compare with the planetary frequency calculated in the seminal work of Mayor et al. (2011) for stars hosting at least one planet.

2. Sample selection and description

The 20 southern-emisphere stars selected for this work are all bright ($V < 9.2$), inactive ($\log R'_{HK} < -4.8$), not significantly evolved ($\log g > 4$) and are not members of visually close binaries, a set of criteria ensuring the overall sample is well suited to the search for low-mass inner planets.

All systems feature a single giant planet orbiting the host star at low to moderate eccentricities ($e < 0.5$), with periastron larger than 1 AU and discovered via the radial velocity method. Additional details on each system's stellar parameters can be found in Table 1, while a global overview of the planets positions relative to stars and habitable zones is given in Fig. 1; all planetary data were retrieved from the most recent published paper discussing each planet's orbital solution and listed in the first column of Tables 2 to 21. Regarding stellar parameters, each star's parallax, visual magnitude, metallicity and $\log R'_{HK}$ were retrieved from the Vizier online catalogue; effective temperatures were instead retrieved by joining the estimates reported in Bonfanti et al. (2015), Sousa et al. (2008) and Stassun et al.

Table 1. Stellar parameters for the sample systems

Star	π [mas]	V [mag]	B-V[a] [mag]	T_{eff} [K]	log$g$[a] [cgs]	[Fe/H]	Mass[a] [$M_\odot$]	Radius[a] [$R_\odot$]	Age[a] [Gyr]	log R'_{HK}	P_{rot}[e] [d]
HD 4208	30.58 ± 1.08	7.795 ± 0.011	0.726 ± 0.008	5717 ± 33[b]	4.501 ± 0.036	−0.28 ± 0.02	0.883 ± 0.024	0.846 ± 0.028	3.813 ± 2.970	-4.77	~25
HD 23127	11.22 ± 0.76	8.576 ± 0.002	0.701 ± 0.013	5843 ± 52[b]	4.146 ± 0.054	0.29 ± 0.03	1.208 ± 0.045	1.490 ± 0.104	4.508 ± 0.788	-5.00	~33
HD 25171	17.84 ± 0.60	7.782 ± 0.013	0.618 ± 0.005	6125 ± 21[b]	4.263 ± 0.031	−0.12 ± 0.04	1.076 ± 0.021	1.230 ± 0.045	4.802 ± 0.619	-4.99	~22
HD 27631	22.45 ± 0.78	8.243 ± 0.012	0.721 ± 0.009	5737 ± 36	4.455 ± 0.038	−0.12 ± 0.05	0.944 ± 0.032	0.923 ± 0.033	4.010 ± 2.892	-4.91	~31
HD 30177	19.93 ± 0.63	8.397	0.773 ± 0.012	5607 ± 47[b]	4.417 ± 0.034	0.39 ± 0.05	1.053 ± 0.023	1.019 ± 0.034	2.525 ± 1.954	-5.07	~45
HD 38801	10.39 ± 1.74	8.224	0.841 ± 0.019	5338 ± 59[b]	3.877 ± 0.084	0.25 ± 0.03	1.207 ± 0.108	2.029 ± 0.286	6.072 ± 1.835	-5.03	~47
HD 48265	11.48 ± 0.72	8.051	0.722 ± 0.013	5733 ± 55[d]	3.970 ± 0.048	0.30 ± 0.04	1.312 ± 0.064	1.901 ± 0.126	4.201 ± 0.625	-5.21	~45
HD 50499	21.02 ± 0.68	7.207 ± 0.004	0.628 ± 0.014	6102 ± 54[b]	4.247 ± 0.033	0.26 ± 0.04	1.253 ± 0.020	1.351 ± 0.054	2.391 ± 0.633	-5.03	~25
HD 66428	18.21 ± 1.07	8.246 ± 0.013	0.717 ± 0.006	5773 ± 23[b]	4.360 ± 0.050	0.23 ± 0.05	1.083 ± 0.022	1.102 ± 0.062	3.515 ± 2.040	-5.07	~38
HD 70642	34.84 ± 0.60	7.169	0.733 ± 0.005	5732 ± 23[b]	4.458 ± 0.017	0.22 ± 0.02	1.078 ± 0.015	0.984 ± 0.022	0.919 ± 0.733	-4.90	~32
HD 73267	18.77 ± 1.00	8.889	0.827 ± 0.003	5387 ± 10[d]	4.447 ± 0.035	0.07 ± 0.04	0.897 ± 0.019	0.909 ± 0.033	8.140 ± 3.505	-4.97	~43
HD 114729	27.69 ± 0.54	6.687 ± 0.005	0.688 ± 0.003	5844 ± 12[c]	4.046 ± 0.016	−0.33 ± 0.03	0.936 ± 0.013	1.473 ± 0.037	10.116 ± 0.344	-5.07	~34
HD 117207	30.37 ± 0.92	7.240	0.727 ± 0.014	5732 ± 53[b]	4.371 ± 0.039	0.19 ± 0.03	1.053 ± 0.028	1.074 ± 0.041	4.192 ± 2.274	-5.06	~39
HD 126525	26.24 ± 0.82	7.847 ± 0.004	0.747 ± 0.003	5638 ± 13[c]	4.382 ± 0.028	−0.10 ± 0.01	0.897 ± 0.010	0.979 ± 0.030	9.670 ± 1.333	-5.03	~40
HD 143361	16.80 ± 1.26	9.200	0.792 ± 0.004	5507 ± 10[d]	4.472 ± 0.043	0.14 ± 0.06	0.968 ± 0.027	0.916 ± 0.041	2.942 ± 2.749	-5.00	~42
HD 152079	11.90 ± 1.40	9.182	0.687 ± 0.014	5907 ± 52	4.365 ± 0.054	0.29 ± 0.07	1.147 ± 0.030	1.128 ± 0.074	1.622 ± 1.369	-4.99	~31
HD 187085	22.02 ± 1.12	7.225	0.622 ± 0.007	6117 ± 27[b]	4.279 ± 0.041	0.12 ± 0.04	1.189 ± 0.023	1.270 ± 0.066	2.747 ± 0.838	-4.93	~21
HD 190647	18.70 ± 1.10	7.779	0.744 ± 0.017	5656 ± 60[b]	4.162 ± 0.054	0.23 ± 0.02	1.069 ± 0.027	1.376 ± 0.089	7.957 ± 1.096	-5.09	~42
HD 216437	37.58 ± 0.56	6.057 ± 0.001	0.677 ± 0.009	5909 ± 31[b]	4.188 ± 0.026	0.20 ± 0.10	1.165 ± 0.046	1.394 ± 0.032	4.750 ± 1.059	-5.01	~30
HD 220689	21.96 ± 0.92	7.795 ± 0.062	0.671 ± 0.007	5921 ± 26	4.360 ± 0.045	−0.07 ± 0.10	1.016 ± 0.048	1.068 ± 0.047	4.586 ± 2.487	-4.99	~29

Notes. All stellar data retrieved from Vizier catalogue, except: [(a)] calculated from PARAM 1.3 (see da Silva et al. 2006) [(b)] retrieved from Bonfanti et al. (2015) [(c)] retrieved from Sousa et al. (2008) [(d)] retrieved from Stassun et al. (2017) [(e)] calculated following Mamajek & Hillenbrand (2008).

(2017). These stellar parameters were then used as input in the online tool PARAM in order to calculate each star's color index, surface gravity, mass, radius and age as detailed in da Silva et al. (2006). Values of stellar rotational period were instead computed using the empirical relations between $(B - V)$, $\log R'_{HK}$ and P_{rot} from Noyes et al. (1984) and Mamajek & Hillenbrand (2008) and here reported with a 1-day precision for the analytical nature of the relations used.

At a general overview of the systems characteristics, it can be noted that all selected stars are reasonably similar to our Sun; two exceptions worthy of note are represented by HD 38801 and HD 48265 whose mass and size (respectively 1.36 $M_\odot$, 2.53 $R_\odot$ and 1.28 $M_\odot$, 2.05 $R_\odot$) suggest that they are in a later stage of their evolution, probably on the sub-giant branch.

Moving on to the planets in the chosen sample, the minimum mass range spans from 0.224 M_J to 10.7 M_J, the most massive planet being HD 38801 b, which also features peculiar zero values of eccentricity and periastron longitude as fixed in the discovery paper (Harakawa et al. 2010) to improve its Keplerian fit quality; such a low value of eccentricity at such intermediate distances from the host star (a = 1.7 AU), it is noted, cannot yet be explained by tidal circularization and therefore represents an interesting conundrum. All the planets in the sample are characterized by long-period orbits, spanning from 1.89 to 7.94 years, and low to moderate eccentricities ($e < 0.52$).

It is also important to note that although each selected system was known to host a single, giant planet at the beginning of our observational program, an additional outer giant planet has been recently discovered in the system HD 30177, as detailed in Wittenmyer et al. (2017). Still, we have nonetheless decided to show rather than discard the results of our observations and analysis on this system, both since the existence of HD 30177 c was not known at the time of observation and because its very long period (P=31.82 yr) causes it not to have a significant dynamical influence on the short-period regions of interest to our study.

We further stress the fact that we verified through extensive simulations using literature and archival RV data that current data on the selected sample do not provide the sensitivity needed to succesfully detect Neptune-mass planets with $P < 50d$, due to large RV errors (≥5 m/s) in the discovery data, poor sampling at short periods, or both.

3. HARPS observations

As discussed in Sect. 1, the present understanding of multiple planetary systems architecture still shows severe gaps, especially regarding the occurence of architectures mimicking that of our Solar System. To try and help filling this gaps we have conducted an intense monitoring on selected stars hosting a single long-period giant planet using the high-precision HARPS spectrograph mounted at the ESO La Silla 3.6m telescope. In order to successfully detect any additional low-mass planets in the selected systems and to further refine the outer giant planet orbit, the selected stars were intensely observed over a time period spanning from April 2014 to March 2015 (ESO programmes 093.C-0919(A) and 094.C-0901(A)); during this period each star was observed for about a semester, and to optimize time sampling the observing nights were split in blocks of two or three nights at the beginning, middle and end of the observing period. Based on the allocated observation time, a total of 514 measurements where obtained during this period, providing about 27 datapoints on average for each of the 20 target stars, a number of observations that, we note, is significantly lower than the ∼40 measurements per star that we originally foresaw in the program proposal.

Depending on magnitude, the target stars were measured with 10 or 15 minutes total exposure, in order to achieve sufficient signal-to-noise ratio to reach the required <1 ms^{-1} precision for all program stars using HARPS in its simultaneous Th-Ar observing mode. The aforementioned integration time is also needed in order to average the oscillation and granulation modes of solar-type stars.

4. Systems analysis

4.1. Fitting methodology

A complete list of the newly acquired high-precision HARPS data for each system in the selected sample is collected in Table 22 at the end of this paper. To use this data for the refinement of the known planets orbital elements we subtracted from the raw timeseries the stellar proper radial motion computed as the mean of the radial velocity dataset. Our datasets were then joined with all literature data available on each system, producing therefore a complete series of radial velocity data comprising discovery datasets, follow-up timeseries and the HARPS data acquired during our survey; when available previous HARPS observations publicly released on the ESO archive were also used. Any HARPS datapoint characterized by a signal-to-noise ratio lower than 30 was removed; details on the excluded datapoints are to be found in each system's paragraph in Subsect. 4.3. Unless otherwise noted, we fit for no offset between the various HARPS datasets, that were therefore treated as a single timeseries. The main purpose of joining various datasets from different observations and instruments is to use the higher precision of HARPS data to further constrain and refine the known planets orbital parameters by refitting the complete timeseries composed of both historic and new data.

The fits have been obtained using the `EXOFAST` suite of routines written for IDL (Eastman et al. 2013), characterizing the orbital parameters and their uncertainties with a differential evolution Markhov Chain Monte Carlo method, the fitting parameters being time of periastron T_{peri}, orbital period P, $\sqrt{e}\cos\omega$, $\sqrt{e}\sin\omega$, semiamplitude K and systematic velocity γ_i and jitter j_i for each instrument in the joined timeseries. The `EXOFAST` routines assumes the stellar jitter to be uncorrelated Gaussian nois that is added in quadrature to the radial velocity measurement error. The known orbital parameters found in the literature and listed in Tables 2 to 21 were used as starting guesses for the MCMC chains to help achieve a better convergence.

After subtracting the best-fit Keplerian curve produced by `EXOFAST`, the residual datapoints were used to produce a generalized Lomb-Scargle periodogram using the IDL routine `GLS` (Zechmeister & Kürster 2009) to investigate the presence of additional inner planetary signals, selecting as signals of potential interest for further investigation only those power peaks characterized by a false alarm probabilty as computed via bootstrap method less than or equal to 1%.

As a further note on the plausibility of the presence of additional inner planets, after obtaining the refined fits on each system we searched for the maximum orbital period allowing dynamical stability for a single additional planet on a circular inner orbit under the gravitational influence of the known outer planet, using the equality on Hill's criterion (see e.g. Murray & Dermott 1999):

$$a_1(1 - e_1) - a_2 \geq 2\sqrt{3}R_H$$

being a_1 and e_1 the major semiaxis and eccentricity of the known giant planet, a_2 the major semiaxis of the test planet's orbit and R_H the known planet's Hill radius defined as:

$$R_H = a_1(1 - e_1)\sqrt[3]{\frac{m_1}{3M_*}}$$

We consider therefore the maximum approach distance between the known outer giant planet and the inner test planet as the limit stability. We varied the test planet's mass in the range 0.1-2 M_J and, since the maximum stable period for the test planet underwent a variation amount to less than one day within this mass range, we provide on each system's paragraph in Subsect. 4.3 a mean value for this maximum stable period and show each system's stability region as a thin blue line in Fig. 1.

Details on overall results and on case-by-case fitting process and results are contained in the following subsections.

4.2. Results overview

The overall results of the new fits obtained joining ours HARPS high-precision data with the available literature time series can be roughly divided in three main categories: fits that confirm the literature without significant changes to the orbital solution, fits than instead significantly change some or all of the published orbital elements and fits that suggest the existence of additional planetary companions in the system. A comparison between the literature results and the parameters obtained from our MCMC chains is shown in each system's Tables 2 to 21, along with the number of measurement used for each orbital solution and the mean radial velocity error for each dataset. It is interesting to note that the values for stellar jitter derived from our orbital solutions are often different between the used dataset, the lowest being usually the one found for HARPS datasets; this may suggest that the jitter is likely dominated by instrumental effects for instruments with lower precision than HARPS.

Out of the 20 planetary systems of our sample, 7 did not significantly benefit from the addition of our new, higher-precision HARPS data, resulting in new orbital solution compatible with the ones found in the literature (HD 23127, HD 25171, HD 27631, HD 114729, HD 117207, HD 187085, HD 220689). We however note that for the most part our orbital solutions feature higher precision of the orbital parameters.

Instead, the addition of the HARPS data obtained from our observation brought significant updates in 12 systems of the sample (HD 4208, HD 30177, HD 38801, HD 48265, HD 66428, HD 70642, HD 73267, HD 126525, HD 143361, hd 152079, HD 190647, HD 216437). For the most part these updates consist in values of eccentricity and period incompatible with those found in the literature best-fits solutions; we also want to explicitly stress that our data produced very different orbital parameters for planet HD 30177 c, the addition of orbital parameters missing in the literature fit for HD 126525 and the detection of a linear trend not previously published for HD 73267.

Finally, we report the characterization of outer giant planet HD 50499 c, the existence of which could be previously inferred in the quadratic trend of Keck data but was never fitted and published before.

4.3. Case-by-case results

HD 4208 This G5V star's only planetary companion was first detected by Vogt et al. (2002) via 35 Keck observations spanning about 5 years. Later observations and improvements in data reduction pipelines reported in Butler et al. (2006) have refined the planet's orbital parameters; additional and further refined Keck data have recently been published in Butler et al. (2017), although no further orbital refinement has yet been anounced.

Using all these literature results as historical data next to the 30 high-precision datapoints obtained during our HARPS survey we obtained a new orbital fit (see Table 2 and Fig. 2) with Keplerian semiamplitude K=$19.03^{+0.85}_{-0.79}$ms^{-1} and period P=$832.97^{+2.15}_{-1.89}$d, from which we estimate the minimum mass of HD 4208 b to be Msin i=$0.810^{+0.014}_{-0.015}$M$_J$, its eccentricity as e=$0.042^{+0.039}_{-0.029}$ and a longitude of periastron of ω=$217.634^{+57.556}_{-67.497}$deg.

Table 2. Fit results comparison for system HD 4208

	HD 4208		
	Butler et al. (2006)		This work
Parameter	Planet b		Planet b
K (ms^{-1})	19.06 ± 0.73		$19.03^{+0.85}_{-0.79}$
P (days)	828.0 ± 8.1		$832.97^{+2.15}_{-1.89}$
$\sqrt{e}\cos\omega$	-		$-0.101^{+0.148}_{-0.121}$
$\sqrt{e}\sin\omega$	-		$-0.092^{+0.147}_{-0.123}$
e	0.052 ± 0.040		$0.042^{+0.039}_{-0.029}$
ω (deg)	345		$217.634^{+57.556}_{-67.497}$
Msin i (M$_J$)	0.804 ± 0.073		$0.810^{+0.014}_{-0.015}$
a (AU)	1.650 ± 0.096		$1.662^{+0.015}_{-0.015}$
T$_{peri}$ (d)	2451040 ± 120		$2456505.5^{+127.3}_{-491.3}$
n$_{obs}$	52		82
	mean RV error (ms^{-1})	γ (ms^{-1})	jitter (ms^{-1})
Keck1	1.52	$0.12^{+0.58}_{-0.58}$	$3.26^{+0.55}_{-0.45}$
Keck2	1.44	$-12.39^{+1.99}_{-1.99}$	$6.36^{+1.86}_{-1.30}$
HARPS	0.48	$-17.31^{+0.88}_{-0.86}$	$1.33^{+0.23}_{-0.19}$

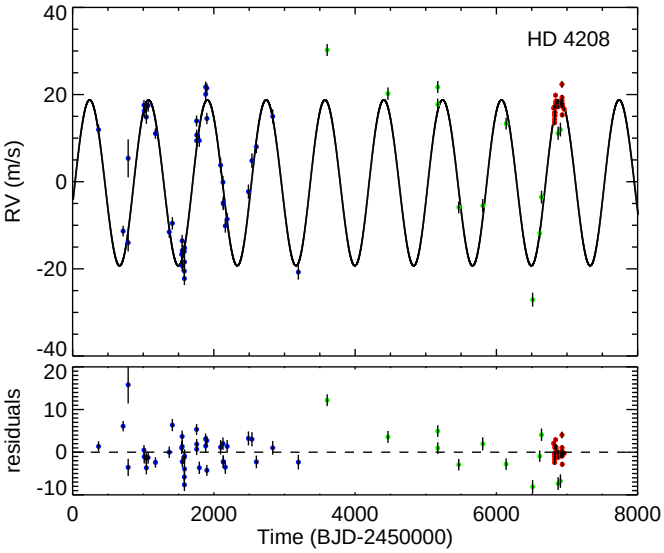

Fig. 2. Analysis results for system HD 4208. In the top panel, our best-fit solution is superimposed as a black curve on the literature datapoints from two Keck surveys (shown in blue and green) and from our HARPS observations (shown in red). The bottom panel shows the residual radial velocities obtained after subtracting pur best-fit solution for HD 4208 b from the original datapoints.

Table 3. Fit results comparison for system HD 23127

HD 23127		
	O'Toole et al. (2007)	This work
Parameter	Planet b	Planet b
K (ms^{-1})	27.5 ± 1	$27.72^{+2.83}_{-2.63}$
P (days)	1214 ± 9	$1211.17^{+11.11}_{-8.91}$
$\sqrt{e}\cos\omega$	-	$-0.613^{+0.088}_{-0.065}$
$\sqrt{e}\sin\omega$	-	$-0.019^{+0.176}_{-0.185}$
e	0.44 ± 0.07	$0.406^{+0.083}_{-0.09}$
ω (deg)	190 ± 6	$181.829^{+17.296}_{-16.507}$
Msin i (M_J)	1.5 ± 0.2	$1.527^{+0.037}_{-0.038}$
a (AU)	2.4 ± 0.3	$2.370^{+0.032}_{-0.032}$
T_{peri} (days)	2450229 ± 19	$2457266.6^{+62.1}_{-43.5}$
n_{obs}	34	58
	mean RV error (ms^{-1})	γ (ms^{-1})	jitter (ms^{-1})
AAT	4.30	$5.55^{+2.32}_{-2.27}$	$11.00^{+2.01}_{-1.60}$
HARPS	0.64	$-1.82^{+4.69}_{-4.53}$	$1.88^{+0.38}_{-0.29}$

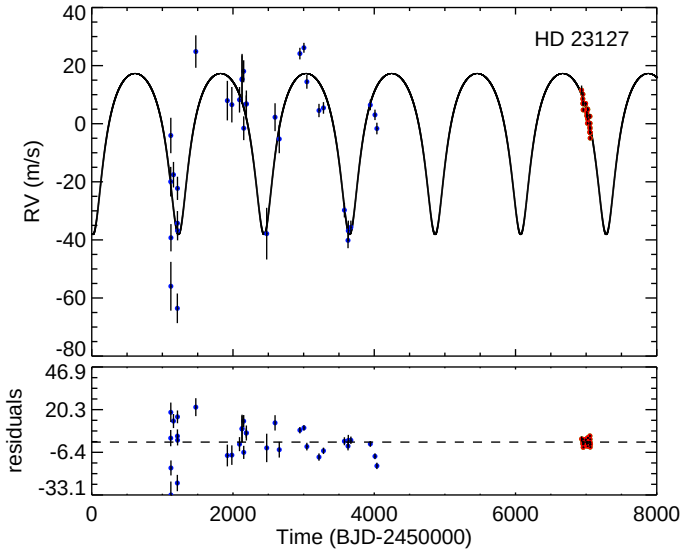

Fig. 3. Same as Fig. 2 but for system HD 23127. The literature AAT data are shown in blue, while our HARPS survey data are shown in red.

Table 4. Fit results comparison for system HD 25171

HD 25171		
	Moutou et al. (2011)	This work
Parameter	Planet b	Planet b
K (ms^{-1})	15.0 ± 3.6	$14.56^{+0.84}_{-0.88}$
P (days)	1845 ± 167	$1802.29^{+24.12}_{-22.92}$
$\sqrt{e}\cos\omega$	-	$-0.006^{+0.175}_{-0.169}$
$\sqrt{e}\sin\omega$	-	$0.028^{+0.159}_{-0.169}$
e	0.08 ± 0.06	$0.042^{+0.046}_{-0.029}$
ω (deg)	96 ± 89	$159.543^{+136.626}_{-104.900}$
Msin i (M_J)	0.95 ± 0.10	$0.915^{+0.011}_{-0.012}$
a (AU)	3.02 ± 0.16	$2.971^{+0.033}_{-0.032}$
T_{peri} (days)	2455301 ± 449	$2457105.7^{+540.5}_{-554.43}$
n_{obs}	24	46
	mean RV error (ms^{-1})	γ (ms^{-1})	jitter (ms^{-1})
HARPS	1.18	$-2.10^{+0.60}_{-0.58}$	$2.40^{+0.39}_{-0.34}$

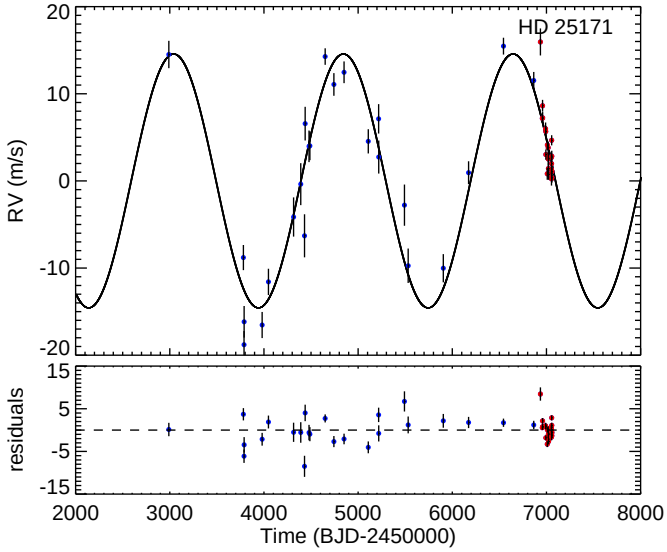

Fig. 4. Same as Fig. 2 but for system HD 25171. The literature HARPS data are shown in blue, while our HARPS survey data are shown in red.

Our results are generally compatible with Butler's, although better constrained; an exception is represented by a very different value of ω. No power peak with FAP≤0.01 was found in the residual data periodogram. Using the Hill criterion we also find the maximum dynamically stable period for an inner planet to be 547.5 days.

HD 23127 A G2V star, its planetary companion has been announced in O'Toole et al. (2007) based on 34 observations collected at the Anglo-Australian Telescope (AAT) over 7.7 yr; no further data nor refinement to the planet's orbital elements have been published since its discovery.

The HARPS observations have produced 25 new datapoint; we excluded a single datapoint taken at epoch 2456989.5 since it showed a radial velocity difference from the observation taken the previous and following nights of ∼30 ms^{-1}, in addition to having an outlier value of bisector; being such a difference difficult to justify as a real radial velocity variation the point was flagged as spurious, probably due to some error occurring during its acquisition, and therefore ignored in the subsequent analysis.

The orbital fit (see Table 3 and Fig. 3) obtained from joining the 34 AAT datapoints with the 24 HARPS observations suggests new orbital elements values of Msin i=$1.527^{+0.037}_{-0.038}$$M_J$, P=$1211.17^{+11.11}_{-8.91}$d and e=$0.406^{+0.083}_{-0.09}$, results compatible to the literature solution. The radial velocity residuals periodogram show no power peak under the 0.01 level of FAP, and we find the maximum stable period for an additional inner planet to be 322.1 days.

HD 25171 This F8V-type star's planet has been discovered and characterized in Moutou et al. (2011) via 24 HARPS observations; 8 additional HARPS datapoints are publicly accessible from the ESO Science Archive. Of these 32 archival HARPS data we excluded a total of 8 datapoints due to SNR lower than 30, namely the data found at epochs 2452946.79, 2452998.59, 2454732.77, 2454813.77, 2455091.89, 2455105.77, 2455261.53 and 2456751.48.

Table 5. Fit results comparison for system HD 27631

HD 27631			
	Marmier et al. (2013)		This work
Parameter	Planet b		Planet b
K (ms^{-1})	23.7 ± 1.9		$24.51^{+1.84}_{-1.82}$
P (days)	2208 ± 66		$2198.14^{+54.11}_{-50.34}$
$\sqrt{e}\cos\omega$	-		$-0.182^{+0.177}_{-0.143}$
$\sqrt{e}\sin\omega$	-		$0.284^{+0.113}_{-0.159}$
e	0.12 ± 0.060		$0.141^{+0.062}_{-0.065}$
ω (deg)	134 ± 44		$122.642^{+33.335}_{-30.158}$
M$\sin i$ (M_J)	1.45 ± 0.14		$1.494^{+0.042}_{-0.042}$
a (AU)	3.25 ± 0.07		$3.242^{+0.070}_{-0.068}$
T_{peri} (days)	2453867 ± 224		$2456086.0^{+193.4}_{-170.8}$
n_{obs}	64		87
	mean RV error (ms^{-1})	γ (ms^{-1})	jitter (ms^{-1})
CORALIE1	5.84	$8.19^{+3.24}_{-3.28}$	$5.29^{+1.97}_{-1.74}$
CORALIE2	3.76	$-3.74^{+1.59}_{-1.68}$	$7.42^{+1.19}_{-1.05}$
HARPS	0.53	$-1.79^{+3.31}_{-3.47}$	$4.24^{+0.79}_{-0.61}$

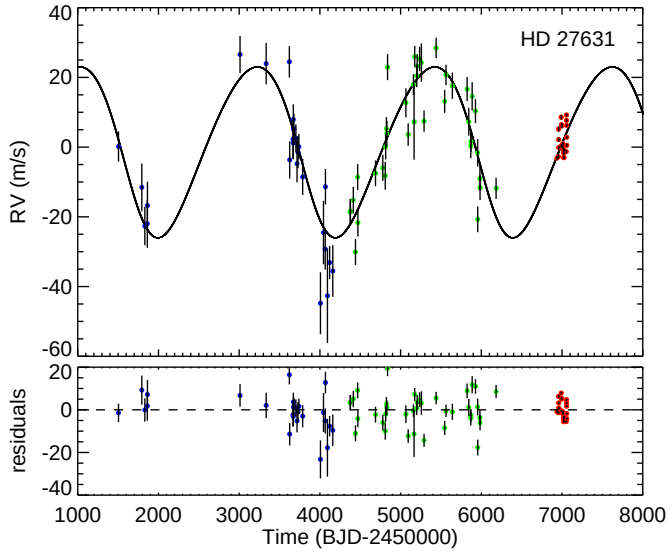

Fig. 5. Same as Fig. 2 but for system HD 27631. The literature CORALIE surveys data are shown in blue and green, while our HARPS survey data are shown in red.

In addition to this literature HARPS data we used our own 22 lower-uncertainties datapoints to obtain a $K=14.56^{+0.85}_{-0.88}$, $P=1802.29^{+24.12}_{-22.92}$d Keplerian fit (see Table 4 and Fig. 4) from which we provide new estimates of minimum mass of $0.915^{+0.012}_{-0.012}M_J$ and eccentricity of $0.0417^{+0.046}_{-0.029}$, in a generally good agreement with the literature fit. No power peak with a sufficiently low false alarm probability is present in the residuals periodogram. The maximum stable period for an inner planet found via the Hill criterion is 1105 days.

HD 27631 The planet orbiting this G3IV star was first discovered by Marmier et al. (2013) using a total of 64 CORALIE measurements, the last 37 of which were obtained after an upgrade of the instrument and are therefore treated as a separate dataset with its own radial velocity offset.

During our HARPS observations we have obtained 23 further datapoints; the joined time series was then used to produce a Keplerian fit having semiamplitude $K=24.51^{+1.84}_{-1.82}ms^{-1}$ and period $P=2198.14^{+54.11}_{-50.34}$d, providing a new estimate of M$\sim i$=$1.494^{+0.042}_{-0.042}M_J$ and eccentricity $e=0.141^{+0.062}_{-0.065}$, an overall solution compatible yet better constrained than the literature fit (see Table 5 and Fig. 5). We also find the maximum stable period for an additional inner planet to be 1107 days.

The generalized Lomb-Scargle periodogram produced from the residual data features no major peak with FAP≤0.01.

HD 30177 The planetary system orbiting this G8V star is a well-studied one and therefore deserves special attention. The first study to detect a planet around the star (Tinney et al. 2003) used fifteen AAT observations and failed to observe the planet's entire orbit, leading to noticeably poor constrained values of $e=0.22 \pm 0.17$ and M$\sin i=7.7 \pm 1.5M_J$. A follow-up study (Butler et al. 2006) refines these values leading to estimates of $e=0.193 \pm 0.025$ and a minimum mass of $10.45 \pm 0.88M_J$. Most recently, Wittenmyer et al. (2017) reports an orbital fit made from 28 additional AAT data and 20 HARPS-TERRA measurements, leading to the latest values of M$\sin i=8.08 \pm 0.10M_J$, $P=2524.4 \pm 9.8$d, $e=0.184 \pm 0.012$; of particular interest is the fact that the authors best-fit solution feature an additional, outer planetary companion HD 30177 c, estimating a minimum mass of $7.60 \pm 3.10M_J$, a period of 11613 ± 1837 days and an eccentricity value of 0.22 ± 0.14.

As already noted and discussed in Sect. 2, the existence of planet c was not known during our targets selection and subsequent HARPS observations, hence the inclusion of this system in an otherwise single-planet sample. We however decided to still include HD 30177 in this paper, since we consider the published outer companion's long period of 31.82 yr not to have a significant dynamical influence in the stability of the short-period (a<1 AU) region of interest in searching for inner, low-mass companions. We therefore report here the result of the fit obtained joining the literature data to the additional 26 HARPS measurements collected in our observations, noting that we excluded from the following analysis four datapoints taken at epochs 2454384.87, 2455563.54, 2455564.57 and 2456631.80 due to low signal-to-noise ratio.

It can be noted that the dataset used in Wittenmyer et al. (2017) fails to cover a significant portion of the orbit of HD 30177 c, covering a total timescale of about only 5840 days out of the 31.7 years proposed orbital period; a fact clearly reflected in the poorly constrained orbital parameters for this proposed outer planet. Moreover, all the MCMC chains we launched in searching for a two-planet solution failed to achieve a satisfactory convergence and parameters resolutions, the acceptance rate never rising above 0.4% and producing exceptionally poorly constrained estimates for the outer companion's orbital parameters, such as a period of $11084.29^{+1235.54}_{-1059.33}$ days and a semiamplitude of $32.71^{+83.55}_{-26.48}$ ms^{-1}.

We interpret the poor parameter constrains in Wittenmyer et al. (2017) and our repeated failure to achieve a satisfactory convergence as evidence that the most recent literature two-planet fit does not constitute a correct interpretation of the available data, while an orbital solution featuring the outer planet as a quadratic trend added to the Keplerian signal of the inner planet may be a better fit to the joined dataset, allowing a further refinement of the orbital parameters for HD 30177 b but only lower limits on the outer planet's semiamplitude, mass and period.

Table 6. Fit results comparison for system HD 30177

	HD 30177			
	Wittenmyer et al. (2017)	This work	Wittenmyer et al. (2017)	This work
Parameter	Planet b	Planet b	Planet c	Planet c
K (ms^{-1})	126.3 ± 1.5	$125.98^{+1.26}_{-1.27}$	70.8 ± 29.5	≥ 16.42
P (days)	2524.4 ± 9.8	$2527.83^{+4.71}_{-4.69}$	11613 ± 1837	≥ 6163.40
$\sqrt{e}\cos\omega$	-	$0.340^{+0.014}_{-0.014}$	-	-
$\sqrt{e}\sin\omega$	-	$0.216^{+0.015}_{-0.016}$	-	-
e	0.184 ± 0.012	$0.162^{+0.010}_{-0.010}$	0.22 ± 0.14	-
ω (deg)	31 ± 3	$32.422^{+2.525}_{-2.563}$	19 ± 30	-
Msin i (M_J)	8.08 ± 0.10	$8.622^{+0.125}_{-0.126}$	7.6 ± 3.1	≥ 1.533
a (AU)	3.58 ± 0.01	$3.704^{+0.027}_{-0.027}$	9.89 ± 1.04	-
T_{peri} (days)	2451434 ± 29	$2456502.4^{+17.9}_{-18.4}$	2448973 ± 1211	-
n_{obs}	63	85		
	mean RV error (ms^{-1})	γ (ms^{-1})	jitter (ms^{-1})	
AAT	3.84	$22.16^{+1.69}_{-1.73}$	$7.43^{+1.38}_{-1.17}$	
HARPS	0.79	$-6.66^{+1.20}_{-1.18}$	$2.19^{+0.39}_{-0.34}$	

Following the example set by Kipping et al. (2011) we therefore fitted the radial velocity data for a single Keplerian orbit plus a quadratic term, so that the overall RV model is expressed as:

$$RV = V_\gamma - K \sin\frac{2\pi(t - t_{peri})}{P} + k_2(t - t_{pivot}) + \frac{1}{2}k_3(t - t_{pivot})^2$$

being t_{pivot} the mean time stamp and k_2, k_3 respectively the linear and quadratic coefficients. From this model we can infer some estimate on minimum mass and period for the outer planet using the relationships:

$$\frac{-k_2 + k_3 t_{pivot}}{k_3} = t_{peri} + \frac{P}{4} \quad ; \quad \frac{k_3}{4\pi^2} = \frac{K}{P^2}$$

Our best-fit curve (see Table 6 and Fig. 6) returns for planet b values for semiamplitude $125.98^{+1.26}_{-1.27} ms^{-1}$,minimum mass of $8.622^{+0.125}_{-0.126}$ M_J, period $2527.83^{+4.71}_{-4.69}$ d and eccentricity $0.162^{+0.010}_{-0.010}$; we find quadratic trend coefficients of k_2=$(-6.7 \pm 0.5) \cdot 10^{-3} ms^{-1} d^{-1}$ and k_2=$(1.20 \pm 0.05) \cdot 10^{-5} ms^{-1} d^{-1}$. Again following Kipping et al. (2011), to determine the lower limits for the outer planet's semiamplitude, mass and period we force a circular orbit, selecting as minimum value of P the one causing a $\delta\chi^2 = 1$ relative to the quadratic fit, and then using this period value for computing a minimum value of K and then minimum mass. The limits thus obtained for the outer planet are P$\geq$ 6163.40d, K$\geq$ 16.42 ms^{-1} and Msin $i \geq$ 1.533 M_J; further datapoints and a greater observation coverage are clearly necessary to better characterize this outer companion.

The most significant peak apparent in the residual data periodogram is located at 771.0 days and has a false alarm probability of 0.1, above our threshold of 1%. The maximum orbital period allowing dynamical stability for an additional inner planet obtained from Hill's criterion is 854.5 days.

HD 38801 This G8IV star is host to a noticeable case of low-eccentricity super-massive planet discovered by Harakawa et al. (2010), deserving a short literature retrospective. Basing its detection on 21 Subaru and Keck joint observations, the authors reported the results of a Keplerian fit with semiamplitude

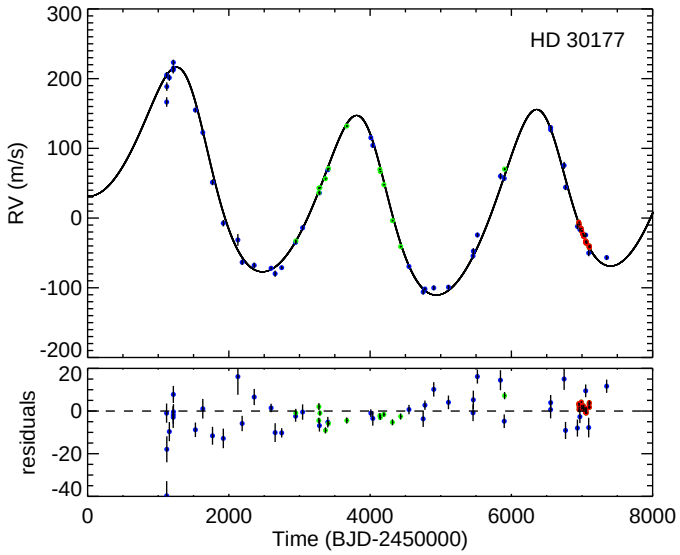

Fig. 6. Same as Fig. 2 but for system HD 30177. The literature AAT data are shown in blue and the literature HARPS data are shown in green; our HARPS survey data are instead shown in red.

$200.0 \pm 3.9 ms^{-1}$ and period of 696.3 ± 2.7 days, obtaining a minimum mass of $10.7 \pm 0.5 M_J$ and an extraordinary low eccentricity, set to zero after its first estimate of 0.04 led to poorly constrained value of ω, also set to zero to improve the fit. HD 38801 b's low eccentricity, the authors note, is of special interest since it cannot be explained by tidal interaction with its host star since the latter's radius of 2.5 $R_\odot$ is too small to effectively circularize the planet's intermediate orbit.

The addition of 16 Keck measurments published in Butler et al. (2017) and of our own 21 HARPS measurements allow us to produce a new best-fit solution (see Table 7 and Fig. 7) with semiamplitude $197.29^{+3.52}_{-3.43} ms^{-1}$ and period $685.25^{+0.85}_{-0.85}$d, obtaining a minimum mass value of $9.698^{+0.573}_{-0.587} M_J$ and still poorly constrained values for e=$0.017^{+0.013}_{-0.011}$ and ω=$97.115^{+238.614}_{-71.900}$deg that will surely benefit from further high-precision and high-sampling observations. We find the dynami-

Table 7. Fit results comparison for system HD 38801

HD 38801		
	Harakawa et al. (2010)	This work
Parameter	Planet b	Planet b
K (ms^{-1})	200.0 ± 3.9	$197.29^{+3.52}_{-3.43}$
P (days)	696.3 ± 2.7	$685.25^{+0.85}_{-0.85}$
$\sqrt{e}\cos\omega$	-	$0.089^{+0.058}_{-0.086}$
$\sqrt{e}\sin\omega$	-	$0.021^{+0.087}_{-0.093}$
e	0.0	$0.017^{+0.013}_{-0.011}$
ω (deg)	0.0	$97.115^{+238.614}_{-71.900}$
Msin i (M_J)	10.7 ± 0.5	$9.698^{+0.573}_{-0.587}$
a (AU)	1.7 ± 0.037	$1.623^{+0.047}_{-0.049}$
T_{peri} (days)	2453966.0 ± 2.1	$2456752.9^{+126.5}_{-102.1}$
n_{obs}	37	58
	mean RV error (ms^{-1})	γ (ms^{-1})	jitter (ms^{-1})
Subaru	2.70	$1.44^{+2.96}_{-2.89}$	$10.81^{+2.20}_{-1.71}$
Keck	0.50	$-20.85^{+2.87}_{-2.95}$	$10.93^{+2.76}_{-1.98}$
HARPS	0.45	$175.71^{+4.63}_{-4.77}$	$10.13^{+2.05}_{-1.58}$

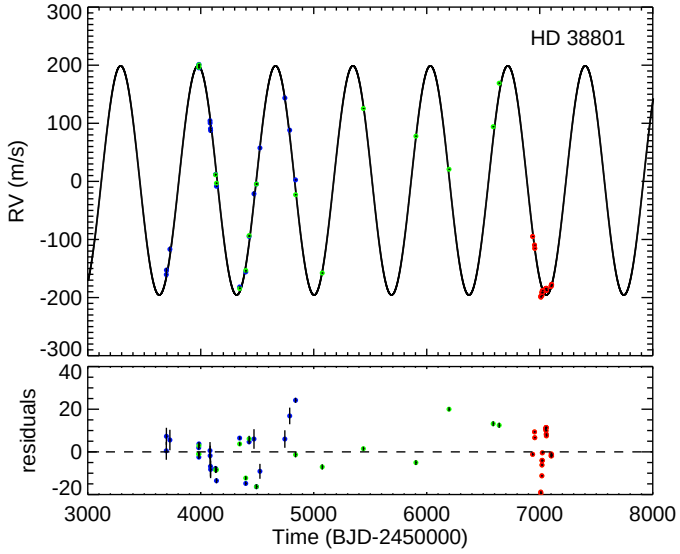

Fig. 7. Same as Fig. 2 but for system HD 38801. The literature Subaru data are shown in blue, literature Keck data is in green, while our HARPS survey data are shown in red.

Table 8. Fit results comparison for system HD 48265

HD 48265		
	Jenkins et al. (2017)	This work
Parameter	Planet b	Planet b
K (ms^{-1})	27.7 ± 1.2	$28.65^{+1.59}_{-1.57}$
P (days)	780.3 ± 4.6	$778.51^{+5.38}_{-5.18}$
$\sqrt{e}\cos\omega$	-	$0.298^{+0.104}_{-0.123}$
$\sqrt{e}\sin\omega$	-	$-0.319^{+0.224}_{-0.123}$
e	0.080 ± 0.050	$0.211^{+0.089}_{-0.096}$
ω (deg)	343.78 ± 137.51	$308.313^{+21.261}_{-23.111}$
Msin i (M_J)	1.47 ± 0.12	$1.525^{+0.049}_{-0.050}$
a (AU)	1.81 ± 0.07	$1.814^{+0.030}_{-0.031}$
T_{peri} (days)	2452892 ± 100	$2456036.7^{+67.7}_{-36.5}$
n_{obs}	60	20
	mean RV error (ms^{-1})	γ (ms^{-1})	jitter (ms^{-1})
MIKE	3.22	$-5.81^{+2.29}_{-2.08}$	$3.38^{+1.89}_{-1.53}$
HARPS	0.54	$-6.37^{+2.68}_{-2.72}$	$3.38^{+1.89}_{-1.53}$
CORALIE	9.40	$-1.23^{+4.45}_{-4.49}$	$15.98^{+3.96}_{-3.21}$

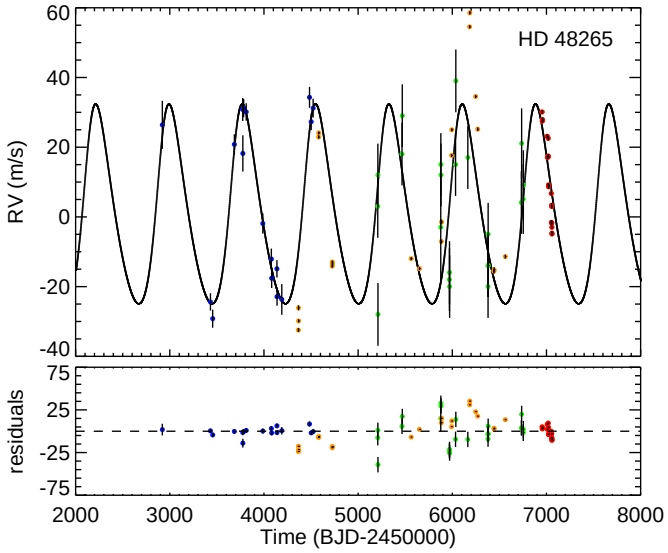

Fig. 8. Same as Fig. 2 but for system HD 48265. The literature MIKE data are shown in blue, the literature HARPS data in orange and literature CORALIE datapoints is in green, while our HARPS survey data are shown in red.

cal stability limit period for additional inner planets to be 322.1 days.

A power peak characterized by a very low FAP of 0.01% is present in the residual radial velocity periodogram around 79 days; as shown in Fig. 24 this peak has however a high correlation with similar peaks in the stellar activity indexes, excluding any planetary origin for this signal.

HD 48265 This G5IV star hosts a planet first characterized in Minniti et al. (2009) via the analysis of 17 observations obtained over 4.4 years with the MIKE echelle spectrograph, and later refined using new HARPS and CORALIE data in Jenkins et al. (2009, 2017).

Our 20 new HARPS observations, when joined with the literature data, lead to a fit characterized by semiamplitude K=$28.65^{+1.59}_{-1.57}$$ms^{-1}$ and period P=$778.51^{+5.38}_{-5.18}$d. From this fit (see Table 8 and Fig. 8) we obtain orbital elements Msin i=$1.525^{+0.049}_{-0.050}$ and e=$0.211^{+0.089}_{-0.096}$. Although most of these fit parameters are reasonably consistent with those found by Jenkins et al. (2017), we note that our estimate of eccentricity is only marginally compatible with the one obtained in the published works. The maximum inner period allowing dynamical stability for additional inner planets is found with Hill's criterion to be 294.7 days.

A power peak with FAP=0.05% is found at 21 days in the residual radial velocity data periodogram, the only stellar activity-related peak at this period being present in the bisector periodogram (see Fig. 25). We therefore tried to find a two-planet solutions for the system, using this residual period and a zero value for eccentricy for the additional planet's initial setting, but found no satisfactory convergence, suggesting that this residual power should be regarded as having stellar origins.

Table 9. Fit results comparison for system HD 50499

HD 50499			
	Vogt et al. (2005)	This work	
Parameter	Planet b	Planet b	Planet c
K (ms^{-1})	22.9 ± 3	$21.99^{+1.08}_{-1.02}$	≥ 8.15
P (days)	2482.7 ± 110	$2447.10^{+21.92}_{-21.72}$	≥ 8256.51
$\sqrt{e}\cos\omega$	-	$0.161^{+0.084}_{-0.089}$	-
$\sqrt{e}\sin\omega$	-	$-0.483^{+0.046}_{-0.041}$	-
e	0.23 ± 0.14	$0.266^{+0.044}_{-0.044}$	-
ω (deg)	262 ± 36	$288.31^{+9.579}_{-10.094}$	-
Msin i (M_J)	1.71 ± 0.2	$1.636^{+0.017}_{-0.017}$	≥ 0.942
a (AU)	3.86 ± 0.6	$3.833^{+0.0305}_{-0.030}$	-
T_{peri} (days)	2451234.6 ± 225	$2456291.1^{+58.7}_{-57.6}$	-
n_{obs}	86	24	
	mean RV error (ms^{-1})	γ (ms^{-1})	jitter (ms^{-1})
Keck	1.71	$2.33^{+1.05}_{-1.07}$	$5.08^{+0.47}_{-0.42}$
HARPS	0.49	$-18.45^{+3.57}_{-3.55}$	$2.15^{+0.39}_{-0.31}$

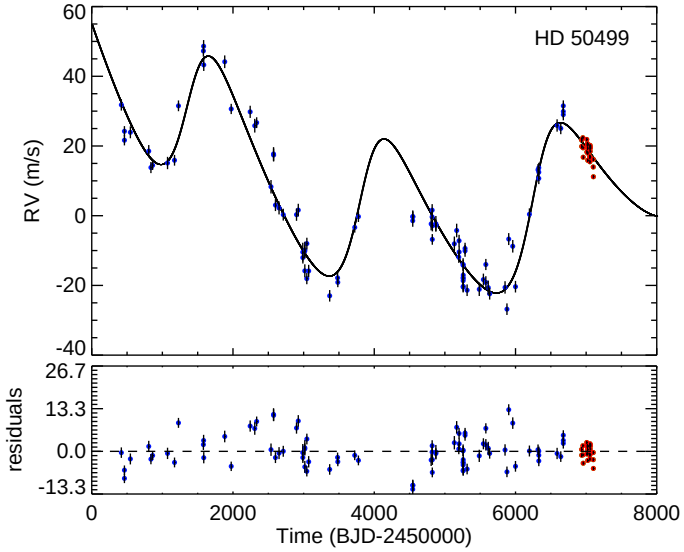

Fig. 9. Same as Fig. 2 but for system HD 50499. The literature Keck data are shown in blue, while our HARPS survey data are shown in red.

HD 50499 The existence of a planet orbiting this G2V star was first reported by Vogt et al. (2005) based on 35 HIRES observations; in the discovery paper a linear trend of -4.8 $ms^{-1}yr^{-1}$ was also noted, suggesting the presence of an outer companion estimated to be located beyond 4 AU and having a minimum mass of at least 2 M_J. The nature of this additional companion was not completely determined, and although an outer star or brown dwarf were dismissed due to system stability considerations, the proposed two-planet solution was not significantly superior to a model consisting of one planet and a linear trend.

However, the recent publication by Butler et al. (2017) of 50 new Keck measurements taken over 8 years for HD 50499 shows this outer trend to be parabolic; Butler's work also provides a new reduction of Vogt's datapoints, forming the complete Keck dataset we joined with the 24 HARPS data collected during our observation to refine the orbital solution for HD 50499 b and provide lower limits on the outer planet's mass and period. Following again the example set by Kipping et al. (2011) we fit the radial velocity data for a single Keplerian orbit plus a quadratic term, obtaining a best-fit curve (see Table 9 and Fig. 9) returning for planet b values for semiamplitude $21.99^{+1.08}_{-1.02} ms^{-1}$, minimum mass of $1.636^{+0.017}_{-0.017} M_J$, period $2447.10^{+21.92}_{-21.72}$d and eccentricity $0.266^{+0.044}_{-0.044}$, in addition to quadratic coefficients $k_2=(-5.6 \pm 0.3) \cdot 10^{-3} ms^{-1}d^{-1}$ and $k_2=(4.6 \pm 0.4) \cdot 10^{-5} ms^{-1}d^{-1}$.

We finally derive lower limits for the outer planet orbital parameters as P$\geq$ 8256.51 d, K$\geq$ 8.15 ms^{-1} and Msin $i \geq$ 0.942 M_J; we additionally note that Kóspál et al. (2009) detects an excess in the star's emission at 70 μm, suggesting the presence of a debris disk at distances larger than 4-5 AU that can provide further constraints on the outer planet's orbital elements; from the outer planet's orbital limits it is possible estimate its major semiaxis as lying beyond $\simeq$8.6 AU and therefore could be placed outside the debris disk. Finally, we find using Hill's criterion the maximum dynamically stable inner period for any additional inner companion to be 959.5 days.

The highest power peak in the residual periodogram's is found at about 13 days and has a FAP level of 4%, above our threshold of 1%.

HD 66428 This G8IV star was first discovered to host a planet in Butler et al. (2006) using 22 Keck observations and its orbital elements were later refined in Feng et al. (2015) using 33 datapoints obtained after the upgrade of HIRES, also reporting a linear trend of $-3.4 \pm 0.2 ms^{-1}yr^{-1}$ suggesting the presence of an outer companion.

Combining the improved data reduction published in Butler et al. (2017), 10 HARPS measurements from two different observation periods publicly available on the ESO archive and our own 18 HARPS datapoints we found a best-fit solution for HD 66428 b (see Table 10 and Fig. 10) with Msin i=$3.204^{+0.043}_{-0.044} M_J$, P=$2263.12^{+6.13}_{-5.94}$d and e=$0.493^{+0.015}_{-0.015}$, with a linear trend value of $-2.58^{+0.11}_{-0.12} ms^{-1}yr^{-1}$. Regarding the system's linear trend and the possible presence of further bodies in the system, we note that Moutou et al. (2017) reports that no additional outer companion above 0.1 $M_\odot$ has been found in the 0.05 to 50 AU range during a VLT/SPHERE high-angular resolution survey, and therefore the yet undetected source of the slope in the data must be a substellar companion. Following the example set by Feng et al. (2015), we can provide an estimate of the minimum mass required of the companion to produce the detected linear slope $\dot{\gamma}$ over the span of observation τ using the equation:

$$M_{min} \approx (0.0164\ M_J)\left(\frac{\tau}{yr}\right)^{4/3}\left|\frac{\dot{\gamma}}{ms^{-1}yr^{-1}}\right|\left(\frac{M_*}{M_\odot}\right)^{2/3} \quad (1)$$

from which we obtain that the outer companion should have a minimum mass of 1.54 M_J, a value not dissimilar from the 1.77 M_J value suggested in the same paper. The maximum period allowing dynamical stability for an additional inner planet is found to be 374.6 days.

No peak with false alarm probability below 0.01 was found in the residual data periodogram.

HD 70642 A G5V star, its known planet was discovered by Carter et al. (2003) using 21 AAT measurements obtained over 5 years of observations; a more tightly constrained orbital solution was later found in Butler et al. (2006).

In addition to 8 archival HARPS datapoints, the acquisition of our 21 high-precision HARPS measurements however lead us to a different orbital solution. We find the best-fit

Table 10. Fit results comparison for system HD 66428

HD 66428		
	Feng et al. (2015)	This work
Parameter	Planet b	Planet b
K (ms^{-1})	52.6 ± 1.1	$54.03^{+1.46}_{-1.43}$
P (days)	2293.9 ± 6.4	$2263.12^{+6.13}_{-5.94}$
$\sqrt{e}\cos\omega$	-	$-0.696^{+0.010}_{-0.010}$
$\sqrt{e}\sin\omega$	-	$-0.086^{+0.025}_{-0.023}$
e	0.440 ± 0.013	$0.493^{+0.015}_{-0.015}$
ω (deg)	180.4 ± 2.6	$187.03^{+1.926}_{-2.07}$
Msin i (M_J)	3.194 ± 0.060	$3.204^{+0.043}_{-0.043}$
a (AU)	3.471 ± 0.069	$3.467^{+0.024}_{-0.024}$
T_{peri} (days)	2452278 ± 16	$2456857.2^{+7.3}_{-7.4}$
slope ($ms^{-1}yr^{-1}$)	−3.4 ± 0.2	$-2.58^{+0.12}_{-0.12}$
n_{obs}	55	83
	mean RV error (ms^{-1})	γ (ms^{-1})	jitter (ms^{-1})
Keck	1.40	$-15.18^{+0.64}_{-0.64}$	$4.00^{+0.55}_{-0.47}$
HARPS	0.68	$18.83^{+1.10}_{-1.01}$	$2.21^{+0.45}_{-0.39}$

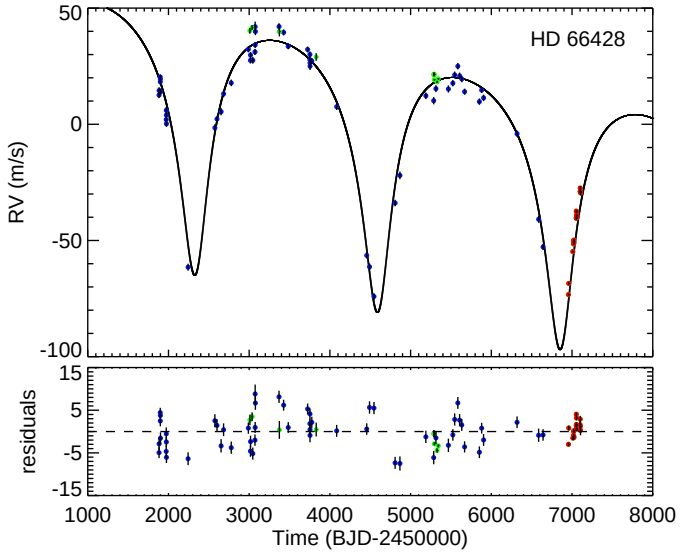

Fig. 10. Same as Fig. 2 but for system HD 66428. The literature Keck data are shown in blue and the literature HARPS observations are shown in green, while our HARPS survey data are shown in red.

curve (see Table 11 and Fig. 11) to be a Keplerian with semi-aplitude K=$30.40^{+1.83}_{-1.91}$$ms^{-1}$ and period P=$2124.54^{+14.65}_{-13.51}$d; from this we characterize HD 70642 b as having minimum mass Msin i=$1.99^{+0.018}_{-0.018}$$M_J$, eccentricity e=$0.175^{+0.045}_{-0.044}$ and periastron longitude ω=$272.840^{+15.584}_{-14.002}$deg; the differences in our fit are especially evident in the values of P and ω, and we also note that our solution features a poorly constrained value for the time of periastron T_{peri}=$2456159.1^{+1912.3}_{-131.9}$d. The maximum period ensuring dynamical stability for an additional inner planet is estimated via Hill's criterion to be 1232.9 days.

No residual velocity periodogram peak with a FAP lower than 1% is found.

HD 73267 The planet hosted by this G5V star was discovered using 39 HARPS observations as detailed in Moutou et al.

Table 11. Fit results comparison for system HD 70642

HD 70642		
	Butler et al. (2006)	This work
Parameter	Planet b	Planet b
K (ms^{-1})	30.4 ± 1.3	$30.40^{+1.83}_{-1.91}$
P (days)	2068 ± 39	$2124.54^{+14.65}_{-13.51}$
$\sqrt{e}\cos\omega$	-	$0.020^{+0.108}_{-0.102}$
$\sqrt{e}\sin\omega$	-	$-0.405^{+0.059}_{-0.054}$
e	0.034 ± 0.043	$0.175^{+0.044}_{-0.044}$
ω (deg)	205	$272.840^{+15.584}_{-14.002}$
Msin i (M_J)	1.97 ± 0.18	$1.993^{+0.018}_{-0.018}$
a (AU)	3.23 ± 0.19	$3.318^{+0.022}_{-0.021}$
T_{peri} (days)	2451350 ± 380	$2456159.1^{+1912.3}_{-131.9}$
n_{obs}	21	50
	mean RV error (ms^{-1})	γ (ms^{-1})	jitter (ms^{-1})
AAT	0.75	$-6.71^{+1.22}_{-1.25}$	$3.99^{+1.46}_{-1.26}$
HARPS	0.38	$5.00^{+2.08}_{-2.25}$	$2.24^{+0.38}_{-0.31}$

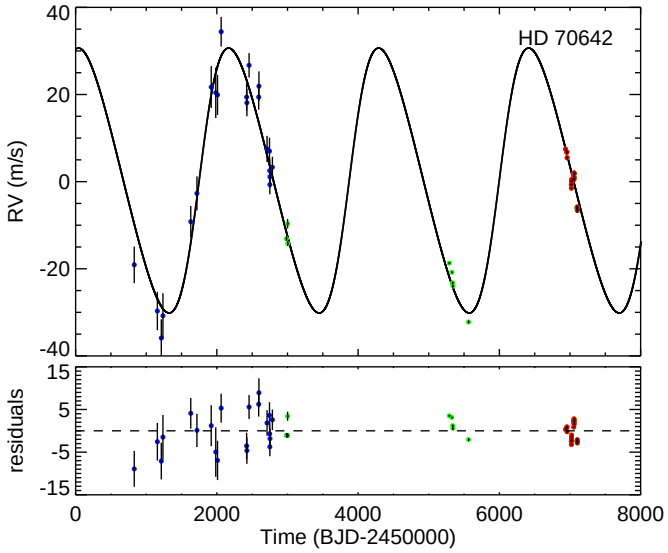

Fig. 11. Same as Fig. 2 but for system HD 70642. The literature AAT data are shown in blue, the literature HARPS data are shown in green while our HARPS survey data are shown in red.

(2009); 10 additional archival HARPS data can also be found on the ESO archive. We exclude from the following analysis five literature datapoints taken on epochs 2453781.72, 2454121.74, 2454232.56, 2454257.49 and 2455563.60 for having low SNR.

After joining this literature data with our 17 new HARPS datapoints we found the best-fit curve (see Table 12 and Fig. 12) to have a semiamplitude value of $64.65^{+0.86}_{-0.87}$$ms^{-1}$ and period $1245.36^{+2.81}_{-2.81}$d, from wich values of mass $3.097^{+0.044}_{-0.043}$$M_J$ and eccentricity $0.230^{+0.014}_{-0.014}$ can be inferred, in good agreement with the literature orbital elements. We also find a previously undetected linear trend of $2.14^{+0.20}_{-0.19}$$ms^{-1}yr^{-1}$, from which using Eq. 1 we derive a minimum mass of 0.83M_J for the outer companion. A solution without linear trend was also tested, returning a Bayesian Information Criterion value of 325.25, higher the the BIC value of 258.15 returned by the fit featuring a slope, which is therefore preferred. The dynamical stability limit for inner planets is found with Hill's criterion to be 416.5 days.

Table 12. Fit results comparison for system HD 73267

HD 73267		
	Moutou et al. (2009)	This work
Parameter	Planet b	Planet b
K (ms^{-1})	64.29 ± 0.48	$64.65^{+0.86}_{-0.87}$
P (days)	1260 ± 7	$1245.36^{+2.81}_{-2.81}$
$\sqrt{e}\cos\omega$	-	$-0.296^{+0.023}_{-0.022}$
$\sqrt{e}\sin\omega$	-	$-0.376^{+0.021}_{-0.020}$
e	0.256 ± 0.009	$0.230^{+0.014}_{-0.014}$
ω (deg)	229.1 ± 1.8	$231.799^{+3.136}_{-3.286}$
Msin i (M_J)	3.06 ± 0.07	$3.097^{+0.044}_{-0.043}$
a (AU)	2.198 ± 0.025	$2.187^{+0.016}_{-0.016}$
T_{peri} (days)	2451821.7 ± 16	$2456842.7^{+11.4}_{-12.0}$
slope ($ms^{-1}yr^{-1}$)	-	$2.14^{+0.21}_{-0.19}$
n_{obs}	39	63
	mean RV error (ms^{-1})	γ (ms^{-1})	jitter (ms^{-1})
HARPS	1.05	$-9.12^{+0.71}_{-0.71}$	$3.70^{+0.43}_{-0.35}$

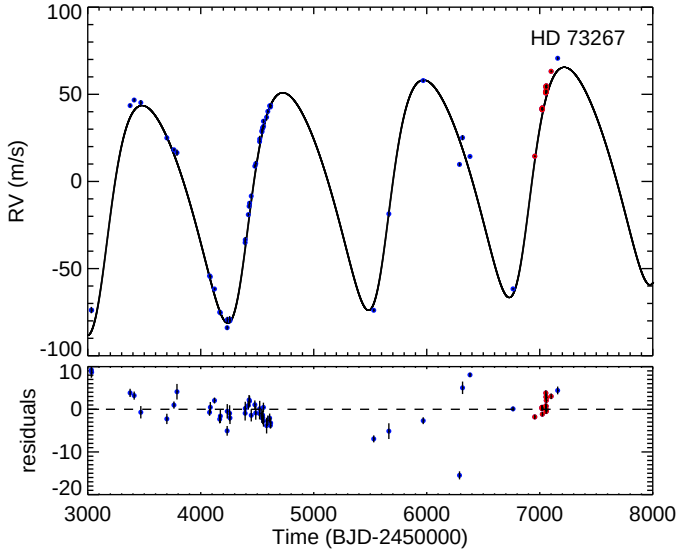

Fig. 12. Same as Fig. 2 but for system HD 73267. The literature HARPS datapoints are shown in blue while our HARPS survey data are shown in red.

Table 13. Fit results comparison for system HD 114729

HD 114729		
	Butler et al. (2006)	This work
Parameter	Planet b	Planet b
K (ms^{-1})	18.8 ± 1.3	$16.91^{+0.53}_{-0.52}$
P (days)	1114 ± 15	$1121.79^{+3.53}_{-3.43}$
$\sqrt{e}\cos\omega$	-	$0.061^{+0.112}_{-0.124}$
$\sqrt{e}\sin\omega$	-	$0.251^{+0.058}_{-0.086}$
e	0.167 ± 0.055	$0.079^{+0.029}_{-0.032}$
ω (deg)	93 ± 30	$77.059^{+27.681}_{-27.685}$
Msin i (M_J)	0.95 ± 0.10	$0.825^{+0.007}_{-0.007}$
a (AU)	2.11 ± 0.12	$2.067^{+0.010}_{-0.010}$
T_{peri} (days)	2450520 ± 67	$2454947.7^{+82.4}_{-82.8}$
n_{obs}	52	109
	mean RV error (ms^{-1})	γ (ms^{-1})	jitter (ms^{-1})
Keck	1.14	$1.46^{+0.64}_{-0.63}$	$3.93^{+0.50}_{-0.44}$
HARPS	0.22	$-6.11^{+0.41}_{-0.42}$	$2.00^{+0.22}_{-0.19}$

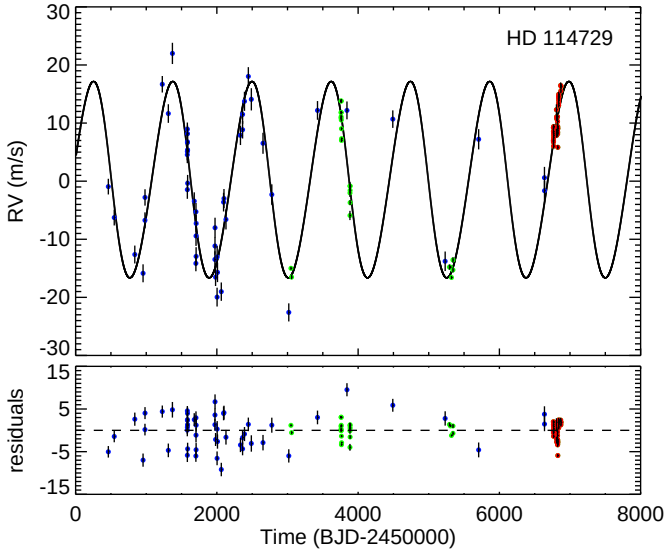

Fig. 13. Same as Fig. 2 but for system HD 114729. The literature Keck data are shown in blue, the literature HARPS data in green, while our HARPS survey data are shown in red.

The residual radial velocity periodogram features no peak with a false alarm probability low enough to justify a MCMC search for additional planetary bodies.

HD 114729 This G0V star's planetary companion orbital elements were first announced and then refined by Butler et al. (2003, 2006), both results being obtained using Keck data.

Using both the 34 HARPS data collected during our observations and the improvement in Keck data reduction provided in Butler et al. (2017) in addition to 23 archival HARPS datapoint from the ESO Archive we obtained a similar yet better constrained orbital fit (see Table 13 and Fig. 13), producing semiamplitude $16.91^{+0.53}_{-0.52}ms^{-1}$, period of $1121.79^{+3.53}_{-3.43}$ days, minimum mass $0.825^{+0.007}_{-0.007}M_J$ and a lower eccentricity of $0.0797^{+0.029}_{-0.032}$. Hill's criterion gives us a maximum period of 697.5 days for dynamical stability of inner planets.

A major residual periodogram peak at 25 days has a low FAP level of 0.4%; this periodogram peak is however matched by peaks at a similar period in the FWHM and Ca II periodograms (see Fig. 26), suggesting a stellar origin for this power peak.

HD 117207 A G8IV star, its planet was first announced in Marcy et al. (2005) and the orbital solution was later refined by Butler et al. (2006). This literature data were later refined and newly reduced in Butler et al. (2017).

We study the timeseries resulting in joining this newly reduced Keck data, 44 archival HARPS measurements, our own 33 HARPS datapoints and 12 further archival HARPS measurements taken after the May 2015 fiber-link update and that are here therefore treated as a independent dataset. We obtain a a significantly better constrained orbital solution (see Table 14 and Fig. 14), with minimum mass $1.926^{+0.034}_{-0.034}M_J$, period of $2621.75^{+8.37}_{-8.53}$d, eccentricity $0.157^{+0.013}_{-0.013}$ as well as periastron lon-

Table 14. Fit results comparison for system HD 117207

HD 117207		
Parameter	Butler et al. (2006) Planet b	This work Planet b
K (ms^{-1})	26.6 ± 0.93	$27.78^{+0.33}_{-0.33}$
P (days)	2597 ± 41	$2621.75^{+8.37}_{-8.53}$
$\sqrt{e}\cos\omega$	-	$-0.001^{+0.038}_{-0.037}$
$\sqrt{e}\sin\omega$	-	$0.394^{+0.016}_{-0.017}$
e	0.144 ± 0.035	$0.157^{+0.013}_{-0.013}$
ω (deg)	73 ± 16	$90.217^{+5.275}_{-5.523}$
Msin i (M_J)	1.88 ± 0.17	$1.926^{+0.034}_{-0.034}$
a (AU)	3.79 ± 0.22	$3.787^{+0.034}_{-0.035}$
T_{peri} (days)	2450630 ± 120	$2455978.9^{+35.7}_{-37.8}$
n_{obs}	51	140
	mean RV error (ms^{-1})	γ (ms^{-1})	jitter (ms^{-1})
Keck	1.54	$-10.58^{+0.52}_{-0.53}$	$3.44^{+0.47}_{-0.40}$
HARPS1	0.35	$4.65^{+0.29}_{-0.29}$	$1.71^{+0.16}_{-0.14}$
HARPS2	0.42	$21.38^{+0.85}_{-0.84}$	$1.88^{+0.55}_{-0.38}$

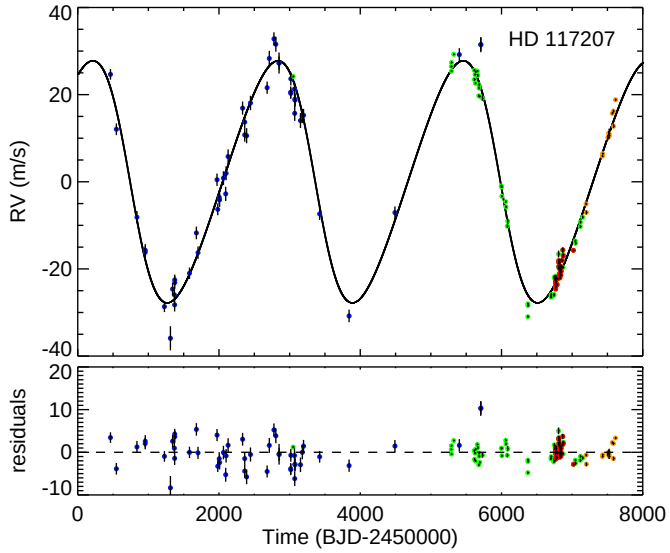

Fig. 14. Same as Fig. 2 but for system HD 117207. The literature Keck data are shown in blue, past HARPS data in green, our HARPS survey data are shown in red while literature HARPS data taken after the fiber-link update of May 2015 are in orange.

gitude of $90.217^{+5.275}_{-5.523}$deg. The maximum period allowing dynamical stability for an inner planet is found with Hill's criterion to be 1263.5 days.

No power peak with FAP$\leq$ 0.01 is found in the residual data periodogram.

HD 126525 This G4V star has been target to various HARPS observational surveys, and Mayor et al. (2011) summary work reports a best-fit solution for its planet; no value for time of periastron passage or longitude is given in the discovery paper, nor the number of measurements used to obtain the orbital solution.

We collected 35 HARPS measurements in our observations, from which we removed a single datapoint at epoch 2456869.5 due to low SNR value. A total of 96 archival HARPS datapoints were also collected, 11 of which were taken after the fiber-link update of May 2015 and are here treated as an independent dataset.

Table 15. Fit results comparison for system HD 126525

HD 126525		
Parameter	Mayor et al. (2011) Planet b	This work Planet b
K (ms^{-1})	5.11 ± 0.34	$5.26^{+0.25}_{-0.25}$
P (days)	948.1 ± 22	$960.41^{+6.19}_{-6.33}$
$\sqrt{e}\cos\omega$	-	$0.045^{+0.143}_{-0.151}$
$\sqrt{e}\sin\omega$	-	$-0.071^{+0.151}_{-0.130}$
e	0.13 ± 0.07	$0.035^{+0.039}_{-0.024}$
ω (deg)	-	$247.506^{+76.249}_{-184.079}$
Msin i (M_J)	0.224 ± 0.0182	$0.237^{+0.002}_{-0.002}$
a (AU)	1.811 ± 0.041	$1.837^{+0.010}_{-0.010}$
T_{peri} (days)	-	$2456161.7^{+534.8}_{-215.7}$
n_{obs}	-	130
	mean RV error (ms^{-1})	γ (ms^{-1})	jitter (ms^{-1})
HARPS1	0.45	$-2.18^{+0.18}_{-0.18}$	$1.56^{+0.12}_{-0.10}$
HARPS2	0.41	$16.89^{+0.81}_{-0.80}$	$2.50^{+0.78}_{-0.54}$

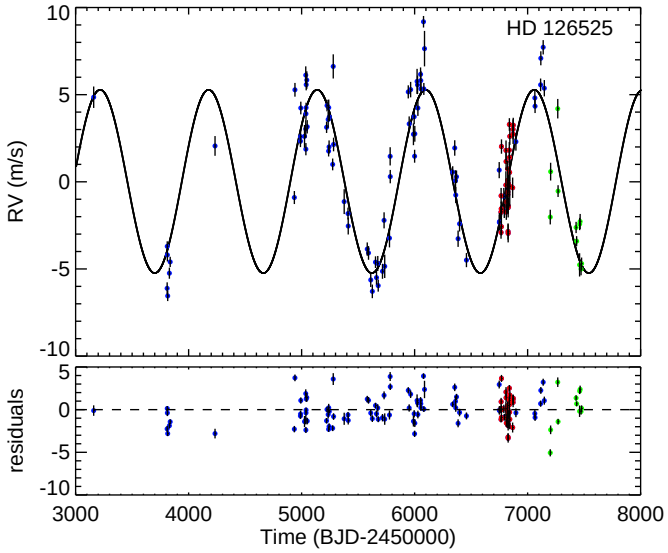

Fig. 15. Same as Fig. 2 but for system HD 126525. Past literature HARPS data are shown in blue, while our HARPS survey data are shown in red and literature HARPS datapoints taken afet the fiber-link update of May 2015 are shown in green.

Joining the literature and the new data we find a fit (see Table 15 and Fig. 15) in which the planet has a minimum mass of $0.237^{+0.002}_{-0.002}M_J$, a period of $960.41^{+6.19}_{-6.33}$d and an eccentricity value of $0.035^{+0.039}_{-0.024}$, a solution generally better constrained than the literature one. The limit on dynamical stability for an additional inner companion is estimated with Hill's criterion to be 707.7 days.

No significant peak is found in the residual data periodogram.

HD 143361 The planet orbiting this G6V star was first discovered and reported in Minniti et al. (2009) as the result of 12 MIKE observation, and later studies (Jenkins et al. 2009,

Table 16. Fit results comparison for system HD 143361

HD 143361			
	Jenkins et al. (2017)		This work
Parameter	Planet b		Planet b
K (ms^{-1})	72.1 ± 1		$73.89^{+0.56}_{-0.58}$
P (days)	1046.2 ± 3.2		$1039.15^{+1.64}_{-1.70}$
$\sqrt{e}\cos\omega$	-		$-0.209^{+0.015}_{-0.014}$
$\sqrt{e}\sin\omega$	-		$-0.392^{+0.010}_{-0.009}$
e	0.193 ± 0.015		$0.197^{+0.006}_{-0.006}$
ω (deg)	241.22 ± 3.44		$241.889^{+2.112}_{-2.051}$
Msin i (M_J)	3.48 ± 0.24		$3.532^{+0.065}_{-0.066}$
a (AU)	1.98 ± 0.07		$1.988^{+0.018}_{-0.018}$
T_{peri} (days)	2453746 ± 147		$2456805.8^{+4.9}_{-4.9}$
n_{obs}	79		107
	mean RV error (ms^{-1})	γ (ms^{-1})	jitter (ms^{-1})
MIKE	3.13	$7.50^{+3.87}_{-3.75}$	$11.47^{+3.59}_{-2.49}$
HARPS	0.87	$10.15^{+0.48}_{-0.48}$	$1.86^{+0.25}_{-0.22}$
CORALIE	14.42	$3.31^{+2.09}_{-2.11}$	$2.23^{+2.47}_{-1.57}$

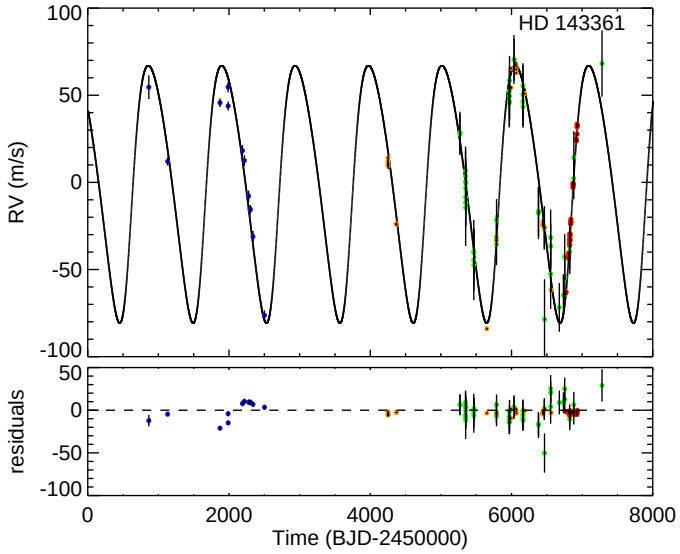

Fig. 16. Same as Fig. 2 but for system HD 143361. The literature MIKE data are shown in blue, literature HARPS data in orange, literature CORALIE datapoints are marked in green, while our HARPS survey data are shown in red.

Table 17. Fit results comparison for system HD 152079

HD 152079			
	Jenkins et al. (2017)		This work
Parameter	Planet b		Planet b
K (ms^{-1})	31.3 ± 1.1		$40.76^{+1.16}_{-1.10}$
P (days)	2899 ± 52		$2918.92^{+37.87}_{-39.28}$
$\sqrt{e}\cos\omega$	-		$0.648^{+0.018}_{-0.018}$
$\sqrt{e}\sin\omega$	-		$-0.331^{+0.025}_{-0.024}$
e	0.52 ± 0.02		$0.532^{+0.015}_{-0.016}$
ω (deg)	324.87 ± 3.44		$332.905^{+2.299}_{-2.195}$
Msin i (M_J)	2.18 ± 0.17		$2.661^{+0.046}_{-0.046}$
a (AU)	3.98 ± 0.15		$4.187^{+0.051}_{-0.053}$
T_{peri} (days)	2453193 ± 260		$2456173.2^{+11.6}_{-11.3}$
slope ($ms^{-1}yr^{-1}$)	1.72 ± 0.47		$0.35^{+0.24}_{-0.24}$
n_{obs}	46		66
	mean RV error (ms^{-1})	γ (ms^{-1})	jitter (ms^{-1})
MIKE	2.98	$-10.34^{+1.51}_{-1.61}$	$4.08^{+1.51}_{-1.22}$
HARPS	0.83	$-7.64^{+0.63}_{-0.63}$	$2.21^{+0.30}_{-0.25}$

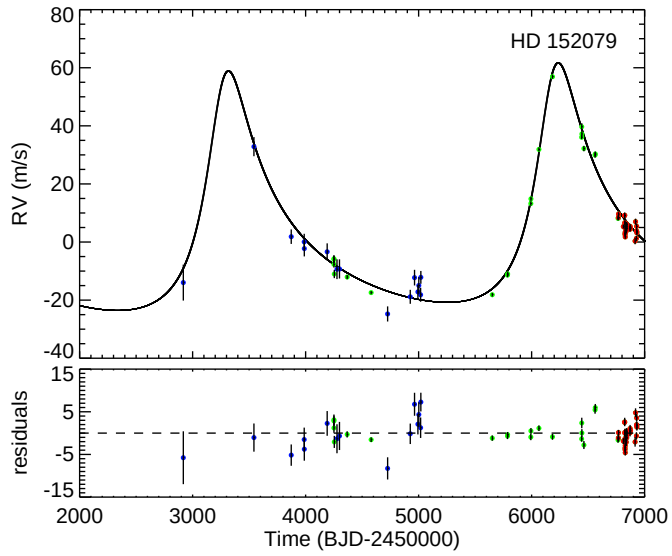

Fig. 17. Same as Fig. 2 but for system HD 152079. Literature MIKE data are shown in blue, literature HARPS data in green while our HARPS survey data are shown in red.

2017) refined the known orbit based on additional HARPS and CORALIE datapoints.

We joined literature data, excluding from the 22 HARPS datapoints the three low-SNR measurements taken at epochs 2454253.77, 2454578.78 and 2454581.80, with our 32 HARPS measurements, from which we exclude a single point at epoch 2456869.62 due to low SNR value. We thusly obtain a best-fit curve (see Table 16 and Fig. 16) of semiamplitude $73.89^{+0.56}_{-0.58}ms^{-1}$ and a $1039.15^{+1.64}_{-1.70}$ days period, slightly shorter than the literature result. We then obtain a minimum mass of $3.532^{+0.065}_{-0.066}M_J$ and an eccentricity value of $0.197^{+0.006}_{-0.006}$, a solution that agrees well with the results of Jenkins et al. (2017) and yet is far better constrained.

The residual data periodogram features no major peak with FAP≤ 0.01.

HD 152079 This G6V star hosts a planet first reported in Arriagada et al. (2010), a discovery based on 15 MIKE datapoints, whose orbit was later refined by Jenkins et al. (2017) using additional 15 CORALIE measurements and 16 HARPS data in good agreement with Arriagada's first findings, also reporting a linear trend of $1.72 \pm 0.47 ms^{-1}yr^{-1}$.

We joined our 32 datapoints to the literature timeseries (from which two low-SNR datapoints at epochs 2455649.80 and 2455650.75 were excluded) and additional 7 HARPS archival data, obtaining a best-fit (see Table 17 and Fig. 17) solution having Msin i=$2.661^{+0.046}_{-0.046}M_J$, period of $2918.92^{+37.87}_{-39.28}$ days and eccentricity value of $0.532^{+0.015}_{-0.016}$, also featuring a linear trend of $0.35^{+0.24}_{-0.24}ms^{-1}yr^{-1}$ which, using again Eq. 1, suggests the presence of an outer companion of at least 0.15 M_J. While generally agreeing to the previously published fit, we note that our solution features slightly higher values for planetary mass and

Table 18. Fit results comparison for system HD 187085

HD 187085			
	Jones et al. (2006)		This work
Parameter	Planet b		Planet b
K (ms^{-1})	17		$15.39^{+2.21}_{-1.98}$
P (days)	986		$1019.74^{+21.29}_{-22.58}$
$\sqrt{e}\cos\omega$	-		$-0.045^{+0.165}_{-0.186}$
$\sqrt{e}\sin\omega$	-		$0.456^{+0.222}_{-0.448}$
e	0.47		$0.251^{+0.221}_{-0.191}$
ω (deg)	94		$98.315^{+78.336}_{-20.027}$
Msin i (M_J)	0.75		$0.836^{+0.011}_{-0.011}$
a (AU)	2.05		$2.100^{+0.032}_{-0.032}$
T_{peri} (days)	2450912		$2456053.6^{+252.4}_{-54.4}$
n_{obs}	40		69
	mean RV error (ms^{-1})	γ (ms^{-1})	jitter (ms^{-1})
AAT	4.51	$-1.66^{+1.20}_{-1.24}$	$5.51^{+1.15}_{-1.00}$
HARPS	0.59	$-13.50^{+2.06}_{-2.00}$	$1.82^{+0.33}_{-0.27}$

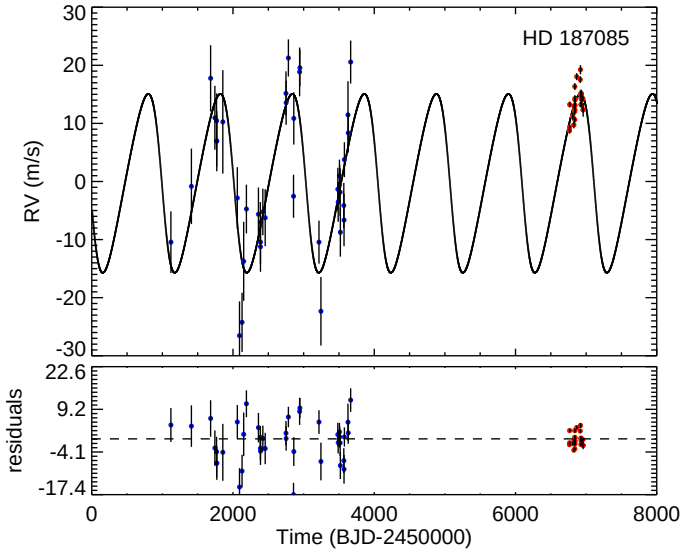

Fig. 18. Same as Fig. 2 but for system HD 187085. The literature AAT data are shown in blue, while our HARPS survey data are shown in red.

major semiaxis and a significantly lower value of linear acceleration. Hill's criterion gives an estimate of 395.9 days for an inner planet's maximum period allowing dynamical stability.

The residual data periodogram features a major peak at 16 days with a false alarm probability of 0.4%; however significant peaks at similar periods can be found in the periodograms obtained for the activity indexes (see Fig. 27), suggesting a non-planetary origin for the signal.

HD 187085 A G0V star hosting a planet first reported in Jones et al. (2006) using 40 AAT measurements; it is however noted in the discovery paper that the data does not manage to effectively sample the sharp drop evident in the radial velocities, allowing therefore for a better fit characterized by a lower eccentricity.

Our 30 HARPS measurements also fail to sample this sharp drop, therefore not conclusively determining whether a lower value of eccentricity would better fit the data. We also report that the datapoint at epoch 2456825.878, was taken with a erroneous exposure time of 5 seconds and is therefore ignored in our analysis; the same night (epoch 2456825.884) a new measurement was immediately taken with a correct exposure time of 600 seconds, this one being used instead in our analysis.

We find a new orbital solution (see Table 18 and Fig. 18) with semiaplitude K=$15.39^{+2.21}_{-1.98}ms^{-1}$, a longer period of $1019.74^{+21.29}_{-22.58}$ days, slightly higher minimum mass of $0.836^{+0.011}_{-0.011}M_J$ and lower but still poorly constrained eccentricity e=$0.251^{+0.221}_{-0.191}$. Although no uncertainty on the published orbital elements were available in the discovery paper, we note that our solution is generally compatible with the nominal values provided in Jones et al. (2006). We find the highest orbital period allowing stability for an additional inner planet's orbit to be 453.2 days.

The residual periodogram show no low FAP significant peak.

HD 190647 This G5V star has been the target of 20 HARPS observations that, as detailed in Naef et al. (2007), led to the discovery of planetary companion HD 190647 b. The authors note however that their data failed to cover the entire orbital period. In the following analysis, we excluded from this literature timeseries the 4 datapoints taken at epochs 2453273.59, 2453274.60, 2453466.90 and 2453493.92 due to low values of SNR.

The 30 HARPS data collected in our survey however manage to sample more efficiently the maximum in RV variation; we removed the datapoint at epoch 2456827.918 since it was taken with an erroneus exposure time of 5 seconds and another datapoint at epoch 2456840.81 for having low SNR. The resulting timeseries lead to two significantly different possible orbital solutions with similar statistical weight (see Table 19); since the main difference between these solutions is found in orbital period we shall refer to them as a 'short period solution' (see Fig. 19) and a 'long period solution' (see Fig. 20). Having respectively a Bayesian Information Criterion value of 99.79 and 101.21 neither solution is clearly preferred.

We characterize the short period solution as having orbital period $878.86^{+1.76}_{-1.65}$d, radial velocity semiamplitude $32.28^{+0.68}_{-0.66}ms^{-1}$, eccentricity of $0.146^{+0.018}_{-0.018}$ and minimum mass of $1.573^{+0.026}_{-0.026}M_J$. The long period solution features instead a period of $1176.45^{+3.10}_{-2.83}$d, semiamplitude $37.51^{+0.82}_{-0.86}ms^{-1}$, eccentricity of $0.224^{+0.014}_{-0.014}$ and minimum planetary mass $1.985^{+0.033}_{-0.033}M_J$.

No peak with FAP$\leq$ 0.01 was found in the residual periodogram obtained for either solution. From Hill's criterion we obtain a stability limit maximum period of 527.4 days for an additional inner planet.

HD 216437 A G2IV star whose planetary companion was independently detected by Jones et al. (2002) using 39 UCLES datapoints and by Mayor et al. (2004) with 21 CORALIE observations, finding similar solutions.

Using the 33 HARPS datapoint obtained from our observations we find (see Table 20 and Fig. 21) significantly higher values for minimum mass Msin i=$2.223^{+0.058}_{-0.058}M_J$ and period P=$1334.28^{+13.07}_{-13.36}$d, while the resulting eccentricity value of e=$0.317^{+0.028}_{-0.027}$ is consistent with the published solution but has a higher accuracy. Hill's criterion gives an orbital period of 427.1 days as a limit on an inner planet's dynamical stability.

No low FAP peak is found in the residual data periodogram.

HD 220689 This G3V star's planetary companion discovery was reported in Marmier et al. (2013) after the acquisition of 48

Table 19. Fit results comparison for system HD 190647

HD 190647					
	Naef et al. (2007)	This work (short period solution)		This work (long period solution)	
Parameter	Planet b	Planet b		Planet b	
K (ms^{-1})	36.4 ± 1.2	$32.28^{+0.68}_{-0.66}$		$37.51^{+0.82}_{-0.86}$	
P (days)	1038.1 ± 4.9	$878.86^{+1.76}_{-1.65}$		$1176.45^{+3.10}_{-2.83}$	
$\sqrt{e}\cos\omega$	-	$-0.071^{+0.042}_{-0.041}$		$-0.364^{+0.038}_{-0.033}$	
$\sqrt{e}\sin\omega$	-	$-0.373^{+0.029}_{-0.026}$		$-0.300^{+0.044}_{-0.043}$	
e	0.18 ± 0.02	$0.146^{+0.018}_{-0.018}$		$0.224^{+0.014}_{-0.014}$	
ω (deg)	232.5 ± 9.4	$259.217^{+6.475}_{-6.744}$		$219.541^{+6.821}_{-6.591}$	
Msin i (M_J)	1.90 ± 0.06	$1.573^{+0.026}_{-0.026}$		$1.985^{+0.033}_{-0.033}$	
a (AU)	2.07 ± 0.06	$1.836^{+0.015}_{-0.016}$		$2.231^{+0.019}_{-0.019}$	
T_{peri} (days)	2453869 ± 24	$2456552.8^{+16.9}_{-21.0}$		$2457373.0^{+25.2}_{-24.5}$	
n_{obs}	20	44			
	mean RV error (ms^{-1})	γ (ms^{-1})	jitter (ms^{-1})	γ (ms^{-1})	jitter (ms^{-1})
HARPS	0.65	$-11.78^{+0.37}_{-0.36}$	$1.32^{+0.22}_{-0.18}$	$-2.62^{+0.61}_{-0.57}$	$1.39^{+0.21}_{-0.17}$
BIC		99.79		101.21	

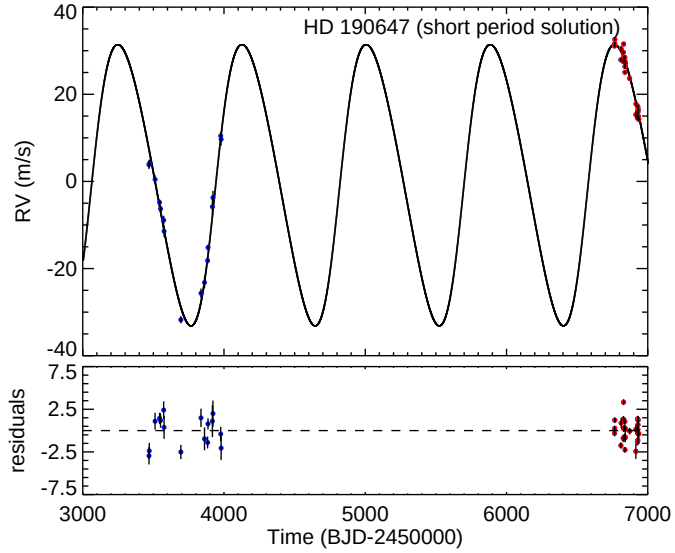

Fig. 19. Same as Fig. 2 but for the short-period solution of system HD 190647. The literature HARPS data are shown in blue, while our HARPS survey data are shown in red.

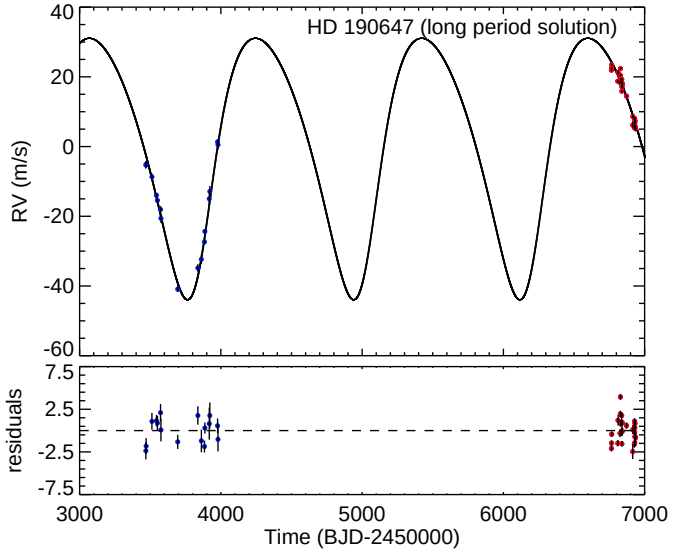

Fig. 20. Same as Fig. 2 but for the long-period solution of system HD 190647. The literature HARPS data are shown in blue, while our HARPS survey data are shown in red.

CORALIE datapoints, the last 34 of which were obtained after an instrument upgrade and are therefore treated as an independent dataset. This planet is also notable for having the lowest radial velocity semiamplitude detected by CORALIE at the time of publication.

Using the 31 HARPS datapoints we collected, we found a compatible but better constrained value for orbital period P=$2266.40^{+65.84}_{-58.77}$d, a higher precision value of eccentricity e=$0.054^{+0.061}_{-0.038}$ and a similarly better determined value of minimum mass Msin i=$1.118^{+0.035}_{-0.035}M_J$ (see Table 21 and Fig. 22). We find the maximum period allowing dynamical stability for an additional inner planet to be 1426.6 days. No peak under 1% level of false alarm probability was found in the residual periodogram.

5. Detection limits and planetary frequency

The calculation of the planetary detection frequency in the star sample was carried out using a standard procedure, which is the production of synthetic circular radial velocity curves for different realizations of the orbital elements pair (P, Msin i) and the statistical analysis of the obtained RV curve in order to determine the detection probability of the signal produced by the simulated planet; a recent application of this technique can be seen in Faria et al. (2016).

For each star in our sample we explored 100 different orbital periods P_j evenly spaced in logarithm from a single day to one year and 100 different planetary mass M_k similarly spaced from 1 $M_\oplus$ to 2 M_J. For each one of these period-mass realization we then computed 20 synthetic radial velocity curves, each one with a different randomly obtained combination of (T_{peri},

Table 20. Fit results comparison for system HD 216437

HD 216437			
	Mayor et al. (2004)		This work
Parameter	Planet b		Planet b
K (ms^{-1})	34.6 ± 5.7		$39.08^{+1.07}_{-1.04}$
P (days)	1256 ± 35		$1334.28^{+13.07}_{-13.36}$
$\sqrt{e}\cos\omega$	-		$0.237^{+0.051}_{-0.052}$
$\sqrt{e}\sin\omega$	-		$0.509^{+0.026}_{-0.028}$
e	0.29 ± 0.12		$0.317^{+0.028}_{-0.027}$
ω (deg)	63 ± 22		$65.092^{+5.515}_{-5.394}$
Msin i (M_J)	1.82		$2.223^{+0.058}_{-0.058}$
a (AU)	2.32		$2.497^{+0.036}_{-0.037}$
T_{peri} (days)	2450693 ± 130		$2457289.2^{+52.2}_{-46.6}$
n_{obs}	21		93
	mean RV error (ms^{-1})	γ (ms^{-1})	jitter (ms^{-1})
UCLES	3.86	$-0.05^{+1.01}_{-1.02}$	$4.11^{+0.912}_{-0.75}$
CORALIE	5.33	$16.13^{+1.90}_{-1.94}$	$6.47^{+1.96}_{-1.65}$
HARPS	0.32	$-12.41^{+5.06}_{-5.36}$	$2.07^{+0.30}_{-0.25}$

Table 21. Fit results comparison for system HD 220689

HD 220689			
	Marmier et al. (2013)		This work
Parameter	Planet b		Planet b
K (ms^{-1})	16.4 ± 1.5		$17.12^{+1.26}_{-1.19}$
P (days)	2209^{+103}_{-81}		$2266.40^{+65.84}_{-58.77}$
$\sqrt{e}\cos\omega$	-		$0.090^{+0.161}_{-0.185}$
$\sqrt{e}\sin\omega$	-		$0.059^{+0.176}_{-0.193}$
e	$0.16^{+0.10}_{-0.07}$		$0.054^{+0.061}_{-0.038}$
ω (deg)	137 ± 75		$112.834^{+194.3244}_{-80.118}$
Msin i (M_J)	1.06 ± 0.09		$1.118^{+0.035}_{-0.035}$
a (AU)	3.36 ± 0.09		$3.396^{+0.084}_{-0.081}$
T_{peri} (days)	245649 ± 413		$2457532.9^{+772.5}_{-478.1}$
n_{obs}	48		79
	mean RV error (ms^{-1})	γ (ms^{-1})	jitter (ms^{-1})
CORALIE1	5.67	$6.87^{+2.40}_{-2.51}$	$4.85^{+2.46}_{-2.25}$
CORALIE2	3.48	$-0.07^{+1.38}_{-1.39}$	$6.02^{+1.16}_{-0.95}$
HARPS	0.59	$-9.89^{+3.16}_{-2.66}$	$1.35^{+0.23}_{-0.19}$

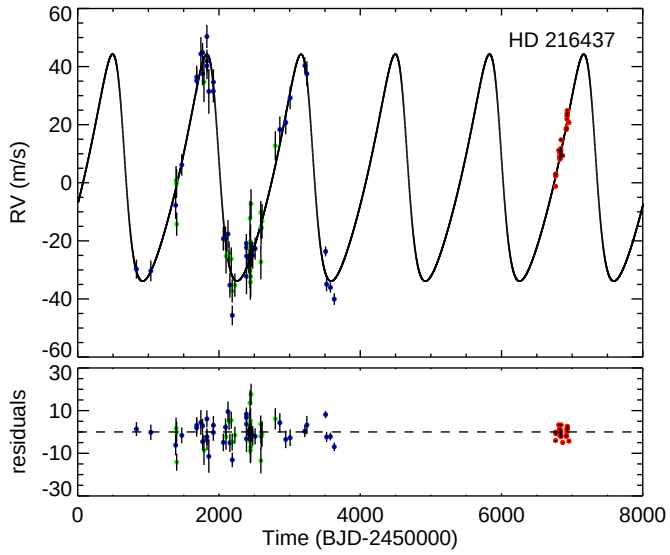

Fig. 21. Same as Fig. 2 but for system HD 216437. The literature UCLES data are shown in blue, CORALIE datapoints are in green while our HARPS survey data are shown in red.

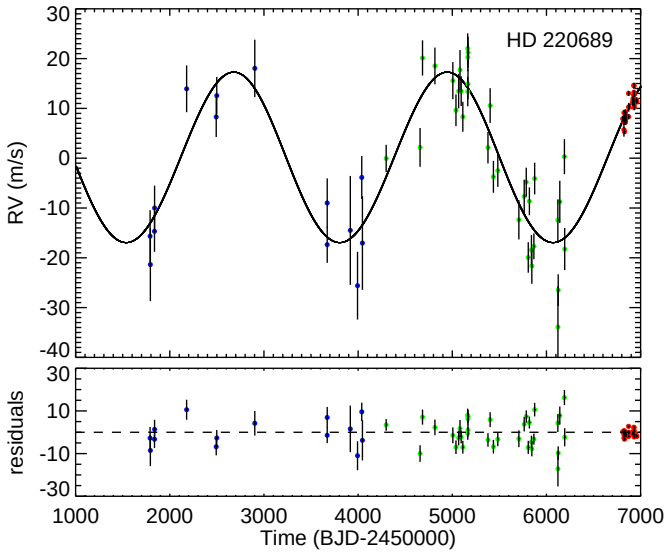

Fig. 22. Same as Fig. 2 but for system HD 220689. The literature CORALIE surveys data are shown in blue and green, while our HARPS survey data are shown in red.

ω); these synthetic radial velocities were obtained by evaluating at each of our survey's observation times t_i the theoretical radial velocity value RV($t_i, P_j, M_k, T_{peri}, \omega$) for the injected period and mass, and then adding to this theoretical values a random gaussian noise with an amplitude equal to the standard deviation of the post-fit residuals data for our high cadence and precision HARPS survey. We then produce a periodogram for each one of the $2{\cdot}10^5$ synthetic signals thus obtained, and the signal is considered as detected only if the injected period power is higher than the power corresponding to a 1% false alarm probability.

It is important to note that our choice to use only our high precision and cadence HARPS residual data for this synthetic curves production leads to a rather conservative evaluation of the detection frequency, being the typical RMS of our post-fit residual data around 3-4 ms^{-1} rather than the $\sim$ 0.5 ms^{-1} RMS of our original HARPS data. Also, choosing not to include the lower-precision literature data could lead to some precision loss at high periods, a fact that has however low influence on our analysis since we choose to study detection for periods up to 1 year. It is also important to note that only in three of the systems of our sample (HD 23127, HD 38801 and HD 48265) a limited portion of the outer region of the period range being considered in this detection limits analysis is subject to instability as calculated throught the Hill criterion (see Sect. 4 and each system's paragraph in Subsect. 4.3).

The detection map produced for the overall HARPS survey, obtained summing and renormalizing each and every system's detection map, is shown in Fig. 23. It can be seen that true uniform completeness for the whole 20-stars sample is achieved for periods below 50 days only for Msin i>30 $M_\oplus$, while for periods less than 150 days we have whole sample completeness only for Msin i>50 $M_\oplus$. For the same period limits we are instead uni-

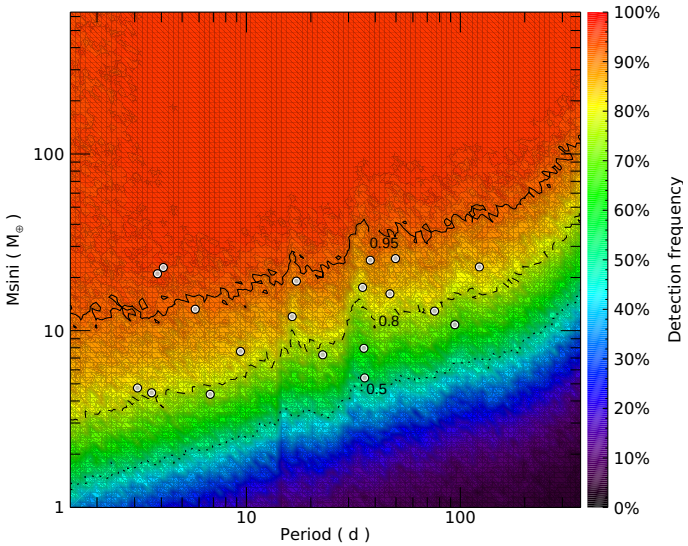

Fig. 23. Color-coded HARPS precision detection frequency map for the whole 20-systems sample studied in this paper, period ranging from one day to one year and masses ranging from 1 $M_\oplus$ to 2 M_J. The detection frequency levels of 50%, 80% and 95% are respectively shown as dotted, dashed and solid curves. The low-mass inner planets of the 11 archival Solar System analogs discussed in Sect. 1 are shown as white circles.

formely sensitive for half our sample respectively for minimum masses ranging from 5 to 10 Earth masses and from 7 to 15 Earth masses. We also note that that for minimum masses ranging from 10 to 30 M⊕ we have completeness below 10 days, a fact that in combination with the lack of additional hot Neptunes found in our analysis suggest a strong absence of such planets around the selected stars.

It is therefore clear that to achieve higher detection frequencies for terrestrial and super-terrestrial planet at all periods, expecially shorter ones, it is necessary to obtain a higher number of observations per target star and ensure a higher-density sampling. Our observing program, as noted in Sect. 3, originally foresaw about 40 measurements per star, a much higher number than the average 27 per star we actually obtained; it can be argued that a number of observations closer to the one originally proposed could push the survey's detection limits to lower planetary masses, ensuring a better coverage and higher detection frequencies for terrestrial and super-terrestrial additional planets. In fact, analytical expressions for close-in low-mass exoplanets detection threshold found in Narayan et al. (2005) show such a dependence on the number of radial velocity measurements. It will also be important in the near future comparing our results with the similarly produced detection map for the parallel HARPS-N survey mentioned in Sect. 1.

From the overall survey detection map one can finally obtain an estimate for the planetary occurence frequency f_p in the presence of a giant outer planet; the probability of obtaining m detection out of a sample of size N is given by the binomial distribution:

$$p(m; N, f_p) = \frac{N!}{m!(N-m)!} f_p^m (1-f_p)^{N-m}$$

The choice of distribution is dictated by the small size of our sample (at most N=20) and has been originally justified in Burgasser et al. (2003) and successfully used in Sozzetti et al. (2009) and Faria et al. (2016), to name a few.

During the analysis of our sample, as detailed in Sect. 4, we found a single new candidate planet, namely the gas giant HD 50499 c, which due to its estimated minimum orbital period P≥8265.51 days lies outside our considered period range of P≤1 yr. Following a section of the analysis reported in the work of Mayor et al. (2011), in which the authors estimated the occurrence frequency of stars with at leats one planet in given regions of orbital period and planetary mass, we focus our interest on sub-giant planets with orbital period less than 150 days and Msin i between 10 and 30 $M_\oplus$, a region for which we are conservatively sensitive to only 50% of our 20-stars sample. Having found no candidate planet falling within this mass-period space, we can only obtain a 1-σ lower limit for occurence frequency of low-mass planets in the presence of a known outer giant planet of f_p<9.84%, a value we note to be much lower than the 38.8±7.1% reported in Mayor et al. (2011) for stars hosting at least one planet in the same period-mass region.

6. Summary and discussion

In this work we have reported the results of an intense observational campaign conducted using the high-precision HARPS spectrograph on 20 stars, obtaining an average of 27 datapoints per star. The stars in the sample were selected in virtue of being bright, inactive and not significantly evolved Sun-like stars hosting at the time of selection a single long-period giant planet previously discovered via radial velocity observations, the final objective of our observations being the search for additional inner low-mass planets and estimating the occurrence frequency of scaled-down Solar System analogs.

By joining the literature radial velocity data with our own measurements we have obtained revised orbital solutions for each known planet in our sample using an MCMC-based fitting algorithm, generally characterized by a higher precision on most of the orbital parameters and significant updates on the orbital parameters for half of the selected systems. We especially stress the achievement of a drastically different set of orbital elements for the previously characterized planet HD 30177 c and the characterization of previously unpublished outer giant planet HD 50499 c, both results obtained fitting the data with a Keplerian curve with a parabolic trend.

Also, three of the systems in our sample (HD 66428, HD 73267 and HD 152079) show a significant slope in the data, one of which (HD 73267) was previously unpublished, suggesting the existence of at least one additional outer companion in the system having a minimum mass >0.83 M_J.

We have also conducted detection simulations on all sample stars in order to calculate the occurrence rate of inner (periods from one day to one year) low mass (10-30 $M_\oplus$) planets in the presence of long-period giants. Having found no candidate planet within these period and mass ranges we can only provide an estimate for the upper limit of said frequency, namely f_p<9.84%, a value which is significantly lower than the one obtained for the same period-mass ranges by Mayor et al. (2011) for stars hosting at least one planet.

The lack of candidate planets found on inner orbits in the sample systems is especially significant when considering again the detection limits of our sample, shown in Fig. 23, from which is clear that we are sensitive to the vast majority of "hot super-Earths" or "mini-Neptunes", defined as planets up to 20 times more massive than the Earth on orbits shorter than 100 days. This type of planet is found to be present around roughly half of all Sun-like stars (Mayor et al. 2011; Howard et al. 2012; Izidoro et al. 2015; Morbidelli & Raymond 2016), often in a

compact low-eccentricity configuration within multiple systems, and is noticeably missing in our own Solar System. The search for the reason of the lack of hot super-Earth in the Solar System has produced several competing formation models for super-Earths (see Morbidelli & Raymond 2016), roughly distinguishable into in situ formation (Hansen & Murray 2012, 2013; Martin & Livio 2016) and inward migration processes (Cossou et al. 2014; Izidoro et al. 2015, 2017). The latter model, proposing that super-Earth embryos form in the outer protoplanetary disk before migrating inward, is especially interesting in interpreting the lack of inner candidate planets found in our sample because, as detailed in Izidoro et al. (2015), if the innermost super-Earth embryo grows into a giant planet core while migrating inward the newly produced gas giant can and will significantly alter the dynamical evolution of the planetary system, blocking the outer super-Earths from further inward migration, with some embryos only occasionally crossing the giant planet's orbit and becoming hot super-Earths or mini-Neptunes. While some studies (Volk & Gladman 2015; Batygin & Laughlin 2015) propose that the early Solar System hosted a close-in population of super-Earths that was either destroyed by erosive collisions or by merging with the Sun, Izidoro & Raymond (2018) points out that the debris generated by erosive processes should have catalyzed further growth of close-in planets and that the existence of an inner edge in the protoplanetary disk should actually prevent planets from simply falling onto the Sun, suggesting instead that the wide, low-eccentricity orbit of Jupiter has had a key role in effectively blocking the formation of close-in super-Earths in the Solar System. The lack of planets found on inner orbits in our sample could be interpreted as evidence for the main observational prediction of the inward migration model, namely the anti-correlation between planetary systems hosting close-in super-Earths and those hosting long-period gas giants.

There is also an interesting formal match between the occurence rate 9.84% of low mass planets in the presence of outer giants derived from our analysis and the preliminary $\sim 10\%$ fraction of Solar System analogs discussed in Sect. 1 that we found amongst the multi-planet systems studied via the radial velocity method; it is also interesting to note from 23 that the inner low-mass planets in these 11 systems would have been detected by our survey in at least 50% of the cases. It could be also argued that the low number of low-mass inner planets in these systems could be examples of the planetary embryos that can occasionally cross the innermost giant planet's orbit in the inward migration formation scenario. However, we stress that the 11 multi-planet systems are not a homogeneous sample, showing a variety of stellar type and planetary characteristics and that were selected in our preliminary search in virtue of the relation between planetary orbits in relation and the circumstellar habitable zone, while the 20-stars sample that is the main focus of this work were all homogeneously selected for their stellar characteristics (as detailed in Sect. 2) and that we did not focus on their habitable zone. While it is interesting to note a suppression of this type of planetary architecture across different spectral types, directly comparing such differently selected groups of systems to draw supportable conclusions about their dynamical history is difficult without further data and higher statistics and beyond the scope of this work.

We finally stress the need for further high-cadence and high-precision observations on the sample stars in order to better characterize certain systems; in particular the constrains on some planets eccentricity and longitude of periastron, such as HD 38801 b and HD 126525 b will greatly benefit from additional intense observations. Exceptional attention will surely be needed in future observations of systems HD 30177 and HD 50499, whose long-period (respectively $\simeq$17 and $\simeq$22 years) outer planet orbits are still incompletely sampled and therefore only partially characterized via semiamplitude, period and mass lower limits.

As a final and future-oriented point of interest we estimated the astrometric signal α of each known giant planet in our sample, using the relation:

$$\alpha = \frac{M_p}{M_*}\frac{a}{d}$$

in order to obtain a quick evaluation of how many and which systems in our sample could be observed by the high-precision astrometric satellite Gaia during its ongoing five-year mission, to fuel further instrument synergies. We find 13 of our systems (namely HD 27631, HD 30177, HD 38801, HD 50499, HD 66428, HD 70642, HD 73267, HD 117207, HD 143361, HD 152079, HD 190647, HD 216437 and HD 220689) to have an astrometric signal $\alpha \gtrsim 50$ μas (expected to be detected by Gaia at high S/N); being however α obviously dependent on the planet's true mass this fraction of astrometrically observable planets could very well be much higher if their orbital inclination turns out to be rather small in value. The importance of evaluating which systems could be observed by Gaia is clear when considering that during its five-year mission the satellite will provide a partial or complete coverage of the known planet's orbit, producing therefore a high-accuracy dataset that could be joined with the literature radial velocity data to further constrain the systems orbital elements and search for additional inner companions in the residuals, an important example of how using different detection methods and instruments can and will help future detailed analysis on exoplanetary systems architecture.

Acknowledgements. We thank the anonymous referee for useful comments. DB acknowledges financial support from INAF and Agenzia Spaziale Italiana (ASI grant n. 014-025-R.1.2015) for the 2016 PhD fellowship programme of INAF. MD acknowledges funding from INAF through the Progetti Premiali funding scheme of the Italian Ministry of Education, University, and Research. The research leading to these results has received funding from the European Union Seventh Framework Programme (FP7/2007-2013) under Grant Agreement No. 313014 (ETAEARTH).

References

Arriagada, P., Butler, R. P., Minniti, D., et al. 2010, ApJ, 711, 1229
Batygin, K. & Laughlin, G. 2015, Proceedings of the National Academy of Science, 112, 4214
Bonfanti, A., Ortolani, S., Piotto, G., & Nascimbeni, V. 2015, A&A, 575, A18
Burgasser, A. J., Kirkpatrick, J. D., Reid, I. N., et al. 2003, ApJ, 586, 512
Butler, R. P., Marcy, G. W., Vogt, S. S., et al. 2003, ApJ, 582, 455
Butler, R. P., Vogt, S. S., Laughlin, G., et al. 2017, AJ, 153, 208
Butler, R. P., Wright, J. T., Marcy, G. W., et al. 2006, ApJ, 646, 505
Cabrera, J., Csizmadia, S., Lehmann, H., et al. 2014, ApJ, 781, 18
Carter, B. D., Butler, R. P., Tinney, C. G., et al. 2003, ApJ, 593, L43
Ciardi, D. R., Fabrycky, D. C., Ford, E. B., et al. 2013, ApJ, 763, 41
Cossou, C., Raymond, S. N., Hersant, F., & Pierens, A. 2014, A&A, 569, A56
da Silva, L., Girardi, L., Pasquini, L., et al. 2006, A&A, 458, 609
Eastman, J., Gaudi, B. S., & Agol, E. 2013, PASP, 125, 83
Faria, J. P., Santos, N. C., Figueira, P., et al. 2016, A&A, 589, A25
Feng, Y. K., Wright, J. T., Nelson, B., et al. 2015, ApJ, 800, 22
Hansen, B. M. S. & Murray, N. 2012, ApJ, 751, 158
Hansen, B. M. S. & Murray, N. 2013, ApJ, 775, 53
Harakawa, H., Sato, B., Fischer, D. A., et al. 2010, ApJ, 715, 550
Hobson, M. J. & Gomez, M. 2017, New A, 55, 1
Howard, A. W., Marcy, G. W., Bryson, S. T., et al. 2012, ApJS, 201, 15
Izidoro, A., Ogihara, M., Raymond, S. N., et al. 2017, MNRAS, 470, 1750
Izidoro, A. & Raymond, S. N. 2018, ArXiv e-prints [arXiv:1803.08830]
Izidoro, A., Raymond, S. N., Morbidelli, A., Hersant, F., & Pierens, A. 2015, ApJ, 800, L22
Jenkins, J. S., Jones, H. R. A., Goździewski, K., et al. 2009, MNRAS, 398, 911

Jenkins, J. S., Jones, H. R. A., Tuomi, M., et al. 2017, MNRAS, 466, 443
Jones, H. R. A., Butler, R. P., Tinney, C. G., et al. 2006, MNRAS, 369, 249
Jones, H. R. A., Paul Butler, R., Marcy, G. W., et al. 2002, MNRAS, 337, 1170
Kipping, D. M., Hartman, J., Bakos, G. Á., et al. 2011, AJ, 142, 95
Kopparapu, R. K., Ramirez, R., Kasting, J. F., et al. 2013, ApJ, 765, 131
Kóspál, Á., Ardila, D. R., Moór, A., & Ábrahám, P. 2009, ApJ, 700, L73
Mamajek, E. E. & Hillenbrand, L. A. 2008, ApJ, 687, 1264
Marcy, G. W., Butler, R. P., Vogt, S. S., et al. 2005, ApJ, 619, 570
Marmier, M., Ségransan, D., Udry, S., et al. 2013, A&A, 551, A90
Martin, R. G. & Livio, M. 2016, ApJ, 822, 90
Mayor, M., Marmier, M., Lovis, C., et al. 2011, ArXiv e-prints [arXiv:1109.2497]
Mayor, M., Udry, S., Naef, D., et al. 2004, A&A, 415, 391
Minniti, D., Butler, R. P., López-Morales, M., et al. 2009, ApJ, 693, 1424
Morbidelli, A. & Raymond, S. N. 2016, Journal of Geophysical Research (Planets), 121, 1962
Moutou, C., Mayor, M., Lo Curto, G., et al. 2011, A&A, 527, A63
Moutou, C., Mayor, M., Lo Curto, G., et al. 2009, A&A, 496, 513
Moutou, C., Vigan, A., Mesa, D., et al. 2017, A&A, 602, A87
Murray, C. D. & Dermott, S. F. 1999, Solar system dynamics
Naef, D., Mayor, M., Benz, W., et al. 2007, A&A, 470, 721
Narayan, R., Cumming, A., & Lin, D. N. C. 2005, ApJ, 620, 1002
Noyes, R. W., Hartmann, L. W., Baliunas, S. L., Duncan, D. K., & Vaughan, A. H. 1984, ApJ, 279, 763
O'Toole, S. J., Butler, R. P., Tinney, C. G., et al. 2007, ApJ, 660, 1636
Raymond, S. N., Barnes, R., & Mandell, A. M. 2008, MNRAS, 384, 663
Sahlmann, J., Lazorenko, P. F., Ségransan, D., et al. 2016, A&A, 595, A77
Schlaufman, K. C. 2014, ApJ, 790, 91
Sousa, S. G., Santos, N. C., Mayor, M., et al. 2008, A&A, 487, 373
Sozzetti, A., Torres, G., Latham, D. W., et al. 2009, ApJ, 697, 544
Stassun, K. G., Collins, K. A., & Gaudi, B. S. 2017, AJ, 153, 136
Tinney, C. G., Butler, R. P., Marcy, G. W., et al. 2003, ApJ, 587, 423
Vogt, S. S., Butler, R. P., Marcy, G. W., et al. 2005, ApJ, 632, 638
Vogt, S. S., Butler, R. P., Marcy, G. W., et al. 2002, ApJ, 568, 352
Volk, K. & Gladman, B. 2015, ApJ, 806, L26
Winn, J. N. & Fabrycky, D. C. 2015, ARA&A, 53, 409
Wittenmyer, R. A., Horner, J., Mengel, M. W., et al. 2017, AJ, 153, 167
Zechmeister, M. & Kürster, M. 2009, A&A, 496, 577

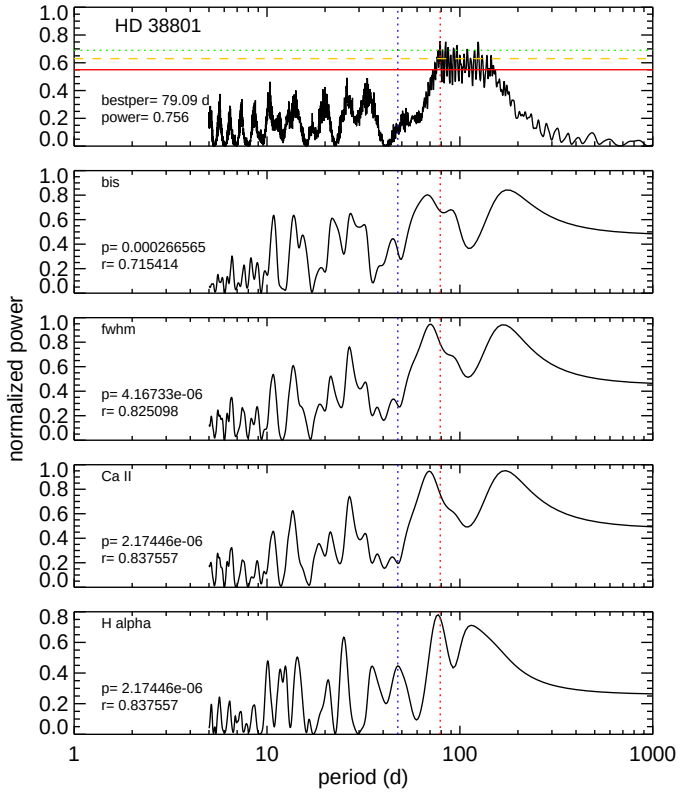

Fig. 24. Activity indexes periodograms for star HD 38801. The topmost panel shows the post-fit residual data periodogram, the most significant period peak value and power shown in the lower left corner, the horizontal lines indicating the false alarm probability levels of 10% (solid red line), 1% (dashed orange line) and 0.1% (dotted green line). The following panels show the periodograms for the activity indexes studied in the paper, respectively bisector, FWHM, Ca II and Hα, the correlation rank r and significance p with the radial velocity residuals shown in each panel's lower left corner. The residual data periodogram's most significant period is highlighted by a vertical red dotted line in all the panels, while the stellar rotation period is shown as a blue dotted vertical line.

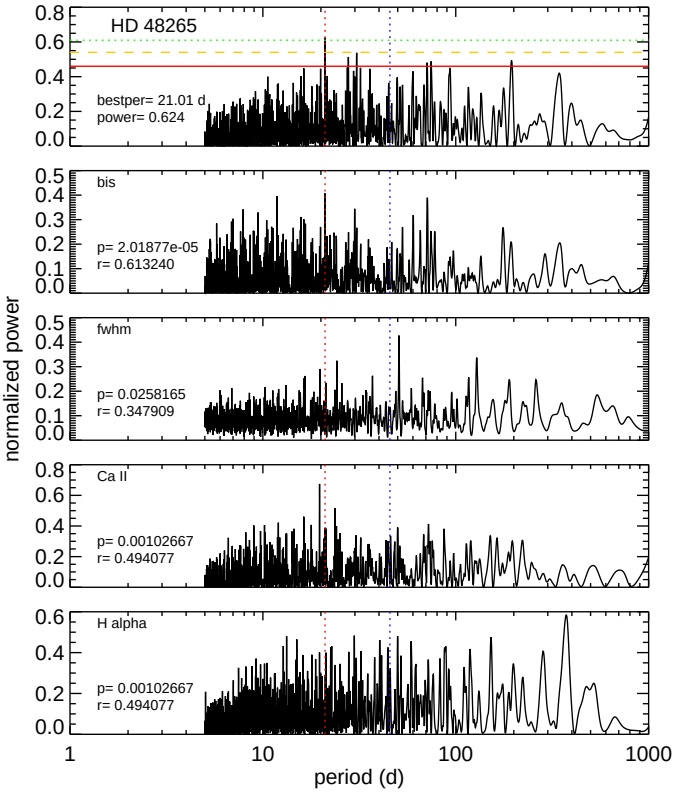

Fig. 25. Same as Fig. 24 but for star HD 48265.

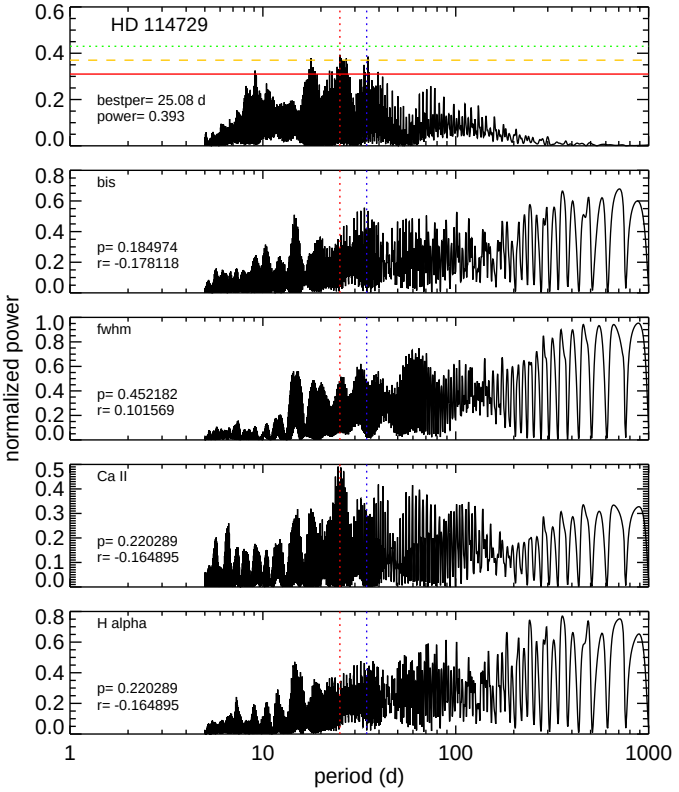

Fig. 26. Same as Fig. 24 but for star HD 114729.

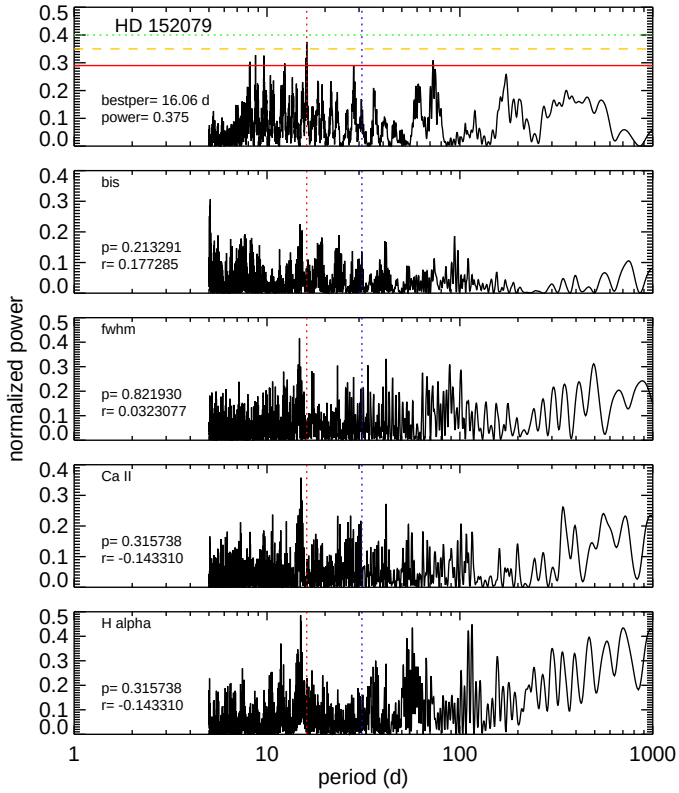

Fig. 27. Same as Fig. 24 but for star HD 152079.

Table 22. RV velocity tables

BJD	T_{exp} [s]	RV [kms^{-1}]	BIS [kms^{-1}]	FWHM [kms^{-1}]	Ca II	Hα	Air mass	SNR
				HD 4208				
2456810.929653	900	56.8184 ± 0.0005	-0.037	6.564	0.00343 ± 0.00004	0.03098 ± 0.00006	1.20	113.10
2456823.914287	900	56.8150 ± 0.0005	-0.037	6.561	0.00345 ± 0.00004	0.03097 ± 0.00005	1.13	119.65
2456824.882368	900	56.8158 ± 0.0004	-0.037	6.565	0.00343 ± 0.00004	0.03107 ± 0.00005	1.25	121.50
2456824.894267	900	56.8170 ± 0.0004	-0.038	6.566	0.00344 ± 0.00003	0.03092 ± 0.00005	1.19	129.65
2456825.936023	900	56.8187 ± 0.0004	-0.041	6.565	0.00349 ± 0.00003	0.03098 ± 0.00005	1.06	127.90
2456826.899682	900	56.8173 ± 0.0004	-0.038	6.566	0.00342 ± 0.00003	0.03092 ± 0.00004	1.15	150.05
2456826.945334	900	56.8166 ± 0.0004	-0.039	6.565	0.00346 ± 0.00003	0.03098 ± 0.00004	1.04	145.65
2456827.892475	900	56.8166 ± 0.0004	-0.039	6.564	0.00343 ± 0.00003	0.03091 ± 0.00004	1.17	139.25
2456828.920515	900	56.8174 ± 0.0005	-0.040	6.563	0.00342 ± 0.00004	0.03088 ± 0.00005	1.07	119.10
2456837.915312	900	56.8213 ± 0.0004	-0.036	6.567	0.00345 ± 0.00003	0.03106 ± 0.00005	1.04	122.95
2456838.892930	900	56.8185 ± 0.0004	-0.039	6.567	0.00353 ± 0.00003	0.03112 ± 0.00005	1.08	124.50
2456839.863290	900	56.8195 ± 0.0005	-0.039	6.568	0.00345 ± 0.00004	0.03090 ± 0.00006	1.16	99.90
2456841.896540	900	56.8194 ± 0.0005	-0.038	6.570	0.00344 ± 0.00004	0.03090 ± 0.00005	1.05	119.40
2456842.896172	900	56.8199 ± 0.0007	-0.040	6.568	0.00356 ± 0.00006	0.03099 ± 0.00009	1.05	72.05
2456872.877254	900	56.8187 ± 0.0005	-0.040	6.567	0.00343 ± 0.00004	0.03090 ± 0.00006	1.00	102.80
2456873.883995	900	56.8199 ± 0.0006	-0.043	6.565	0.00344 ± 0.00005	0.03112 ± 0.00007	1.01	90.00
2456874.858882	900	56.8198 ± 0.0004	-0.039	6.565	0.00347 ± 0.00003	0.03105 ± 0.00005	1.00	123.20
2456915.766156	900	56.8192 ± 0.0005	-0.040	6.568	0.00344 ± 0.00004	0.03099 ± 0.00006	1.00	101.90
2456916.746847	900	56.8198 ± 0.0006	-0.037	6.563	0.00349 ± 0.00005	0.03106 ± 0.00007	1.00	93.05
2456919.795010	900	56.8194 ± 0.0005	-0.038	6.569	0.00344 ± 0.00004	0.03096 ± 0.00006	1.04	109.15
2456927.671189	900	56.8193 ± 0.0004	-0.043	6.568	0.00342 ± 0.00003	0.03098 ± 0.00005	1.04	127.85
2456928.630821	900	56.8238 ± 0.0008	-0.041	6.575	0.00339 ± 0.00006	0.03102 ± 0.00009	1.13	70.25
2456928.778030	900	56.8201 ± 0.0004	-0.039	6.568	0.00342 ± 0.00003	0.03096 ± 0.00005	1.06	142.50
2456929.748528	900	56.8208 ± 0.0006	-0.042	6.566	0.00357 ± 0.00005	0.03102 ± 0.00008	1.02	88.60
2456931.631361	900	56.8188 ± 0.0005	-0.038	6.565	0.00350 ± 0.00004	0.03098 ± 0.00005	1.11	137.20
2456931.815259	900	56.8194 ± 0.0004	-0.039	6.568	0.00341 ± 0.00003	0.03097 ± 0.00005	1.20	120.50
2456932.659389	900	56.8168 ± 0.0005	-0.038	6.568	0.00346 ± 0.00004	0.03099 ± 0.00006	1.04	142.80
2456932.858518	899	56.8191 ± 0.0005	-0.040	6.567	0.00351 ± 0.00004	0.03090 ± 0.00006	1.48	111.00
2456936.706301	900	56.8188 ± 0.0005	-0.041	6.567	0.00345 ± 0.00004	0.03106 ± 0.00006	1.00	110.70
2456959.525588	900	56.8181 ± 0.0004	-0.042	6.567	0.00348 ± 0.00003	0.03098 ± 0.00005	1.21	107.95
				HD 23127				
2456935.862138	900	19.4190 ± 0.0016	0.009	7.972	0.00175 ± 0.00008	0.03067 ± 0.00017	1.19	36.15
2456952.755413	900	19.4160 ± 0.0006	0.001	7.976	0.00273 ± 0.00005	0.03024 ± 0.00007	1.17	89.30
2456953.670819	900	19.4176 ± 0.0008	-0.000	7.980	0.00275 ± 0.00006	0.03013 ± 0.00009	1.28	67.35
2456955.719775	900	19.4144 ± 0.0005	-0.002	7.974	0.00272 ± 0.00004	0.03030 ± 0.00006	1.19	109.30
2456957.831460	900	19.4143 ± 0.0008	0.001	7.977	0.00256 ± 0.00006	0.03024 ± 0.00009	1.23	67.30
2456958.752593	900	19.4122 ± 0.0006	-0.003	7.969	0.00271 ± 0.00005	0.03035 ± 0.00008	1.16	85.85
2456959.648656	900	19.4146 ± 0.0007	-0.002	7.983	0.00276 ± 0.00005	0.03032 ± 0.00008	1.30	80.55
2456989.593729	900	19.3767 ± 0.0008	-1.600	7.970	0.00271 ± 0.00006	0.03009 ± 0.00009	1.23	66.30
2456990.602025	900	19.4142 ± 0.0006	-0.001	7.978	0.00267 ± 0.00005	0.03022 ± 0.00007	1.21	85.15
2456992.658442	899	19.4144 ± 0.0005	-0.001	7.983	0.00270 ± 0.00004	0.03030 ± 0.00006	1.16	102.05
2457008.689356	900	19.4102 ± 0.0007	0.002	7.979	0.00251 ± 0.00005	0.03029 ± 0.00008	1.23	81.90
2457009.665346	900	19.4112 ± 0.0006	-0.001	7.982	0.00254 ± 0.00004	0.03020 ± 0.00007	1.20	91.20
2457018.541477	899	19.4076 ± 0.0005	-0.004	7.979	0.00271 ± 0.00004	0.03014 ± 0.00006	1.19	105.55
2457019.554249	900	19.4102 ± 0.0006	-0.008	7.982	0.00277 ± 0.00005	0.03009 ± 0.00007	1.18	83.45
2457020.559139	900	19.4091 ± 0.0005	-0.005	7.980	0.00268 ± 0.00004	0.03020 ± 0.00006	1.17	104.90
2457021.571019	900	19.4125 ± 0.0006	0.003	7.979	0.00279 ± 0.00005	0.02998 ± 0.00007	1.17	90.60
2457022.566152	900	19.4123 ± 0.0005	-0.004	7.980	0.00278 ± 0.00004	0.03012 ± 0.00006	1.17	99.70
2457051.610389	900	19.4046 ± 0.0006	-0.002	7.978	0.00252 ± 0.00004	0.03019 ± 0.00007	1.32	94.05
2457052.598641	900	19.4062 ± 0.0007	-0.002	7.983	0.00247 ± 0.00005	0.03015 ± 0.00009	1.30	73.35
2457053.560319	900	19.4100 ± 0.0008	-0.001	7.975	0.00239 ± 0.00005	0.03019 ± 0.00009	1.22	67.80
2457054.598141	900	19.4058 ± 0.0005	-0.004	7.974	0.00257 ± 0.00004	0.03011 ± 0.00006	1.31	100.70
2457055.551568	900	19.4076 ± 0.0006	-0.001	7.979	0.00263 ± 0.00004	0.03031 ± 0.00007	1.21	94.20
2457056.553593	900	19.4044 ± 0.0005	-0.003	7.979	0.00254 ± 0.00004	0.03017 ± 0.00006	1.22	100.95
2457057.547262	900	19.4025 ± 0.0006	-0.005	7.981	0.00246 ± 0.00004	0.03031 ± 0.00008	1.22	83.95
2457058.559138	900	19.4043 ± 0.0005	-0.003	7.975	0.00256 ± 0.00004	0.03024 ± 0.00006	1.24	100.65
				HD 25171				
2456935.872116	600	43.6576 ± 0.0016	0.032	7.335	0.00257 ± 0.00007	0.02840 ± 0.00015	1.26	43.05

Table 22. continued.

BJD	T_{exp} [s]	RV [kms^{-1}]	BIS [kms^{-1}]	FWHM [kms^{-1}]	Ca II	Hα	Air mass	SNR
2456955.771155	600	43.6489 ± 0.0005	0.022	7.326	0.00291 ± 0.00003	0.02813 ± 0.00005	1.23	139.30
2456958.762118	600	43.6503 ± 0.0007	0.026	7.321	0.00290 ± 0.00004	0.02815 ± 0.00007	1.23	101.40
2456959.658655	600	43.6489 ± 0.0007	0.023	7.330	0.00297 ± 0.00004	0.02805 ± 0.00006	1.36	102.65
2456990.611825	600	43.6477 ± 0.0007	0.024	7.327	0.00291 ± 0.00004	0.02825 ± 0.00007	1.28	94.15
2456992.668540	600	43.6474 ± 0.0006	0.025	7.331	0.00285 ± 0.00003	0.02831 ± 0.00006	1.23	106.95
2456993.625498	600	43.6447 ± 0.0006	0.024	7.332	0.00292 ± 0.00003	0.02820 ± 0.00005	1.25	118.05
2457008.699323	600	43.6425 ± 0.0007	0.024	7.325	0.00293 ± 0.00004	0.02825 ± 0.00007	1.29	99.55
2457009.675204	600	43.6458 ± 0.0006	0.025	7.328	0.00288 ± 0.00003	0.02819 ± 0.00006	1.26	114.80
2457018.599408	600	43.6455 ± 0.0007	0.022	7.328	0.00285 ± 0.00004	0.02820 ± 0.00007	1.23	96.20
2457019.600822	600	43.6442 ± 0.0008	0.024	7.331	0.00285 ± 0.00004	0.02818 ± 0.00007	1.23	86.20
2457020.591912	600	43.6431 ± 0.0006	0.020	7.327	0.00288 ± 0.00003	0.02828 ± 0.00006	1.23	114.20
2457021.604517	600	43.6443 ± 0.0006	0.022	7.327	0.00283 ± 0.00003	0.02816 ± 0.00005	1.24	120.10
2457022.623234	600	43.6424 ± 0.0006	0.028	7.331	0.00288 ± 0.00003	0.02821 ± 0.00006	1.25	109.80
2457051.568172	600	43.6444 ± 0.0006	0.022	7.333	0.00294 ± 0.00003	0.02801 ± 0.00006	1.27	118.50
2457052.540611	600	43.6430 ± 0.0006	0.024	7.331	0.00292 ± 0.00003	0.02796 ± 0.00006	1.25	115.90
2457053.525724	600	43.6419 ± 0.0008	0.024	7.328	0.00281 ± 0.00004	0.02812 ± 0.00007	1.24	88.20
2457054.587873	600	43.6437 ± 0.0007	0.024	7.329	0.00286 ± 0.00004	0.02813 ± 0.00006	1.32	104.75
2457055.527559	600	43.6464 ± 0.0006	0.022	7.327	0.00292 ± 0.00003	0.02808 ± 0.00005	1.24	119.15
2457056.530045	600	43.6445 ± 0.0006	0.023	7.329	0.00286 ± 0.00003	0.02807 ± 0.00006	1.25	111.55
2457057.524429	600	43.6421 ± 0.0006	0.023	7.327	0.00289 ± 0.00003	0.02823 ± 0.00005	1.25	122.95
2457058.535874	600	43.6428 ± 0.0006	0.028	7.330	0.00289 ± 0.00003	0.02809 ± 0.00005	1.26	125.95
HD 27631								
2456936.848558	900	21.1485 ± 0.0006	-0.026	6.816	0.00366 ± 0.00005	0.03060 ± 0.00007	1.02	87.35
2456953.716151	900	21.1486 ± 0.0006	-0.027	6.813	0.00371 ± 0.00005	0.03072 ± 0.00007	1.12	87.20
2456957.846968	900	21.1562 ± 0.0008	-0.030	6.815	0.00349 ± 0.00006	0.03070 ± 0.00010	1.08	67.80
2456958.742151	900	21.1537 ± 0.0006	-0.032	6.808	0.00353 ± 0.00005	0.03050 ± 0.00007	1.05	89.65
2456959.671038	900	21.1510 ± 0.0005	-0.028	6.812	0.00357 ± 0.00004	0.03063 ± 0.00006	1.21	99.80
2456989.607087	900	21.1598 ± 0.0007	-0.023	6.819	0.00378 ± 0.00006	0.03069 ± 0.00008	1.15	79.95
2456990.717359	900	21.1520 ± 0.0005	-0.026	6.814	0.00375 ± 0.00004	0.03060 ± 0.00006	1.03	114.75
2456993.638757	900	21.1578 ± 0.0005	-0.028	6.818	0.00382 ± 0.00004	0.03060 ± 0.00006	1.06	105.70
2456994.661945	900	21.1580 ± 0.0006	-0.026	6.818	0.00373 ± 0.00005	0.03058 ± 0.00007	1.03	92.65
2457008.732293	900	21.1515 ± 0.0005	-0.027	6.811	0.00356 ± 0.00004	0.03052 ± 0.00006	1.13	107.35
2457009.706466	900	21.1522 ± 0.0006	-0.030	6.809	0.00340 ± 0.00004	0.03041 ± 0.00007	1.08	98.05
2457018.611596	900	21.1507 ± 0.0005	-0.028	6.806	0.00340 ± 0.00004	0.03030 ± 0.00007	1.03	99.55
2457019.625102	900	21.1503 ± 0.0006	-0.028	6.814	0.00326 ± 0.00005	0.03034 ± 0.00008	1.03	83.05
2457020.629973	900	21.1482 ± 0.0005	-0.029	6.811	0.00348 ± 0.00004	0.03039 ± 0.00006	1.03	107.10
2457021.629127	900	21.1479 ± 0.0004	-0.031	6.806	0.00346 ± 0.00004	0.03025 ± 0.00005	1.03	123.50
2457022.647145	900	21.1503 ± 0.0005	-0.031	6.812	0.00343 ± 0.00004	0.03040 ± 0.00006	1.05	118.00
2457051.623308	900	21.1504 ± 0.0004	-0.027	6.812	0.00357 ± 0.00004	0.03030 ± 0.00005	1.16	123.90
2457054.634532	900	21.1592 ± 0.0004	-0.030	6.810	0.00345 ± 0.00004	0.03042 ± 0.00005	1.23	124.55
2457055.565159	900	21.1603 ± 0.0005	-0.030	6.807	0.00350 ± 0.00004	0.03021 ± 0.00006	1.06	120.00
2457056.566454	900	21.1574 ± 0.0005	-0.033	6.814	0.00342 ± 0.00004	0.03026 ± 0.00005	1.06	121.60
2457057.560562	900	21.1546 ± 0.0004	-0.030	6.809	0.00341 ± 0.00003	0.03048 ± 0.00005	1.06	144.40
2457058.572019	900	21.1517 ± 0.0004	-0.028	6.811	0.00342 ± 0.00003	0.03044 ± 0.00005	1.08	138.40
2457103.507064	600	21.1555 ± 0.0007	-0.028	6.812	0.00354 ± 0.00006	0.03007 ± 0.00009	1.28	70.85
HD 30177								
2456953.817942	900	62.7138 ± 0.0004	-0.034	7.310	0.00301 ± 0.00005	0.03267 ± 0.00006	1.14	104.50
2456955.781822	900	62.7126 ± 0.0004	-0.031	7.310	0.00303 ± 0.00004	0.03281 ± 0.00005	1.15	117.50
2456957.880537	900	62.7098 ± 0.0007	-0.035	7.316	0.00279 ± 0.00006	0.03278 ± 0.00010	1.22	66.45
2456959.681474	900	62.7103 ± 0.0005	-0.034	7.312	0.00309 ± 0.00005	0.03272 ± 0.00006	1.31	97.20
2456989.651462	900	62.7048 ± 0.0004	-0.036	7.312	0.00287 ± 0.00004	0.03274 ± 0.00006	1.19	108.00
2456993.693334	900	62.7018 ± 0.0004	-0.034	7.312	0.00294 ± 0.00004	0.03279 ± 0.00006	1.14	105.65
2456994.672176	900	62.7005 ± 0.0005	-0.031	7.309	0.00279 ± 0.00005	0.03280 ± 0.00007	1.15	94.30
2457008.766271	900	62.6971 ± 0.0004	-0.035	7.309	0.00285 ± 0.00004	0.03271 ± 0.00006	1.28	104.70
2457009.717459	900	62.6971 ± 0.0004	-0.033	7.310	0.00290 ± 0.00004	0.03284 ± 0.00007	1.18	104.00
2457018.621743	900	62.6948 ± 0.0005	-0.038	7.313	0.00301 ± 0.00005	0.03274 ± 0.00007	1.14	93.25
2457019.611064	900	62.6956 ± 0.0005	-0.034	7.312	0.00284 ± 0.00005	0.03285 ± 0.00008	1.14	82.50
2457020.616728	900	62.6946 ± 0.0005	-0.034	7.310	0.00287 ± 0.00005	0.03290 ± 0.00008	1.14	85.80
2457021.615898	900	62.6939 ± 0.0004	-0.034	7.307	0.00302 ± 0.00004	0.03277 ± 0.00005	1.14	122.00
2457022.634200	900	62.6931 ± 0.0004	-0.036	7.311	0.00290 ± 0.00004	0.03279 ± 0.00006	1.14	114.15

Table 22. continued.

BJD	T_{exp} [s]	RV [kms^{-1}]	BIS [kms^{-1}]	FWHM [kms^{-1}]	Ca II	Hα	Air mass	SNR
2457051.634458	900	62.6852 ± 0.0005	-0.036	7.310	0.00289 ± 0.00004	0.03281 ± 0.00007	1.25	101.35
2457052.612146	900	62.6866 ± 0.0005	-0.034	7.310	0.00294 ± 0.00004	0.03276 ± 0.00007	1.21	101.05
2457053.595215	900	62.6865 ± 0.0005	-0.037	7.313	0.00278 ± 0.00004	0.03267 ± 0.00007	1.18	94.55
2457054.621848	900	62.6847 ± 0.0005	-0.034	7.315	0.00300 ± 0.00005	0.03286 ± 0.00007	1.24	97.20
2457055.631433	900	62.6843 ± 0.0005	-0.033	7.310	0.00291 ± 0.00005	0.03272 ± 0.00006	1.27	101.10
2457056.633599	900	62.6862 ± 0.0005	-0.035	7.313	0.00296 ± 0.00005	0.03281 ± 0.00007	1.28	98.65
2457057.613127	900	62.6847 ± 0.0004	-0.034	7.311	0.00297 ± 0.00004	0.03289 ± 0.00006	1.24	114.00
2457058.633799	900	62.6834 ± 0.0004	-0.035	7.310	0.00285 ± 0.00003	0.03276 ± 0.00005	1.30	131.05
2457100.552195	600	62.6780 ± 0.0006	-0.038	7.317	0.00279 ± 0.00006	0.03264 ± 0.00009	1.44	72.50
2457101.529138	600	62.6794 ± 0.0008	-0.034	7.317	0.00286 ± 0.00008	0.03269 ± 0.00012	1.35	54.25
2457103.534912	600	62.6796 ± 0.0009	-0.034	7.319	0.00303 ± 0.00009	0.03271 ± 0.00013	1.40	48.50
2457104.543893	600	62.6773 ± 0.0007	-0.033	7.316	0.00302 ± 0.00007	0.03254 ± 0.00009	1.45	67.15
HD 38801								
2456936.860622	900	-25.3693 ± 0.0006	0.039	6.859	0.00529 ± 0.00008	0.03308 ± 0.00008	1.11	70.90
2456953.784607	900	-25.3842 ± 0.0004	0.037	6.871	0.00548 ± 0.00006	0.03257 ± 0.00006	1.19	104.90
2456955.832551	900	-25.3898 ± 0.0003	0.038	6.868	0.00544 ± 0.00005	0.03251 ± 0.00005	1.08	120.25
2457008.782827	900	-25.4724 ± 0.0004	0.036	6.851	0.00453 ± 0.00005	0.03318 ± 0.00006	1.18	111.85
2457009.746532	900	-25.4737 ± 0.0004	0.038	6.849	0.00445 ± 0.00006	0.03310 ± 0.00007	1.10	93.45
2457018.646800	900	-25.4711 ± 0.0004	0.036	6.859	0.00512 ± 0.00006	0.03309 ± 0.00007	1.10	92.45
2457019.648939	900	-25.4666 ± 0.0005	0.037	6.864	0.00531 ± 0.00007	0.03297 ± 0.00007	1.09	84.00
2457020.654572	900	-25.4651 ± 0.0005	0.036	6.861	0.00548 ± 0.00007	0.03306 ± 0.00007	1.08	86.75
2457021.665724	900	-25.4655 ± 0.0004	0.036	6.864	0.00535 ± 0.00005	0.03307 ± 0.00006	1.07	110.10
2457022.709779	900	-25.4625 ± 0.0003	0.039	6.867	0.00539 ± 0.00005	0.03288 ± 0.00005	1.10	121.85
2457051.669172	900	-25.4593 ± 0.0004	0.042	6.898	0.00712 ± 0.00006	0.03281 ± 0.00006	1.20	113.75
2457052.636512	900	-25.4593 ± 0.0005	0.048	6.898	0.00722 ± 0.00007	0.03267 ± 0.00007	1.12	89.15
2457055.589403	900	-25.4602 ± 0.0004	0.048	6.900	0.00729 ± 0.00006	0.03272 ± 0.00006	1.07	107.20
2457056.590811	900	-25.4587 ± 0.0004	0.049	6.902	0.00735 ± 0.00007	0.03275 ± 0.00007	1.07	96.30
2457056.666628	900	-25.4587 ± 0.0004	0.052	6.901	0.00739 ± 0.00006	0.03277 ± 0.00006	1.24	114.00
2457057.645895	900	-25.4618 ± 0.0003	0.046	6.899	0.00722 ± 0.00006	0.03268 ± 0.00005	1.18	129.75
2457058.666628	900	-25.4625 ± 0.0003	0.052	6.903	0.00721 ± 0.00006	0.03283 ± 0.00005	1.27	125.15
2457100.543862	600	-25.4553 ± 0.0006	0.045	6.890	0.00661 ± 0.00009	0.03263 ± 0.00008	1.26	74.75
2457101.539715	600	-25.4537 ± 0.0007	0.047	6.887	0.00665 ± 0.00011	0.03284 ± 0.00010	1.25	62.80
2457103.545193	600	-25.4531 ± 0.0008	0.047	6.890	0.00680 ± 0.00012	0.03281 ± 0.00011	1.31	54.10
2457104.554170	600	-25.4519 ± 0.0005	0.044	6.885	0.00652 ± 0.00009	0.03263 ± 0.00008	1.38	77.70
HD 48265								
2456953.854454	600	23.4656 ± 0.0006	0.008	8.173	0.00300 ± 0.00005	0.02999 ± 0.00006	1.08	97.35
2456955.791552	600	23.4630 ± 0.0005	0.011	8.174	0.00292 ± 0.00004	0.03004 ± 0.00006	1.18	105.20
2456958.840131	600	23.4634 ± 0.0007	0.013	8.166	0.00276 ± 0.00005	0.03013 ± 0.00008	1.08	74.75
2457008.812809	600	23.4587 ± 0.0005	0.007	8.169	0.00281 ± 0.00004	0.02984 ± 0.00006	1.13	107.45
2457009.774675	600	23.4526 ± 0.0006	0.009	8.171	0.00283 ± 0.00004	0.02995 ± 0.00007	1.08	97.90
2457018.708409	599	23.4581 ± 0.0006	0.013	8.174	0.00279 ± 0.00005	0.02985 ± 0.00007	1.06	86.20
2457019.722966	600	23.4530 ± 0.0006	0.009	8.174	0.00285 ± 0.00004	0.03002 ± 0.00007	1.06	92.25
2457019.740952	600	23.4527 ± 0.0005	0.009	8.172	0.00290 ± 0.00004	0.02992 ± 0.00006	1.07	100.70
2457020.727928	600	23.4445 ± 0.0007	0.013	8.165	0.00270 ± 0.00005	0.03006 ± 0.00008	1.06	78.70
2457021.725782	600	23.4447 ± 0.0006	0.008	8.166	0.00289 ± 0.00004	0.02986 ± 0.00006	1.06	96.60
2457022.742468	600	23.4442 ± 0.0005	0.009	8.165	0.00273 ± 0.00004	0.02996 ± 0.00006	1.08	104.95
2457051.687850	599	23.4423 ± 0.0006	0.011	8.175	0.00298 ± 0.00005	0.02985 ± 0.00007	1.11	96.50
2457052.684171	600	23.4339 ± 0.0007	0.013	8.179	0.00287 ± 0.00005	0.02979 ± 0.00008	1.11	80.85
2457053.668779	600	23.4339 ± 0.0007	0.007	8.177	0.00300 ± 0.00006	0.02974 ± 0.00009	1.09	73.90
2457054.765711	600	23.4388 ± 0.0006	0.011	8.172	0.00306 ± 0.00005	0.02978 ± 0.00007	1.42	87.00
2457055.643525	600	23.4385 ± 0.0005	0.008	8.175	0.00288 ± 0.00004	0.02959 ± 0.00006	1.07	100.90
2457056.645921	600	23.4338 ± 0.0005	0.009	8.170	0.00285 ± 0.00004	0.02980 ± 0.00006	1.08	106.30
2457057.625144	600	23.4326 ± 0.0005	0.008	8.173	0.00274 ± 0.00004	0.02990 ± 0.00005	1.06	119.20
2457057.774645	600	23.4309 ± 0.0006	0.006	8.170	0.00278 ± 0.00005	0.02980 ± 0.00007	1.53	92.65
2457058.645617	600	23.4307 ± 0.0005	0.012	8.167	0.00284 ± 0.00003	0.02983 ± 0.00006	1.08	117.40
HD 50499								
2456935.879347	600	36.8651 ± 0.0008	0.017	8.605	0.00295 ± 0.00005	0.02879 ± 0.00008	1.07	76.20
2456936.869088	600	36.8633 ± 0.0006	0.016	8.610	0.00295 ± 0.00003	0.02874 ± 0.00005	1.09	117.75
2456953.837807	600	36.8658 ± 0.0005	0.015	8.610	0.00300 ± 0.00003	0.02861 ± 0.00005	1.06	134.65
2456955.819928	600	36.8629 ± 0.0004	0.015	8.610	0.00286 ± 0.00002	0.02872 ± 0.00004	1.09	173.90

Table 22. continued.

BJD	T_{exp} [s]	RV [kms^{-1}]	BIS [kms^{-1}]	FWHM [kms^{-1}]	Ca II	Hα	Air mass	SNR
2456958.785515	600	36.8602 ± 0.0005	0.010	8.604	0.00293 ± 0.00003	0.02855 ± 0.00005	1.17	125.70
2457008.864886	600	36.8653 ± 0.0005	0.011	8.607	0.00288 ± 0.00003	0.02858 ± 0.00004	1.22	150.50
2457009.784340	600	36.8617 ± 0.0005	0.011	8.612	0.00291 ± 0.00002	0.02850 ± 0.00005	1.02	146.45
2457018.717800	600	36.8641 ± 0.0005	0.016	8.607	0.00303 ± 0.00003	0.02843 ± 0.00005	1.00	130.40
2457019.733265	600	36.8638 ± 0.0005	0.015	8.608	0.00299 ± 0.00003	0.02861 ± 0.00005	1.00	147.35
2457019.751043	600	36.8637 ± 0.0004	0.014	8.608	0.00296 ± 0.00002	0.02850 ± 0.00004	1.02	157.10
2457020.737329	600	36.8628 ± 0.0005	0.015	8.611	0.00288 ± 0.00003	0.02852 ± 0.00005	1.01	136.70
2457021.736507	600	36.8614 ± 0.0005	0.014	8.605	0.00295 ± 0.00003	0.02842 ± 0.00005	1.01	143.25
2457022.751749	600	36.8593 ± 0.0005	0.013	8.607	0.00290 ± 0.00003	0.02848 ± 0.00005	1.02	139.70
2457051.774505	600	36.8604 ± 0.0005	0.014	8.604	0.00283 ± 0.00003	0.02853 ± 0.00005	1.37	128.80
2457052.772786	600	36.8589 ± 0.0005	0.013	8.604	0.00281 ± 0.00003	0.02853 ± 0.00004	1.38	150.80
2457053.678416	600	36.8602 ± 0.0006	0.013	8.601	0.00281 ± 0.00003	0.02843 ± 0.00006	1.04	105.30
2457054.775131	600	36.8627 ± 0.0005	0.011	8.605	0.00283 ± 0.00003	0.02846 ± 0.00005	1.43	137.10
2457055.662427	600	36.8636 ± 0.0004	0.013	8.609	0.00284 ± 0.00002	0.02843 ± 0.00004	1.03	168.15
2457056.676432	600	36.8633 ± 0.0004	0.013	8.614	0.00288 ± 0.00002	0.02864 ± 0.00004	1.05	162.45
2457057.656294	600	36.8619 ± 0.0004	0.015	8.612	0.00287 ± 0.00002	0.02865 ± 0.00004	1.03	162.65
2457058.714684	600	36.8629 ± 0.0004	0.016	8.603	0.00283 ± 0.00002	0.02857 ± 0.00004	1.17	189.00
2457100.578272	600	36.8574 ± 0.0005	0.013	8.608	0.00286 ± 0.00003	0.02853 ± 0.00005	1.10	145.40
2457101.491235	600	36.8596 ± 0.0005	0.012	8.606	0.00292 ± 0.00003	0.02862 ± 0.00005	1.00	128.20
2457102.605344	600	36.8546 ± 0.0005	0.013	8.606	0.00287 ± 0.00003	0.02867 ± 0.00004	1.22	150.20
HD 66428								
2456955.872121	900	44.1379 ± 0.0004	-0.033	7.125	0.00299 ± 0.00004	0.03156 ± 0.00006	1.26	111.55
2456958.862979	900	44.1427 ± 0.0006	-0.034	7.125	0.00285 ± 0.00005	0.03150 ± 0.00008	1.26	83.25
2457009.815770	900	44.1564 ± 0.0004	-0.035	7.127	0.00296 ± 0.00004	0.03142 ± 0.00006	1.14	105.95
2457018.778631	900	44.1597 ± 0.0004	-0.030	7.126	0.00292 ± 0.00003	0.03140 ± 0.00005	1.13	127.05
2457019.816847	900	44.1609 ± 0.0004	-0.031	7.126	0.00299 ± 0.00003	0.03142 ± 0.00005	1.17	131.95
2457020.780406	900	44.1613 ± 0.0005	-0.032	7.123	0.00292 ± 0.00004	0.03118 ± 0.00007	1.13	102.10
2457021.792959	900	44.1600 ± 0.0004	-0.032	7.125	0.00303 ± 0.00003	0.03137 ± 0.00006	1.15	119.35
2457022.810475	900	44.1605 ± 0.0004	-0.032	7.126	0.00293 ± 0.00003	0.03114 ± 0.00005	1.18	121.35
2457051.713524	900	44.1710 ± 0.0005	-0.028	7.130	0.00298 ± 0.00004	0.03136 ± 0.00006	1.15	103.60
2457052.710691	900	44.1739 ± 0.0004	-0.033	7.127	0.00300 ± 0.00003	0.03140 ± 0.00005	1.15	128.55
2457053.691352	900	44.1707 ± 0.0005	-0.034	7.125	0.00297 ± 0.00005	0.03141 ± 0.00008	1.14	85.45
2457054.673794	900	44.1719 ± 0.0005	-0.033	7.125	0.00296 ± 0.00004	0.03144 ± 0.00008	1.13	87.25
2457054.748330	899	44.1735 ± 0.0006	-0.032	7.125	0.00291 ± 0.00005	0.03147 ± 0.00008	1.25	84.85
2457058.683034	900	44.1719 ± 0.0004	-0.034	7.128	0.00295 ± 0.00004	0.03145 ± 0.00006	1.14	113.55
2457100.644690	600	44.1822 ± 0.0008	-0.036	7.133	0.00293 ± 0.00007	0.03122 ± 0.00011	1.37	57.85
2457101.552307	600	44.1838 ± 0.0008	-0.029	7.127	0.00273 ± 0.00006	0.03156 ± 0.00011	1.13	61.05
2457102.616913	600	44.1822 ± 0.0006	-0.034	7.126	0.00298 ± 0.00005	0.03140 ± 0.00008	1.26	85.05
2457104.623597	600	44.1818 ± 0.0012	-0.036	7.133	0.00324 ± 0.00010	0.03127 ± 0.00015	1.31	43.70
HD 70642								
2456936.886243	600	49.4926 ± 0.0004	-0.037	6.991	0.00318 ± 0.00003	0.03141 ± 0.00005	1.24	126.95
2456953.844342	600	49.4919 ± 0.0003	-0.036	6.991	0.00328 ± 0.00003	0.03083 ± 0.00004	1.23	145.25
2456955.860682	600	49.4919 ± 0.0003	-0.038	6.988	0.00321 ± 0.00003	0.03116 ± 0.00004	1.15	154.10
2456958.816899	600	49.4906 ± 0.0004	-0.037	6.986	0.00319 ± 0.00003	0.03122 ± 0.00005	1.29	122.85
2457018.786913	600	49.4844 ± 0.0003	-0.035	6.988	0.00325 ± 0.00002	0.03124 ± 0.00004	1.02	185.70
2457019.824954	600	49.4836 ± 0.0003	-0.036	6.990	0.00323 ± 0.00002	0.03123 ± 0.00004	1.04	180.85
2457020.811672	599	49.4852 ± 0.0003	-0.037	6.986	0.00325 ± 0.00003	0.03120 ± 0.00004	1.03	155.50
2457021.801214	600	49.4845 ± 0.0003	-0.039	6.987	0.00327 ± 0.00003	0.03120 ± 0.00004	1.02	160.50
2457022.830850	600	49.4856 ± 0.0003	-0.034	6.991	0.00321 ± 0.00003	0.03116 ± 0.00004	1.06	160.15
2457051.823653	599	49.4868 ± 0.0003	-0.036	6.992	0.00322 ± 0.00003	0.03119 ± 0.00004	1.29	146.30
2457052.818286	600	49.4856 ± 0.0003	-0.035	6.991	0.00320 ± 0.00003	0.03119 ± 0.00004	1.27	175.85
2457053.810730	600	49.4869 ± 0.0003	-0.038	6.990	0.00322 ± 0.00003	0.03122 ± 0.00004	1.25	155.55
2457054.823162	600	49.4869 ± 0.0003	-0.035	6.991	0.00321 ± 0.00003	0.03126 ± 0.00004	1.32	166.30
2457055.803844	600	49.4869 ± 0.0003	-0.035	6.993	0.00326 ± 0.00003	0.03114 ± 0.00004	1.24	148.15
2457056.800534	600	49.4862 ± 0.0003	-0.036	6.992	0.00323 ± 0.00003	0.03126 ± 0.00004	1.24	149.20
2457057.686214	600	49.4872 ± 0.0003	-0.036	6.990	0.00318 ± 0.00003	0.03136 ± 0.00004	1.02	180.75
2457058.773017	600	49.4859 ± 0.0003	-0.035	6.988	0.00315 ± 0.00002	0.03135 ± 0.00004	1.16	189.55
2457100.686503	600	49.4791 ± 0.0004	-0.035	6.991	0.00329 ± 0.00003	0.03111 ± 0.00005	1.27	139.15
2457102.689323	600	49.4793 ± 0.0005	-0.035	6.994	0.00321 ± 0.00004	0.03130 ± 0.00006	1.31	100.65
2457103.681410	600	49.4785 ± 0.0005	-0.034	6.993	0.00337 ± 0.00005	0.03126 ± 0.00007	1.29	97.75

Table 22. continued.

BJD	T_{exp} [s]	RV [kms^{-1}]	BIS [kms^{-1}]	FWHM [kms^{-1}]	Ca II	Hα	Air mass	SNR
2457104.632432	600	49.4789 ± 0.0008	-0.034	6.995	0.00320 ± 0.00007	0.03129 ± 0.00011	1.12	64.35
				HD 73267				
2456955.849837	900	51.9375 ± 0.0005	-0.002	6.250	0.00336 ± 0.00006	0.03412 ± 0.00007	1.23	83.95
2457018.831975	900	51.9644 ± 0.0005	-0.001	6.250	0.00329 ± 0.00005	0.03426 ± 0.00008	1.02	89.10
2457019.843771	900	51.9645 ± 0.0005	-0.003	6.252	0.00325 ± 0.00005	0.03426 ± 0.00008	1.04	86.95
2457020.831365	900	51.9651 ± 0.0005	-0.001	6.253	0.00341 ± 0.00005	0.03420 ± 0.00008	1.03	85.35
2457021.833183	900	51.9652 ± 0.0005	-0.004	6.253	0.00310 ± 0.00006	0.03414 ± 0.00008	1.03	80.90
2457022.842072	900	51.9642 ± 0.0005	-0.002	6.252	0.00324 ± 0.00005	0.03405 ± 0.00008	1.05	84.40
2457052.581993	900	51.9739 ± 0.0007	-0.005	6.253	0.00308 ± 0.00007	0.03419 ± 0.00010	1.27	66.25
2457052.783201	900	51.9739 ± 0.0004	-0.001	6.251	0.00330 ± 0.00005	0.03420 ± 0.00006	1.10	108.05
2457053.629419	900	51.9777 ± 0.0007	-0.001	6.252	0.00332 ± 0.00007	0.03431 ± 0.00010	1.08	65.60
2457053.792153	900	51.9747 ± 0.0005	-0.003	6.253	0.00330 ± 0.00006	0.03427 ± 0.00009	1.13	80.60
2457054.803962	900	51.9771 ± 0.0006	0.003	6.252	0.00338 ± 0.00007	0.03428 ± 0.00009	1.18	69.10
2457055.813734	900	51.9752 ± 0.0005	-0.004	6.251	0.00324 ± 0.00006	0.03410 ± 0.00007	1.23	82.40
2457056.810843	900	51.9741 ± 0.0005	-0.003	6.251	0.00309 ± 0.00006	0.03443 ± 0.00008	1.23	81.90
2457057.804084	900	51.9770 ± 0.0006	-0.002	6.256	0.00327 ± 0.00006	0.03422 ± 0.00009	1.21	78.00
2457058.754419	900	51.9749 ± 0.0004	-0.003	6.251	0.00336 ± 0.00005	0.03418 ± 0.00006	1.07	107.90
2457058.840658	900	51.9779 ± 0.0008	0.002	6.254	0.00335 ± 0.00009	0.03429 ± 0.00012	1.44	53.90
2457100.697446	900	51.9862 ± 0.0007	-0.004	6.253	0.00333 ± 0.00007	0.03415 ± 0.00010	1.27	65.35
				HD 114729				
2456764.574095	600	65.0005 ± 0.0003	0.012	7.082	0.00294 ± 0.00002	0.02897 ± 0.00003	1.22	192.95
2456764.695832	600	64.9984 ± 0.0003	0.013	7.083	0.00293 ± 0.00002	0.02900 ± 0.00003	1.00	224.85
2456765.595697	600	64.9999 ± 0.0004	0.010	7.082	0.00295 ± 0.00002	0.02905 ± 0.00003	1.13	182.25
2456765.828175	600	64.9981 ± 0.0003	0.011	7.079	0.00290 ± 0.00002	0.02894 ± 0.00003	1.40	195.00
2456766.642460	600	64.9996 ± 0.0003	0.012	7.079	0.00292 ± 0.00002	0.02895 ± 0.00003	1.02	199.40
2456767.554128	600	64.9974 ± 0.0004	0.012	7.077	0.00291 ± 0.00003	0.02909 ± 0.00004	1.27	154.40
2456767.757045	600	64.9988 ± 0.0004	0.014	7.078	0.00295 ± 0.00002	0.02894 ± 0.00004	1.10	180.20
2456768.531431	600	65.0007 ± 0.0004	0.011	7.082	0.00291 ± 0.00002	0.02887 ± 0.00004	1.40	173.15
2456768.767264	600	64.9992 ± 0.0003	0.012	7.080	0.00297 ± 0.00002	0.02894 ± 0.00003	1.14	201.85
2456807.718511	600	65.0036 ± 0.0009	0.010	7.080	0.00303 ± 0.00006	0.02910 ± 0.00010	1.45	64.10
2456808.666223	600	64.9998 ± 0.0005	0.011	7.086	0.00298 ± 0.00003	0.02908 ± 0.00005	1.17	124.80
2456809.640101	600	65.0024 ± 0.0004	0.010	7.080	0.00297 ± 0.00003	0.02904 ± 0.00004	1.10	144.00
2456810.606942	600	64.9992 ± 0.0004	0.012	7.081	0.00297 ± 0.00002	0.02905 ± 0.00004	1.03	168.20
2456811.619670	600	65.0021 ± 0.0003	0.013	7.079	0.00290 ± 0.00002	0.02904 ± 0.00003	1.06	188.85
2456822.548127	600	65.0006 ± 0.0006	0.013	7.078	0.00299 ± 0.00003	0.02892 ± 0.00006	1.01	113.60
2456822.670190	600	65.0001 ± 0.0005	0.009	7.081	0.00294 ± 0.00003	0.02885 ± 0.00005	1.40	139.40
2456823.484286	600	65.0016 ± 0.0005	0.012	7.084	0.00295 ± 0.00003	0.02888 ± 0.00005	1.02	134.10
2456823.711353	600	65.0024 ± 0.0006	0.013	7.080	0.00287 ± 0.00003	0.02877 ± 0.00007	1.86	104.70
2456824.494304	600	64.9995 ± 0.0005	0.014	7.082	0.00293 ± 0.00003	0.02913 ± 0.00005	1.01	135.70
2456825.641290	600	64.9998 ± 0.0004	0.013	7.078	0.00293 ± 0.00002	0.02908 ± 0.00004	1.27	171.10
2456826.516097	600	65.0007 ± 0.0004	0.012	7.082	0.00296 ± 0.00002	0.02901 ± 0.00004	1.00	176.35
2456827.517109	600	64.9972 ± 0.0004	0.012	7.079	0.00297 ± 0.00002	0.02905 ± 0.00004	1.00	186.50
2456828.524114	600	65.0004 ± 0.0004	0.010	7.077	0.00296 ± 0.00002	0.02904 ± 0.00004	1.00	180.65
2456837.566047	600	65.0057 ± 0.0004	0.010	7.085	0.00290 ± 0.00002	0.02906 ± 0.00004	1.11	167.90
2456838.499892	600	65.0048 ± 0.0003	0.012	7.078	0.00291 ± 0.00002	0.02902 ± 0.00003	1.01	203.85
2456838.630378	600	65.0053 ± 0.0004	0.013	7.080	0.00294 ± 0.00002	0.02906 ± 0.00004	1.44	165.40
2456839.469254	600	65.0044 ± 0.0004	0.013	7.079	0.00294 ± 0.00002	0.02897 ± 0.00004	1.00	174.00
2456839.607229	600	65.0063 ± 0.0005	0.010	7.079	0.00290 ± 0.00003	0.02894 ± 0.00004	1.30	139.90
2456840.466646	600	65.0058 ± 0.0006	0.010	7.077	0.00288 ± 0.00003	0.02912 ± 0.00006	1.00	102.95
2456841.475692	900	65.0060 ± 0.0004	0.011	7.082	0.00293 ± 0.00002	0.02902 ± 0.00004	1.00	170.20
2456841.616340	900	65.0059 ± 0.0006	0.012	7.080	0.00295 ± 0.00004	0.02901 ± 0.00006	1.39	99.55
2456867.520010	600	65.0078 ± 0.0005	0.008	7.081	0.00293 ± 0.00003	0.02884 ± 0.00005	1.26	125.55
2456870.480462	600	65.0069 ± 0.0004	0.012	7.080	0.00293 ± 0.00002	0.02892 ± 0.00004	1.13	176.25
2456874.457065	600	65.0077 ± 0.0005	0.011	7.077	0.00294 ± 0.00003	0.02906 ± 0.00005	1.10	140.45
				HD 117207				
2456764.583768	900	-17.3911 ± 0.0003	-0.036	7.126	0.00305 ± 0.00002	0.03177 ± 0.00003	1.23	184.70
2456765.605401	900	-17.3905 ± 0.0003	-0.036	7.123	0.00309 ± 0.00003	0.03175 ± 0.00004	1.14	162.40
2456765.839420	900	-17.3921 ± 0.0003	-0.034	7.125	0.00303 ± 0.00003	0.03179 ± 0.00004	1.38	174.90
2456766.600875	600	-17.3916 ± 0.0003	-0.035	7.127	0.00298 ± 0.00003	0.03178 ± 0.00004	1.14	142.35
2456766.690413	600	-17.3935 ± 0.0003	-0.036	7.123	0.00305 ± 0.00003	0.03170 ± 0.00004	1.01	166.80

Table 22. continued.

BJD	T_{exp} [s]	RV [kms^{-1}]	BIS [kms^{-1}]	FWHM [kms^{-1}]	Ca II	Hα	Air mass	SNR
2456767.562354	600	-17.3920 ± 0.0004	-0.036	7.121	0.00307 ± 0.00004	0.03183 ± 0.00005	1.28	115.40
2456767.765516	600	-17.3908 ± 0.0004	-0.037	7.125	0.00305 ± 0.00003	0.03185 ± 0.00005	1.09	131.00
2456768.557247	600	-17.3910 ± 0.0003	-0.035	7.128	0.00297 ± 0.00003	0.03178 ± 0.00004	1.30	143.60
2456768.844378	600	-17.3928 ± 0.0004	-0.035	7.125	0.00304 ± 0.00004	0.03171 ± 0.00005	1.49	123.15
2456807.730364	600	-17.3854 ± 0.0008	-0.035	7.120	0.00243 ± 0.00006	0.03173 ± 0.00010	1.43	59.50
2456808.689344	600	-17.3885 ± 0.0005	-0.038	7.127	0.00299 ± 0.00005	0.03163 ± 0.00007	1.21	92.05
2456809.649514	600	-17.3873 ± 0.0004	-0.034	7.128	0.00305 ± 0.00004	0.03166 ± 0.00006	1.09	108.75
2456810.614938	600	-17.3883 ± 0.0004	-0.036	7.121	0.00310 ± 0.00003	0.03167 ± 0.00005	1.03	126.00
2456811.640381	599	-17.3870 ± 0.0004	-0.034	7.125	0.00301 ± 0.00004	0.03170 ± 0.00006	1.08	112.00
2456822.571757	600	-17.3888 ± 0.0005	-0.039	7.125	0.00309 ± 0.00004	0.03165 ± 0.00007	1.02	95.55
2456822.678995	600	-17.3904 ± 0.0004	-0.037	7.124	0.00296 ± 0.00004	0.03160 ± 0.00006	1.37	111.30
2456823.568472	600	-17.3899 ± 0.0005	-0.039	7.125	0.00301 ± 0.00005	0.03166 ± 0.00006	1.02	96.65
2456824.566831	600	-17.3904 ± 0.0004	-0.038	7.123	0.00304 ± 0.00003	0.03184 ± 0.00005	1.02	123.20
2456824.688616	600	-17.3901 ± 0.0004	-0.037	7.125	0.00301 ± 0.00003	0.03166 ± 0.00005	1.48	128.40
2456825.622973	600	-17.3901 ± 0.0003	-0.034	7.123	0.00302 ± 0.00003	0.03168 ± 0.00004	1.14	145.25
2456826.525815	600	-17.3902 ± 0.0004	-0.034	7.121	0.00299 ± 0.00003	0.03171 ± 0.00005	1.01	131.05
2456827.525826	600	-17.3909 ± 0.0003	-0.038	7.122	0.00306 ± 0.00003	0.03167 ± 0.00004	1.01	148.45
2456828.546227	600	-17.3904 ± 0.0004	-0.036	7.125	0.00304 ± 0.00003	0.03176 ± 0.00005	1.01	130.40
2456837.458667	600	-17.3895 ± 0.0004	-0.036	7.131	0.00305 ± 0.00004	0.03168 ± 0.00006	1.03	110.60
2456837.612092	600	-17.3891 ± 0.0005	-0.035	7.127	0.00306 ± 0.00004	0.03176 ± 0.00006	1.23	103.25
2456838.508780	599	-17.3893 ± 0.0003	-0.036	7.123	0.00296 ± 0.00003	0.03170 ± 0.00004	1.01	155.50
2456838.640552	600	-17.3903 ± 0.0004	-0.037	7.127	0.00306 ± 0.00004	0.03176 ± 0.00005	1.41	126.35
2456839.492682	600	-17.3883 ± 0.0005	-0.038	7.122	0.00300 ± 0.00005	0.03164 ± 0.00006	1.01	100.05
2456840.512959	900	-17.3894 ± 0.0004	-0.038	7.125	0.00307 ± 0.00003	0.03172 ± 0.00005	1.01	128.15
2456841.573324	899	-17.3894 ± 0.0004	-0.035	7.124	0.00297 ± 0.00004	0.03170 ± 0.00006	1.12	107.75
2456842.478203	600	-17.3883 ± 0.0004	-0.037	7.124	0.00304 ± 0.00003	0.03176 ± 0.00005	1.01	131.90
2456867.552677	600	-17.3845 ± 0.0006	-0.037	7.123	0.00289 ± 0.00005	0.03173 ± 0.00008	1.38	79.20
2456874.503436	600	-17.3859 ± 0.0004	-0.036	7.124	0.00294 ± 0.00004	0.03172 ± 0.00006	1.21	109.20
				HD 126525				
2456764.654448	900	13.1371 ± 0.0004	-0.038	6.869	0.00333 ± 0.00003	0.03117 ± 0.00004	1.18	142.70
2456764.737657	900	13.1359 ± 0.0004	-0.038	6.866	0.00325 ± 0.00003	0.03117 ± 0.00004	1.08	152.50
2456765.649276	900	13.1380 ± 0.0005	-0.035	6.873	0.00328 ± 0.00004	0.03123 ± 0.00005	1.19	119.25
2456766.609969	900	13.1373 ± 0.0004	-0.038	6.872	0.00333 ± 0.00004	0.03112 ± 0.00005	1.30	128.25
2456766.700065	900	13.1371 ± 0.0004	-0.039	6.867	0.00322 ± 0.00003	0.03121 ± 0.00005	1.10	132.35
2456767.690897	900	13.1362 ± 0.0005	-0.036	6.869	0.00334 ± 0.00004	0.03120 ± 0.00006	1.10	106.55
2456768.566515	900	13.1408 ± 0.0004	-0.038	6.870	0.00328 ± 0.00003	0.03111 ± 0.00005	1.50	130.20
2456768.853689	900	13.1372 ± 0.0004	-0.039	6.868	0.00322 ± 0.00004	0.03115 ± 0.00005	1.31	131.25
2456807.741732	900	13.1386 ± 0.0008	-0.036	6.872	0.00339 ± 0.00007	0.03112 ± 0.00009	1.29	65.00
2456808.700323	900	13.1406 ± 0.0006	-0.035	6.869	0.00332 ± 0.00005	0.03135 ± 0.00007	1.17	93.30
2456809.660544	900	13.1400 ± 0.0005	-0.036	6.871	0.00326 ± 0.00004	0.03121 ± 0.00006	1.11	108.70
2456810.625266	900	13.1377 ± 0.0004	-0.040	6.864	0.00331 ± 0.00003	0.03116 ± 0.00005	1.09	129.05
2456811.674441	900	13.1371 ± 0.0004	-0.037	6.868	0.00331 ± 0.00004	0.03114 ± 0.00005	1.14	120.90
2456822.624174	900	13.1389 ± 0.0005	-0.036	6.872	0.00325 ± 0.00004	0.03107 ± 0.00006	1.11	110.25
2456823.597919	900	13.1396 ± 0.0005	-0.038	6.871	0.00333 ± 0.00004	0.03104 ± 0.00005	1.09	114.75
2456824.591420	900	13.1382 ± 0.0005	-0.036	6.868	0.00336 ± 0.00004	0.03116 ± 0.00006	1.09	111.70
2456824.736819	900	13.1381 ± 0.0004	-0.036	6.871	0.00331 ± 0.00004	0.03105 ± 0.00005	1.50	125.00
2456825.584272	900	13.1374 ± 0.0004	-0.037	6.868	0.00330 ± 0.00003	0.03112 ± 0.00005	1.09	134.50
2456825.677416	900	13.1375 ± 0.0005	-0.035	6.871	0.00331 ± 0.00004	0.03122 ± 0.00006	1.24	113.55
2456826.590791	900	13.1374 ± 0.0004	-0.036	6.867	0.00330 ± 0.00003	0.03109 ± 0.00004	1.09	150.55
2456826.735055	900	13.1360 ± 0.0005	-0.037	6.870	0.00328 ± 0.00004	0.03109 ± 0.00005	1.52	115.85
2456827.589577	900	13.1359 ± 0.0005	-0.035	6.870	0.00324 ± 0.00004	0.03136 ± 0.00006	1.09	104.00
2456827.732869	900	13.1373 ± 0.0006	-0.037	6.868	0.00330 ± 0.00005	0.03111 ± 0.00007	1.53	95.40
2456828.588617	900	13.1387 ± 0.0004	-0.037	6.867	0.00333 ± 0.00004	0.03122 ± 0.00005	1.09	125.55
2456837.577973	900	13.1406 ± 0.0005	-0.038	6.866	0.00338 ± 0.00004	0.03115 ± 0.00005	1.10	116.60
2456838.544805	900	13.1421 ± 0.0004	-0.036	6.866	0.00327 ± 0.00003	0.03127 ± 0.00004	1.08	150.15
2456839.532457	900	13.1402 ± 0.0004	-0.036	6.868	0.00337 ± 0.00004	0.03111 ± 0.00005	1.08	122.40
2456840.565083	199	13.1394 ± 0.0005	-0.038	6.870	0.00328 ± 0.00004	0.03115 ± 0.00006	1.10	105.70
2456841.585532	200	13.1386 ± 0.0012	-0.034	6.865	0.00261 ± 0.00009	0.03131 ± 0.00013	1.13	46.15
2456842.574801	900	13.1414 ± 0.0005	-0.034	6.867	0.00326 ± 0.00004	0.03113 ± 0.00006	1.12	110.10
2456867.590749	900	13.1385 ± 0.0006	-0.038	6.866	0.00331 ± 0.00005	0.03088 ± 0.00007	1.35	91.15

Table 22. continued.

BJD	T_{exp} [s]	RV [kms^{-1}]	BIS [kms^{-1}]	FWHM [kms^{-1}]	Ca II	Hα	Air mass	SNR
2456869.598407	900	13.1465 ± 0.0032	-0.034	6.886	0.00237 ± 0.00016	0.03170 ± 0.00029	1.42	20.30
2456870.541643	900	13.1418 ± 0.0006	-0.037	6.869	0.00337 ± 0.00005	0.03095 ± 0.00007	1.21	93.55
2456871.492611	900	13.1416 ± 0.0006	-0.040	6.870	0.00329 ± 0.00005	0.03095 ± 0.00007	1.11	95.90
2456872.507022	900	13.1421 ± 0.0004	-0.036	6.866	0.00328 ± 0.00004	0.03095 ± 0.00005	1.14	127.70
				HD 143361				
2456767.703024	900	-0.5053 ± 0.0007	-0.042	6.942	0.00307 ± 0.00008	0.03327 ± 0.00011	1.16	56.30
2456768.688091	900	-0.5045 ± 0.0006	-0.047	6.943	0.00317 ± 0.00007	0.03318 ± 0.00009	1.20	69.95
2456768.901876	900	-0.5047 ± 0.0006	-0.047	6.945	0.00323 ± 0.00006	0.03315 ± 0.00008	1.21	76.60
2456807.753635	900	-0.4854 ± 0.0015	-0.050	6.945	0.00281 ± 0.00012	0.03368 ± 0.00018	1.10	33.45
2456808.713390	900	-0.4846 ± 0.0008	-0.049	6.944	0.00336 ± 0.00008	0.03338 ± 0.00011	1.05	56.20
2456809.672727	900	-0.4823 ± 0.0007	-0.044	6.954	0.00320 ± 0.00008	0.03321 ± 0.00010	1.04	60.05
2456810.693151	900	-0.4833 ± 0.0007	-0.043	6.939	0.00335 ± 0.00007	0.03327 ± 0.00011	1.04	61.80
2456822.638661	900	-0.4768 ± 0.0007	-0.044	6.946	0.00290 ± 0.00007	0.03324 ± 0.00011	1.04	58.20
2456823.677271	900	-0.4744 ± 0.0007	-0.049	6.942	0.00300 ± 0.00007	0.03337 ± 0.00010	1.05	62.10
2456824.605684	900	-0.4777 ± 0.0008	-0.047	6.939	0.00306 ± 0.00008	0.03332 ± 0.00011	1.05	54.75
2456826.603673	900	-0.4753 ± 0.0006	-0.043	6.933	0.00312 ± 0.00006	0.03312 ± 0.00008	1.05	75.35
2456826.748229	900	-0.4739 ± 0.0007	-0.045	6.939	0.00286 ± 0.00007	0.03327 ± 0.00010	1.23	65.05
2456827.601028	900	-0.4725 ± 0.0007	-0.050	6.940	0.00286 ± 0.00007	0.03320 ± 0.00010	1.05	62.40
2456827.746579	900	-0.4714 ± 0.0007	-0.044	6.941	0.00299 ± 0.00008	0.03323 ± 0.00011	1.23	57.95
2456828.614827	900	-0.4750 ± 0.0006	-0.048	6.938	0.00323 ± 0.00007	0.03333 ± 0.00009	1.04	66.90
2456828.769220	900	-0.4712 ± 0.0007	-0.045	6.943	0.00336 ± 0.00008	0.03315 ± 0.00010	1.35	63.75
2456837.591880	900	-0.4644 ± 0.0008	-0.042	6.946	0.00295 ± 0.00008	0.03318 ± 0.00011	1.04	56.30
2456838.653233	900	-0.4645 ± 0.0006	-0.048	6.941	0.00307 ± 0.00007	0.03328 ± 0.00009	1.07	67.20
2456839.585285	900	-0.4657 ± 0.0007	-0.045	6.949	0.00322 ± 0.00008	0.03319 ± 0.00011	1.04	58.25
2456840.663451	500	-0.4643 ± 0.0006	-0.047	6.947	0.00312 ± 0.00006	0.03332 ± 0.00009	1.09	71.30
2456841.696977	900	-0.4629 ± 0.0008	-0.048	6.946	0.00284 ± 0.00009	0.03331 ± 0.00012	1.19	51.05
2456869.627125	900	-0.4498 ± 0.0025	-0.040	6.947	0.00242 ± 0.00016	0.03351 ± 0.00025	1.22	23.55
2456870.584619	900	-0.4447 ± 0.0009	-0.044	6.947	0.00283 ± 0.00008	0.03348 ± 0.00013	1.11	50.15
2456871.615463	900	-0.4422 ± 0.0012	-0.046	6.937	0.00262 ± 0.00010	0.03325 ± 0.00016	1.20	39.00
2456872.520217	900	-0.4434 ± 0.0006	-0.050	6.940	0.00281 ± 0.00006	0.03319 ± 0.00009	1.04	72.30
2456873.521108	900	-0.4428 ± 0.0008	-0.042	6.943	0.00296 ± 0.00008	0.03316 ± 0.00012	1.04	51.70
2456915.571456	900	-0.4168 ± 0.0016	-0.050	6.950	0.00264 ± 0.00013	0.03318 ± 0.00019	1.70	31.60
2456919.558495	900	-0.4179 ± 0.0014	-0.057	6.964	0.00283 ± 0.00012	0.03313 ± 0.00017	1.68	34.70
2456927.473099	900	-0.4141 ± 0.0012	-0.049	6.948	0.00307 ± 0.00011	0.03308 ± 0.00016	1.26	39.45
2456928.479257	900	-0.4100 ± 0.0007	-0.049	6.946	0.00316 ± 0.00008	0.03327 ± 0.00011	1.30	57.20
2456929.473193	900	-0.4084 ± 0.0009	-0.050	6.942	0.00282 ± 0.00009	0.03313 ± 0.00013	1.28	47.75
2456931.494758	900	-0.4094 ± 0.0008	-0.050	6.947	0.00275 ± 0.00008	0.03327 ± 0.00011	1.43	55.35
				HD 152079				
2456764.704569	900	-21.2455 ± 0.0007	-0.029	7.223	0.00275 ± 0.00006	0.03100 ± 0.00009	1.33	70.60
2456767.723564	900	-21.2453 ± 0.0008	-0.029	7.219	0.00269 ± 0.00007	0.03133 ± 0.00011	1.22	56.20
2456767.897800	900	-21.2453 ± 0.0007	-0.027	7.225	0.00249 ± 0.00006	0.03114 ± 0.00009	1.11	63.45
2456768.732984	900	-21.2440 ± 0.0007	-0.026	7.225	0.00277 ± 0.00006	0.03105 ± 0.00008	1.18	71.45
2456811.703038	900	-21.2483 ± 0.0007	-0.026	7.225	0.00277 ± 0.00006	0.03103 ± 0.00009	1.05	67.80
2456822.692812	900	-21.2445 ± 0.0007	-0.026	7.221	0.00285 ± 0.00006	0.03112 ± 0.00009	1.05	68.80
2456823.834735	900	-21.2445 ± 0.0010	-0.027	7.226	0.00239 ± 0.00008	0.03108 ± 0.00012	1.44	48.75
2456824.716983	900	-21.2471 ± 0.0008	-0.032	7.223	0.00287 ± 0.00006	0.03098 ± 0.00010	1.07	62.80
2456825.764772	900	-21.2470 ± 0.0009	-0.025	7.223	0.00269 ± 0.00007	0.03123 ± 0.00011	1.16	55.60
2456826.615258	900	-21.2507 ± 0.0007	-0.025	7.221	0.00305 ± 0.00006	0.03110 ± 0.00009	1.09	69.00
2456826.760500	900	-21.2511 ± 0.0007	-0.027	7.221	0.00286 ± 0.00006	0.03110 ± 0.00010	1.16	67.50
2456827.613288	900	-21.2488 ± 0.0012	-0.020	7.221	0.00273 ± 0.00010	0.03114 ± 0.00014	1.09	42.30
2456827.757927	900	-21.2485 ± 0.0008	-0.022	7.221	0.00256 ± 0.00006	0.03116 ± 0.00011	1.16	60.05
2456828.626570	900	-21.2519 ± 0.0007	-0.028	7.227	0.00298 ± 0.00006	0.03117 ± 0.00009	1.07	71.30
2456828.780978	900	-21.2502 ± 0.0007	-0.025	7.223	0.00273 ± 0.00006	0.03130 ± 0.00010	1.24	67.90
2456837.603850	900	-21.2499 ± 0.0009	-0.032	7.223	0.00290 ± 0.00008	0.03120 ± 0.00011	1.06	54.00
2456838.699997	900	-21.2478 ± 0.0006	-0.025	7.226	0.00263 ± 0.00006	0.03104 ± 0.00008	1.10	74.60
2456839.621205	900	-21.2477 ± 0.0008	-0.034	7.228	0.00291 ± 0.00007	0.03112 ± 0.00010	1.05	59.95
2456840.705845	500	-21.2474 ± 0.0007	-0.030	7.230	0.00269 ± 0.00006	0.03118 ± 0.00010	1.11	68.20
2456841.751329	900	-21.2490 ± 0.0008	-0.025	7.224	0.00272 ± 0.00006	0.03121 ± 0.00010	1.27	63.00
2456842.682962	900	-21.2484 ± 0.0010	-0.026	7.233	0.00220 ± 0.00007	0.03129 ± 0.00012	1.09	50.70
2456870.596671	900	-21.2492 ± 0.0008	-0.030	7.225	0.00252 ± 0.00007	0.03103 ± 0.00011	1.07	56.50

Table 22. continued.

BJD	T_{exp} [s]	RV [kms^{-1}]	BIS [kms^{-1}]	FWHM [kms^{-1}]	Ca II	Hα	Air mass	SNR
2456871.542981	900	-21.2483 ± 0.0008	-0.023	7.223	0.00252 ± 0.00007	0.03108 ± 0.00011	1.05	56.55
2456872.532459	900	-21.2489 ± 0.0007	-0.025	7.221	0.00276 ± 0.00006	0.03119 ± 0.00009	1.05	66.50
2456873.534724	900	-21.2488 ± 0.0009	-0.027	7.221	0.00252 ± 0.00007	0.03120 ± 0.00012	1.05	53.25
2456915.608909	900	-21.2533 ± 0.0011	-0.032	7.227	0.00232 ± 0.00008	0.03094 ± 0.00013	1.70	44.65
2456919.592116	900	-21.2466 ± 0.0010	-0.023	7.224	0.00265 ± 0.00009	0.03078 ± 0.00013	1.65	46.25
2456927.485539	900	-21.2524 ± 0.0009	-0.028	7.231	0.00283 ± 0.00007	0.03094 ± 0.00012	1.18	54.30
2456928.503715	900	-21.2498 ± 0.0007	-0.026	7.224	0.00270 ± 0.00006	0.03109 ± 0.00009	1.25	66.35
2456929.498641	900	-21.2483 ± 0.0009	-0.029	7.222	0.00240 ± 0.00007	0.03093 ± 0.00011	1.24	52.70
2456930.530717	900	-21.2501 ± 0.0008	-0.027	7.223	0.00254 ± 0.00007	0.03093 ± 0.00011	1.41	55.80
2456931.519915	900	-21.2505 ± 0.0008	-0.030	7.223	0.00277 ± 0.00007	0.03118 ± 0.00011	1.36	58.35
				HD 187085				
2456764.898456	600	15.3146 ± 0.0005	0.025	8.754	0.00279 ± 0.00003	0.02853 ± 0.00004	1.06	153.05
2456765.898643	600	15.3152 ± 0.0005	0.026	8.749	0.00277 ± 0.00002	0.02851 ± 0.00004	1.05	172.70
2456766.876814	600	15.3191 ± 0.0005	0.026	8.747	0.00281 ± 0.00002	0.02841 ± 0.00004	1.09	162.45
2456810.914436	600	15.3171 ± 0.0006	0.028	8.749	0.00281 ± 0.00003	0.02835 ± 0.00005	1.11	118.15
2456825.878411	5	15.3163 ± 0.0057	0.061	8.710	0.00301 ± 0.00024	0.02916 ± 0.00057	1.13	10.55
2456825.884534	600	15.3156 ± 0.0006	0.024	8.748	0.00274 ± 0.00003	0.02845 ± 0.00005	1.13	138.55
2456828.870475	900	15.3188 ± 0.0004	0.024	8.756	0.00275 ± 0.00002	0.02838 ± 0.00004	1.11	176.40
2456837.651572	600	15.3179 ± 0.0006	0.026	8.752	0.00274 ± 0.00003	0.02843 ± 0.00005	1.21	120.15
2456837.774237	600	15.3189 ± 0.0005	0.025	8.745	0.00276 ± 0.00003	0.02846 ± 0.00005	1.01	144.95
2456838.751424	600	15.3165 ± 0.0005	0.027	8.751	0.00277 ± 0.00002	0.02837 ± 0.00004	1.01	163.65
2456839.716457	600	15.3201 ± 0.0006	0.028	8.747	0.00275 ± 0.00003	0.02825 ± 0.00005	1.03	139.70
2456839.840592	600	15.3222 ± 0.0006	0.025	8.753	0.00280 ± 0.00003	0.02834 ± 0.00006	1.12	119.30
2456840.782752	900	15.3182 ± 0.0005	0.022	8.749	0.00274 ± 0.00002	0.02838 ± 0.00005	1.02	145.65
2456841.783651	600	15.3190 ± 0.0005	0.023	8.749	0.00279 ± 0.00002	0.02833 ± 0.00004	1.03	161.20
2456842.824225	600	15.3199 ± 0.0007	0.025	8.746	0.00274 ± 0.00003	0.02838 ± 0.00006	1.10	108.10
2456866.796207	600	15.3239 ± 0.0006	0.029	8.751	0.00279 ± 0.00003	0.02830 ± 0.00005	1.22	131.05
2456916.611674	600	15.3234 ± 0.0006	0.020	8.749	0.00273 ± 0.00003	0.02825 ± 0.00005	1.08	121.10
2456919.693856	600	15.3251 ± 0.0008	0.025	8.744	0.00274 ± 0.00004	0.02815 ± 0.00006	1.48	97.80
2456927.498514	600	15.3211 ± 0.0006	0.024	8.751	0.00281 ± 0.00003	0.02821 ± 0.00005	1.01	117.45
2456927.645086	600	15.3208 ± 0.0006	0.028	8.753	0.00278 ± 0.00003	0.02820 ± 0.00005	1.31	135.25
2456928.528409	600	15.3191 ± 0.0005	0.027	8.751	0.00274 ± 0.00002	0.02820 ± 0.00004	1.02	151.80
2456929.523410	600	15.3191 ± 0.0005	0.028	8.749	0.00276 ± 0.00002	0.02823 ± 0.00004	1.01	163.10
2456930.544358	600	15.3202 ± 0.0006	0.025	8.756	0.00276 ± 0.00003	0.02825 ± 0.00005	1.03	133.60
2456931.512255	600	15.3209 ± 0.0006	0.028	8.751	0.00272 ± 0.00003	0.02835 ± 0.00005	1.01	129.55
2456931.646895	600	15.3209 ± 0.0005	0.028	8.751	0.00278 ± 0.00003	0.02821 ± 0.00005	1.39	142.10
2456932.515171	600	15.3200 ± 0.0007	0.023	8.752	0.00268 ± 0.00004	0.02835 ± 0.00006	1.01	100.45
2456936.545975	600	15.3204 ± 0.0008	0.023	8.750	0.00276 ± 0.00004	0.02845 ± 0.00007	1.06	91.00
2456953.587223	600	15.3201 ± 0.0005	0.028	8.755	0.00279 ± 0.00002	0.02803 ± 0.00004	1.41	149.55
2456956.547603	600	15.3182 ± 0.0005	0.027	8.750	0.00271 ± 0.00002	0.02819 ± 0.00004	1.23	170.40
2456957.547439	600	15.3182 ± 0.0012	0.032	8.752	0.00293 ± 0.00006	0.02831 ± 0.00011	1.25	56.00
				HD 190647				
2456764.907841	900	-40.2354 ± 0.0004	-0.021	7.236	0.00283 ± 0.00003	0.03159 ± 0.00005	1.06	130.90
2456765.907774	900	-40.2348 ± 0.0003	-0.021	7.237	0.00273 ± 0.00003	0.03153 ± 0.00004	1.06	157.15
2456766.904524	900	-40.2338 ± 0.0003	-0.024	7.240	0.00279 ± 0.00003	0.03155 ± 0.00004	1.06	154.25
2456809.934925	900	-40.2385 ± 0.0004	-0.025	7.241	0.00281 ± 0.00003	0.03172 ± 0.00005	1.11	124.40
2456811.946449	600	-40.2360 ± 0.0006	-0.025	7.238	0.00274 ± 0.00005	0.03148 ± 0.00008	1.17	74.75
2456825.894518	600	-40.2389 ± 0.0004	-0.026	7.234	0.00289 ± 0.00004	0.03163 ± 0.00006	1.13	104.30
2456827.918178	5	-40.2506 ± 0.0058	-0.038	7.235	0.00361 ± 0.00041	0.03047 ± 0.00054	1.25	8.60
2456827.938966	900	-40.2368 ± 0.0004	-0.020	7.240	0.00284 ± 0.00003	0.03149 ± 0.00005	1.34	122.55
2456828.814213	900	-40.2380 ± 0.0004	-0.024	7.237	0.00274 ± 0.00003	0.03156 ± 0.00006	1.01	118.50
2456828.881566	900	-40.2349 ± 0.0003	-0.023	7.238	0.00278 ± 0.00003	0.03159 ± 0.00005	1.11	141.10
2456837.680740	900	-40.2380 ± 0.0004	-0.023	7.238	0.00282 ± 0.00003	0.03151 ± 0.00006	1.15	114.75
2456837.784216	900	-40.2388 ± 0.0004	-0.023	7.236	0.00279 ± 0.00003	0.03150 ± 0.00005	1.01	129.70
2456838.761826	900	-40.2414 ± 0.0003	-0.023	7.238	0.00284 ± 0.00003	0.03155 ± 0.00004	1.01	146.60
2456839.747515	780	-40.2401 ± 0.0005	-0.024	7.239	0.00282 ± 0.00004	0.03140 ± 0.00007	1.01	90.50
2456839.904845	900	-40.2400 ± 0.0006	-0.022	7.240	0.00282 ± 0.00005	0.03139 ± 0.00007	1.32	83.60
2456840.815171	602	-40.2458 ± 0.0026	-0.029	7.261	0.00289 ± 0.00015	0.03175 ± 0.00024	1.04	23.70
2456841.816030	900	-40.2393 ± 0.0004	-0.022	7.238	0.00276 ± 0.00003	0.03152 ± 0.00005	1.04	124.05
2456871.745223	900	-40.2428 ± 0.0004	-0.022	7.238	0.00280 ± 0.00003	0.03160 ± 0.00005	1.06	123.40

Table 22. continued.

BJD	T_{exp} [s]	RV [kms^{-1}]	BIS [kms^{-1}]	FWHM [kms^{-1}]	Ca II	Hα	Air mass	SNR
2456915.712236	900	-40.2511 ± 0.0009	-0.025	7.237	0.00258 ± 0.00007	0.03156 ± 0.00011	1.44	52.80
2456916.685503	900	-40.2487 ± 0.0005	-0.019	7.237	0.00287 ± 0.00005	0.03141 ± 0.00007	1.28	87.85
2456927.547450	900	-40.2518 ± 0.0004	-0.021	7.237	0.00280 ± 0.00003	0.03156 ± 0.00006	1.01	119.25
2456928.519285	900	-40.2492 ± 0.0003	-0.023	7.238	0.00279 ± 0.00003	0.03158 ± 0.00005	1.01	138.75
2456928.643197	900	-40.2493 ± 0.0004	-0.023	7.240	0.00282 ± 0.00004	0.03168 ± 0.00005	1.24	122.30
2456929.514566	900	-40.2506 ± 0.0003	-0.024	7.236	0.00281 ± 0.00003	0.03164 ± 0.00004	1.01	141.80
2456929.658164	900	-40.2519 ± 0.0004	-0.021	7.237	0.00280 ± 0.00003	0.03167 ± 0.00005	1.34	131.50
2456930.579458	900	-40.2502 ± 0.0004	-0.021	7.239	0.00295 ± 0.00004	0.03162 ± 0.00005	1.06	120.25
2456931.555434	900	-40.2514 ± 0.0004	-0.023	7.236	0.00279 ± 0.00003	0.03162 ± 0.00005	1.03	124.95
2456931.673131	900	-40.2499 ± 0.0004	-0.024	7.240	0.00275 ± 0.00003	0.03167 ± 0.00005	1.49	133.90
2456932.552680	900	-40.2516 ± 0.0004	-0.023	7.238	0.00285 ± 0.00004	0.03164 ± 0.00006	1.03	108.70
2456936.556163	900	-40.2522 ± 0.0006	-0.022	7.242	0.00286 ± 0.00005	0.03164 ± 0.00007	1.05	84.90
				HD 216437				
2456764.929357	600	-2.2378 ± 0.0003	-0.003	7.640	0.00274 ± 0.00002	0.02995 ± 0.00003	1.59	210.85
2456765.928927	600	-2.2338 ± 0.0002	-0.005	7.641	0.00277 ± 0.00002	0.02991 ± 0.00003	1.58	236.35
2456766.926054	600	-2.2343 ± 0.0003	-0.006	7.640	0.00275 ± 0.00002	0.02996 ± 0.00003	1.58	211.50
2456767.934605	600	-2.2340 ± 0.0003	-0.004	7.641	0.00278 ± 0.00002	0.02991 ± 0.00003	1.54	193.25
2456768.932242	600	-2.2335 ± 0.0003	-0.002	7.640	0.00277 ± 0.00002	0.02979 ± 0.00003	1.54	221.35
2456810.923037	600	-2.2254 ± 0.0003	-0.005	7.639	0.00272 ± 0.00002	0.02989 ± 0.00004	1.33	179.70
2456822.869248	600	-2.2262 ± 0.0006	-0.006	7.638	0.00273 ± 0.00005	0.02987 ± 0.00007	1.35	86.70
2456823.955318	600	-2.2258 ± 0.0003	-0.003	7.638	0.00274 ± 0.00002	0.02995 ± 0.00003	1.33	191.45
2456824.860351	600	-2.2277 ± 0.0003	-0.003	7.638	0.00275 ± 0.00002	0.02986 ± 0.00003	1.36	182.85
2456825.870341	600	-2.2274 ± 0.0003	-0.004	7.640	0.00271 ± 0.00002	0.03002 ± 0.00003	1.34	176.15
2456825.949811	600	-2.2283 ± 0.0003	-0.005	7.640	0.00275 ± 0.00002	0.02992 ± 0.00003	1.33	212.15
2456826.867413	600	-2.2284 ± 0.0003	-0.004	7.641	0.00273 ± 0.00002	0.02984 ± 0.00004	1.34	175.30
2456826.925413	600	-2.2284 ± 0.0003	-0.002	7.640	0.00275 ± 0.00002	0.02987 ± 0.00003	1.32	207.40
2456827.860329	600	-2.2256 ± 0.0003	-0.004	7.639	0.00277 ± 0.00002	0.02985 ± 0.00003	1.35	198.35
2456828.889333	600	-2.2261 ± 0.0003	-0.004	7.640	0.00277 ± 0.00002	0.02994 ± 0.00003	1.32	218.40
2456837.858963	600	-2.2254 ± 0.0003	-0.004	7.640	0.00275 ± 0.00002	0.02989 ± 0.00003	1.33	202.55
2456837.950724	300	-2.2258 ± 0.0005	-0.003	7.640	0.00274 ± 0.00003	0.02988 ± 0.00005	1.36	115.45
2456838.869000	600	-2.2265 ± 0.0003	-0.003	7.637	0.00274 ± 0.00002	0.02986 ± 0.00003	1.32	196.35
2456839.880680	399	-2.2248 ± 0.0005	-0.005	7.644	0.00276 ± 0.00004	0.02992 ± 0.00006	1.32	111.30
2456840.895195	600	-2.2275 ± 0.0004	-0.003	7.640	0.00272 ± 0.00003	0.03003 ± 0.00004	1.32	132.45
2456841.840078	600	-2.2271 ± 0.0003	-0.003	7.642	0.00277 ± 0.00002	0.02994 ± 0.00004	1.33	178.35
2456842.860644	600	-2.2218 ± 0.0004	-0.005	7.639	0.00268 ± 0.00003	0.02987 ± 0.00005	1.32	136.60
2456866.851835	600	-2.2272 ± 0.0003	-0.007	7.634	0.00274 ± 0.00002	0.02982 ± 0.00003	1.34	191.55
2456915.721437	600	-2.2180 ± 0.0005	-0.004	7.636	0.00272 ± 0.00004	0.02991 ± 0.00005	1.34	108.80
2456916.702693	600	-2.2183 ± 0.0004	-0.005	7.637	0.00278 ± 0.00003	0.02974 ± 0.00005	1.33	130.40
2456919.717320	600	-2.2177 ± 0.0003	-0.005	7.640	0.00276 ± 0.00002	0.02989 ± 0.00004	1.35	173.55
2456927.598681	600	-2.2147 ± 0.0003	-0.002	7.638	0.00274 ± 0.00002	0.02985 ± 0.00003	1.34	226.00
2456928.563669	600	-2.2137 ± 0.0002	-0.004	7.640	0.00273 ± 0.00002	0.02982 ± 0.00003	1.38	234.10
2456928.716891	600	-2.2133 ± 0.0002	-0.003	7.637	0.00274 ± 0.00002	0.02986 ± 0.00003	1.38	240.90
2456929.685281	600	-2.2128 ± 0.0003	-0.002	7.640	0.00277 ± 0.00002	0.02986 ± 0.00003	1.34	201.50
2456930.602238	600	-2.2126 ± 0.0003	-0.004	7.641	0.00285 ± 0.00002	0.02976 ± 0.00003	1.33	189.20
2456931.638424	599	-2.2117 ± 0.0002	-0.004	7.640	0.00275 ± 0.00002	0.02989 ± 0.00003	1.32	231.25
2456954.528844	600	-2.2158 ± 0.0002	-0.004	7.641	0.00270 ± 0.00002	0.02980 ± 0.00002	1.33	257.30
				HD 220689				
2456809.940935	600	12.2313 ± 0.0006	-0.004	7.410	0.00304 ± 0.00004	0.02945 ± 0.00006	1.04	106.80
2456822.856165	900	12.2291 ± 0.0014	-0.007	7.395	0.00277 ± 0.00008	0.02958 ± 0.00014	1.17	43.25
2456823.891285	900	12.2312 ± 0.0005	-0.005	7.408	0.00305 ± 0.00003	0.02939 ± 0.00005	1.07	119.15
2456823.942412	900	12.2325 ± 0.0006	-0.008	7.409	0.00297 ± 0.00004	0.02943 ± 0.00006	1.01	106.00
2456824.921380	900	12.2306 ± 0.0005	-0.009	7.404	0.00310 ± 0.00003	0.02947 ± 0.00005	1.02	119.55
2456825.858064	900	12.2315 ± 0.0006	-0.007	7.408	0.00297 ± 0.00003	0.02955 ± 0.00006	1.14	110.60
2456828.910589	900	12.2287 ± 0.0005	-0.009	7.401	0.00312 ± 0.00003	0.02952 ± 0.00005	1.02	125.60
2456837.903577	900	12.2326 ± 0.0006	-0.005	7.405	0.00309 ± 0.00004	0.02947 ± 0.00005	1.01	114.45
2456838.857641	900	12.2306 ± 0.0005	-0.005	7.405	0.00305 ± 0.00003	0.02932 ± 0.00005	1.05	123.90
2456838.947324	900	12.2311 ± 0.0005	-0.006	7.409	0.00309 ± 0.00003	0.02944 ± 0.00005	1.04	142.40
2456839.914375	900	12.2311 ± 0.0006	-0.004	7.405	0.00299 ± 0.00004	0.02945 ± 0.00007	1.01	101.05
2456840.909227	200	12.2308 ± 0.0007	-0.008	7.401	0.00312 ± 0.00005	0.02966 ± 0.00007	1.01	86.65
2456841.853230	900	12.2315 ± 0.0006	-0.008	7.412	0.00300 ± 0.00004	0.02936 ± 0.00006	1.05	106.55

Table 22. continued.

BJD	T_{exp} [s]	RV [kms^{-1}]	BIS [kms^{-1}]	FWHM [kms^{-1}]	Ca II	Hα	Air mass	SNR
2456842.870780	900	12.2320 ± 0.0007	-0.004	7.410	0.00306 ± 0.00004	0.02939 ± 0.00007	1.02	95.60
2456871.899889	900	12.2364 ± 0.0005	-0.006	7.404	0.00302 ± 0.00003	0.02938 ± 0.00005	1.13	128.25
2456872.866641	900	12.2317 ± 0.0005	-0.010	7.408	0.00306 ± 0.00003	0.02946 ± 0.00006	1.05	119.05
2456873.874920	900	12.2336 ± 0.0009	-0.008	7.408	0.00307 ± 0.00006	0.02946 ± 0.00010	1.07	63.45
2456874.848892	900	12.2337 ± 0.0005	-0.004	7.405	0.00303 ± 0.00003	0.02943 ± 0.00005	1.03	139.60
2456915.735102	900	12.2347 ± 0.0007	-0.004	7.408	0.00306 ± 0.00004	0.02929 ± 0.00007	1.03	94.00
2456916.716881	900	12.2346 ± 0.0007	-0.003	7.410	0.00302 ± 0.00004	0.02945 ± 0.00008	1.02	87.35
2456919.761695	900	12.2353 ± 0.0007	-0.003	7.405	0.00302 ± 0.00004	0.02948 ± 0.00007	1.11	92.95
2456927.659196	900	12.2360 ± 0.0005	-0.006	7.407	0.00304 ± 0.00003	0.02932 ± 0.00005	1.01	140.25
2456927.809793	900	12.2380 ± 0.0005	-0.004	7.409	0.00300 ± 0.00003	0.02929 ± 0.00005	1.47	138.90
2456928.622102	900	12.2366 ± 0.0005	-0.005	7.406	0.00302 ± 0.00003	0.02936 ± 0.00005	1.04	134.55
2456929.623756	900	12.2361 ± 0.0004	-0.006	7.410	0.00309 ± 0.00002	0.02933 ± 0.00004	1.04	161.15
2456929.791053	900	12.2379 ± 0.0006	-0.004	7.409	0.00298 ± 0.00004	0.02936 ± 0.00006	1.36	108.05
2456931.620091	900	12.2336 ± 0.0006	-0.005	7.408	0.00302 ± 0.00003	0.02945 ± 0.00006	1.03	112.20
2456931.791380	900	12.2339 ± 0.0005	-0.006	7.411	0.00299 ± 0.00003	0.02922 ± 0.00005	1.41	140.05
2456932.729895	900	12.2348 ± 0.0005	-0.007	7.413	0.00301 ± 0.00003	0.02931 ± 0.00005	1.11	125.75
2456954.521088	900	12.2351 ± 0.0004	-0.006	7.404	0.00304 ± 0.00003	0.02899 ± 0.00004	1.10	155.95
2456959.550174	900	12.2347 ± 0.0005	-0.005	7.406	0.00301 ± 0.00003	0.02913 ± 0.00005	1.02	129.15